



Universiteit
Leiden
The Netherlands

Imaging functional brain connectivity : pharmacological modulation, aging and Alzheimer's disease

Klaassens, B.L.

Citation

Klaassens, B. L. (2018, September 6). *Imaging functional brain connectivity : pharmacological modulation, aging and Alzheimer's disease*. Retrieved from <https://hdl.handle.net/1887/65052>

Version: Not Applicable (or Unknown)

License: [Licence agreement concerning inclusion of doctoral thesis in the Institutional Repository of the University of Leiden](#)

Downloaded from: <https://hdl.handle.net/1887/65052>

Note: To cite this publication please use the final published version (if applicable).

Cover Page



Universiteit Leiden



The handle <http://hdl.handle.net/1887/65052> holds various files of this Leiden University dissertation.

Author: Klaassens, B.L.

Title: Imaging functional brain connectivity : pharmacological modulation, aging and Alzheimer's disease

Issue Date: 2018-09-06

Imaging functional brain connectivity

Pharmacological modulation, aging and Alzheimer's disease

Bernadet Klaassens

Cover Het IJzeren Gordijn
Layout Renate Siebes | Proefschrift.nu
Printed by Gildeprint
ISBN 978-94-6233-965-1

The research as described in this thesis was supported by the Netherlands Initiative Brain and Cognition, a part of the Netherlands Organization for Scientific Research (NWO), and the Centre for Human Drug Research.

Printing of this thesis was sponsored by Alzheimer Nederland, Brain Research Center, Pfizer PFE bv and Chipsoft.

Copyright © 2018 Bernadet Klaassens

All rights reserved. No part of this publication may be reproduced, stored or transmitted in any form or by any means without permission of the author, or, when applicable, of the publisher of scientific papers.

Imaging functional brain connectivity

Pharmacological modulation, aging and Alzheimer's disease

Proefschrift

ter verkrijging van
de graad van Doctor aan de Universiteit Leiden,
op gezag van Rector Magnificus prof. mr. C.J.J.M. Stolker,
volgens besluit van het College voor Promoties
te verdedigen op donderdag 6 september 2018
klokke 16.15 uur

door

Bernadet Louise Klaassens

geboren te Leiderdorp
in 1980

Promotoren

Prof. dr. S.A.R.B. Rombouts

Prof. dr. J.M.A. van Gerven

Copromotor

Dr. J. van der Grond

Leden promotiecommissie

Prof. dr. M.J. de Rooij

Prof. dr. J.C. van Swieten, Erasmus Medisch Centrum

Prof. dr. H.A.M. Middelkoop, Leids Universitair Medisch Centrum

Dr. G.J. Groeneveld, Centre for Human Drug Research

Dr. M. de Rover, Leids Universitair Medisch Centrum

TABLE OF CONTENTS

Chapter 1	General introduction	7
Part I	Pharmacological challenge effects on brain connectivity in healthy young adults	15
Chapter 2	Single-dose serotonergic stimulation shows widespread effects on functional brain connectivity <i>NeuroImage 2015; 122:440-450</i>	17
Chapter 3	Time related effects on functional brain connectivity after serotonergic and cholinergic neuromodulation <i>Human Brain Mapping 2017; 38(1):308-325</i>	37
Part II	Functional brain connectivity and neuromodulation in older age and Alzheimer's disease	61
Chapter 4	Diminished posterior precuneus connectivity with the default mode network differentiates normal aging from Alzheimer's disease <i>Frontiers in Aging Neuroscience 2017; 9:1-13</i>	63
Chapter 5	Serotonergic and cholinergic modulation of functional brain connectivity: a comparison between young and older adults <i>NeuroImage 2018; 169:312-322</i>	85
Chapter 6	Imaging cholinergic and serotonergic neurotransmitter networks in Alzheimer's disease in vivo <i>Submitted for publication</i>	107
Chapter 7	Summary and general discussion	131
Chapter 8	Nederlandse samenvatting	143
Appendix	Abbreviations	153
	References	155
	Dankwoord	177
	Curriculum vitae	179

Chapter 1

General introduction

INTRODUCTION

Brain function relies heavily on neural communication and connections. Better understanding of the mechanisms that are related to maintenance or deterioration of brain function requires a technique that takes into account the elaborate nature of the central nervous system (CNS). A useful method for that purpose is to assess the brain's functional connectivity. Brain regions are functionally connected to each other when they exhibit correlating activation patterns [1], illustrating the complex organization of neural networks. Interactions between regions and within networks largely depend on chemical transmission between neurons. Functional connectivity might therefore also be regarded as representative of healthy or affected neural transmission that accompanies aging or neurodegeneration as seen in Alzheimer's disease (AD). The work as described in this thesis is aimed at elucidating the neural connections and serotonergic and cholinergic neurotransmitter pathways in healthy young and older adults and patients with AD.

Functional brain networks

Functional magnetic resonance imaging (fMRI) of the brain measures the change in the blood-oxygenation-level dependent (BOLD) signal over time for each voxel [2]. Based on the premise that active neurons consume more oxygen, the BOLD signal is considered to correspond to functional activity in these areas. More specifically, increased blood flow towards active brain regions alters the ratio of oxygenated to deoxygenated haemoglobin, leading to changes in MR images that are sensitive to the level of deoxyhaemoglobin [3, 4]. The term functional connectivity refers to temporal correlations between remote neurophysiological events [1]. Resting state fMRI (RS-fMRI) has been discovered as a suitable, non-invasive approach to study whole brain functional connections during rest as opposed to during the performance of an active task. Investigating resting state networks instead of task-related regional changes in activation has several advantages. With a relatively short duration of scanning sessions and the absence of complicated task instructions, it is more easily employed within specific patient populations and without the danger of different performance strategies. In addition, task fMRI is restricted to limited flexibility of designs and does not take into account the large-scale and interacting nature of the CNS [5].

Covariation of spontaneous low-frequency fluctuations in the BOLD response seems to reflect functional network interactions [6-8]. Even cortical regions that are spatially distant from each other can belong to the same functional network when its intrinsic activity is temporally coherent. Several resting state networks have consistently been detected in the brain and related to specific functions as visual, auditory and salience processing, motor performance and executive control [9, 10]. A typical resting state network is the default mode network (DMN), comprising the precuneus, posterior cingulate, temporal, parietal and medial prefrontal cortex [11, 12]. The

DMN is one of the most robust resting state networks that shows increased activation during rest as opposed to during the performance of active tasks, and is known to be involved in self-reference, introspection and episodic memory [13, 14].

Functional connectivity in aging and Alzheimer's disease

Measurements of brain network connectivity are increasingly being implemented as a means to investigate neurologic and psychiatric disease [6]. AD, the most common cause of dementia among older adults, is a neurodegenerative disease with a slow onset that progressively affects multiple cognitive domains. It is primarily associated with a deterioration of memory, and additional loss of functions related to language, orientation in time and place, visuospatial and executive functioning as well as changes in personality and behavior [15]. One of the major risk factors for AD is advancing age and because of the aging population, the number of patients with AD is expected to keep on rising considerably [16, 17]. The increased prevalence of AD and the burden it poses on health care and the daily life of patients and their proxies calls for development of early diagnostic markers and improved insight into disruption of neural processes. Examination of altered connectivity is especially relevant since AD is nowadays recognized as a disorder of vanished functional connections [18, 19].

AD is mainly characterized by reduced hippocampal and DMN connectivity [20, 21]. A few studies show that frontoparietal, visual, executive, sensory, motor, cerebellum/basal ganglia and salience networks are affected in AD as well, with evidence for increases as well as decreases in connectivity [22-26]. Although exact causal mechanisms are not completely understood, connectivity alterations are possibly representative of decrements in metabolism [27], white matter integrity [28-30], amyloid deposition [31] and structural atrophy [18, 32]. In line with findings on connectivity disruptions, these hallmarks are frequently found at regions within the DMN and the interrelated hippocampus. Functional connectivity abnormalities have also been found in patients suffering from mild cognitive impairment [33, 34] and healthy subjects with a genetic risk for the development of AD [35, 36]. But 'normal' aging appears to have an influence on DMN coherence as well, as connectivity with anterior and posterior components is compromised in healthy older adults [20, 37]. An age-appropriate degradation in mental functioning might be associated with this decline in DMN connectivity [28, 37]. Studies on the effect of aging on other functional networks are scarce, but indicative of reduced connectivity with dorsal attention, salience, motor, somatosensory and visual networks [28, 38-42].

Neurotransmitter systems in aging and Alzheimer's disease

Apart from a decline in functional connectivity, aging and Alzheimer's disease are characterized by decreased neurotransmitter functioning [43-45]. Neurotransmission is crucial for communication

between neurons and consequently affects behavior and mental processes. Two neurotransmitters that are implicated in both aging and AD are serotonin (5-hydroxytryptamine; 5-HT) and acetylcholine [46]. The serotonergic system comprises a complex organization of pathways that influences the brain from early development through degeneration with aging. With 7 different main classes (5-HT₁₋₇) and 14 subclasses, not only present in the central nervous system but also in the digestive tract and blood platelets, serotonin influences a wide range of functions and is related to multiple mental, behavioral and physiological states [47, 48]. Serotonin is a monoamine that is released by the dorsal and ventral raphe nuclei in the midbrain towards a vast part of the cortex, limbic areas, hypothalamus, basal ganglia, brain stem and cerebellum [49, 50]. In aging and AD, diminished serotonin activity, as demonstrated by reduced pre- and postsynaptic binding, is mostly associated with changes in behavior and the increased prevalence of depression and mood disorders [45-47, 51]. Selective serotonin reuptake inhibitors (SSRIs) are commonly used as medication for depression and anxiety disorders. SSRIs prevent the natural reuptake of serotonin by presynaptic receptors, thereby increasing the available amount of serotonin in postsynaptic terminals that leads to prolonged action on adjacent neurons [52].

The neurotransmitter acetylcholine has been related to changes in cognitive performance in both normal aging and AD [53, 54]. Cholinergic receptors are subdivided into the muscarinic (M) and nicotinic (N) families, together consisting of 17 subclasses that are located in the central and peripheral nervous system, at the neuromuscular junction, the heart and smooth muscles [55-57]. In the CNS, acetylcholine is primarily synthesized in the basal forebrain and binds to receptors that are present throughout the cortex, thalamus, amygdala and hippocampus [58, 59]. A reduction of choline acetyltransferase and acetylcholinesterase activity in AD [60-62] is explained by the notion that basal forebrain atrophy and associated neuronal loss leads to reduced transmitter release towards the cortex, hippocampus and thalamus, hence affecting memory and attentional processes [63, 64]. It is possible that the cholinergic system integrity is compromised by the deposition of amyloid- β and formation of tangles in AD, which show a high density at locations of neuronal and synaptic loss [65-67]. Acetylcholinesterase inhibitors (AChEIs) inhibit the hydrolysis of acetylcholine by the enzyme acetylcholinesterase, thereby increasing acetylcholine levels in the synaptic cleft. As treatment of cognitive symptoms, AChEIs are mainly useful in the early stages of AD when the decrease of neurotransmitter release is still limited [68, 69]. Although the effectiveness of reducing the breakdown of acetylcholine (or butyrylcholine) in AD is far from satisfactory, there are currently not many alternatives [70-72]. Despite the hypothesized cholinergic dysfunction in normal aging, there is minor evidence of cognitive improvement by AChEI treatment in elderly without AD [73].

Pharmacological challenge effects on functional brain connectivity

The concept of pharmacological challenges implies a promising approach to discover the underlying neurobiological mechanisms behind drug action and neurotransmitter-related disease [74]. This method uses the principles of a pharmacokinetic study with dosing of a drug, followed by a series of measurements at intervals predicted to be relevant for the particular drug being studied. Challenging the CNS with drugs that selectively alter central neurotransmission and are aimed at restoring synaptic connections is an efficient procedure to examine the role of neurotransmitters in healthy and pathological brain functioning [75]. Resting state networks are representative of interactions between different brain areas and therefore sensitive to changes in neurotransmission. Using RS-fMRI to measure challenge effects offers the possibility to visualize and localize patterns and deficits in neurotransmitter systems by imaging pharmacologically induced alterations of related pathways in the brain. An advantage of RS-fMRI measurements in pharmacological research is that they can be repeated frequently, which allows studies of network variations over limited time periods, with changing drug concentrations or diurnal fluctuations. RS-fMRI studies of challenges with dopamine (ant)agonists, morphine, ketamine, Δ^9 -tetrahydrocannabinol (THC) and ethanol have shown convincing agent-specific network responses [76-81]. In this thesis, we used the pharmacological challenge technique to investigate the serotonergic and cholinergic neurotransmitter systems by measuring acute SSRI and AChEI effects on resting state functional connectivity.

Single-dose and short-term administration of SSRIs has been demonstrated to mainly lower connectivity in healthy and depressed young subjects [82-87], which is in line with opposite observations of increased connections in depression [88]. Most of these studies restricted their analysis to the DMN, although Schaefer et al. [83] also show connectivity change in many cortical and subcortical regions outside this network. Long-term treatment with AChEIs in AD patients seems to enhance connectivity of DMN and hippocampal areas [89-94]. Single-dose effects on resting state connectivity and the action of AChEIs on functional connections in healthy brains are thus far not investigated but might provide additional knowledge on the role of acetylcholine in neural communication and functions. Likewise, the effects of SSRIs on resting state connectivity in elderly and AD patients are unknown but could improve our understanding of age- and AD-related changes in serotonin pathways. Since serotonergic and cholinergic neurotransmitter systems are known to be altered in AD, and RS-fMRI is known to be sensitive to pharmacological challenges, provoking these neurotransmitter systems with drug challenges combined with RS-fMRI was hypothesized to reveal greater differences between AD and non-diseased elderly compared to changes in functional connectivity alone. In that case, the challenge approach might even lead to a better differentiation of AD from healthy aging and, ideally, to an earlier diagnostic tool.

AIMS AND OUTLINE OF THIS THESIS

The main objective of this thesis was to investigate the serotonergic and cholinergic systems of the brain and the association of older age and AD with changes in neurotransmission and functional connections. The included studies were intended to provide more insight into neural trajectories in health and the way these are affected in aging and dementia. For that purpose, we examined patterns of functional connectivity using RS-fMRI with and without pharmacological challenges in healthy young and older adults, and patients with AD. In all studies we implemented a standardized and comprehensive method and design, by examining whole brain connectivity and functional change induced by serotonergic and cholinergic drugs and/or associated with age or disease. To assess these effects, we used RS-fMRI and the computerized NeuroCart® test battery, developed for quantifying CNS function with tasks and visual analogue scales measuring mood, alertness, calmness, memory, emotional processing, executive functioning and reaction time [95-103]. In case of pharmacological experiments, additional measures of pharmacokinetics, cortisol and prolactin were taken to monitor the drugs' absorption rate and investigate neurotransmitter function based on the neuroendocrine response, which may also be modulated by SSRIs and AChEIs [104-106]. Repeated pharmacodynamic measures (RS-fMRI, NeuroCart® and neuroendocrine parameters) after drug or placebo administration followed a strict time schedule conform the pharmacokinetic characteristics to ensure appropriate and standard measurements, and enable adequate comparison of results across and within studies. Several methods exist to measure functional connectivity, such as graph theory [107] and seed-based analyses [108]. In our studies, we applied a standardized approach to study functional network change by using ten predefined resting state components as networks of interest [10].

Part I: Pharmacological challenge effects on brain connectivity in healthy young adults

The first part of this thesis concerns two pharmacological studies that were executed in healthy young subjects. These studies were intended to determine the sensitivity of brain connectivity to serotonergic and cholinergic challenges, and to gain more insight into the mechanisms of drug action of SSRIs and AChEIs. **Chapter 2** describes the randomized, double blind, placebo-controlled, crossover study on the SSRI sertraline in 12 young volunteers. After drug or placebo intake, RS-fMRI scans and measures of cognitive and subjective functioning were repeatedly collected. Multiple blood samples were taken as well to define neuroendocrine and pharmacokinetic levels. In **chapter 3**, we further investigate acute pharmacological effects in young volunteers. The SSRI citalopram and the AChEI galantamine were administered to 12 subjects that were matched for age and gender with the subject group of chapter 2. A randomized, double blind, placebo-controlled, crossover design was used with repeated measures before and after drug or placebo intake, including blood samples, NeuroCart® task performance and RS-fMRI.

Part II: Functional brain connectivity and neuromodulation in older age and Alzheimer's disease

The second part of this thesis was aimed at discovering changes in brain connectivity and serotonergic and cholinergic systems in old age and AD. The results of these studies may lead to a better understanding of neurotransmitter system decline, and the possible rehabilitative effects of SSRIs and AChEIs in old age and AD. **Chapter 4** includes the outcomes of a study that was conducted to investigate differences in resting state functional connectivity without pharmacological modulation between 12 young and 12 elderly adults and 12 patients with AD. To examine whether functional connectivity changes might be (partially) explained by atrophy of brain structure, the results of this study were presented with and without correction for local gray matter volume. In the final two chapters, effects of an SSRI and AChEI on brain connectivity were compared between young and older adults and between older adults and AD patients. In **chapter 5** we present the results of a randomized, placebo-controlled, double blind, crossover study in 12 young and 17 older adults. The effects of the SSRI citalopram and the AChEI galantamine on resting state connectivity and task performance were compared between young and older adults. Outcome measures (RS-fMRI, blood samples and NeuroCart® task performance) were repeatedly taken before and after drug or placebo intake. The same design was used for the study as described in **chapter 6**, which shows the results of a comparison between 12 patients with AD and 12 elderly controls after a serotonergic and cholinergic challenge.

To conclude, a summary and general discussion of the presented results and future perspectives are provided in **chapter 7**.



Part I

- Pharmacological challenge effects on brain connectivity in healthy young adults

Chapter 2

Single-dose serotonergic stimulation shows widespread effects on functional brain connectivity

Published in NeuroImage 2015; 122:440-450

Bernadet L. Klaassens^{a,b,c}, Helene C. van Gorsel^d, Najmeh Khalili-Mahani^e, Jeroen van der Grond^b, Bradley T. Wyman^f, Brandon Whitcher^f, Serge A.R.B. Rombouts^{a,b,c}, Joop M.A. van Gerven^d

^aLeiden University, Institute of Psychology, Leiden, the Netherlands, ^bLeiden University Medical Center, Department of Radiology, Leiden, the Netherlands, ^cLeiden University, Leiden Institute for Brain and Cognition, Leiden, the Netherlands, ^dCentre for Human Drug Research, Leiden, the Netherlands, ^eMcGill University, Montreal Neurological Institute, Montreal, Quebec, Canada, ^fPfizer Inc., Cambridge, MA, USA

ABSTRACT

The serotonergic system is widely distributed throughout the central nervous system. It is well known as a mood regulating system, although it also contributes to many other functions. With resting state functional magnetic resonance imaging (RS-fMRI) it is possible to investigate whole brain functional connectivity. We used this non-invasive neuroimaging technique to measure acute pharmacological effects of the selective serotonin reuptake inhibitor sertraline (75 mg) in 12 healthy volunteers. In this randomized, double blind, placebo-controlled, crossover study, RS-fMRI scans were repeatedly acquired during both visits (at baseline and 3, 5, 7 and 9 h after administering sertraline or placebo). Within-group comparisons of voxelwise functional connectivity with ten functional networks were examined ($p < 0.005$, corrected) using a mixed effects model with cerebrospinal fluid, white matter, motion parameters, heart rate and respiration as covariates. Sertraline induced widespread effects on functional connectivity with multiple networks; the default mode network, the executive control network, visual networks, the sensorimotor network and the auditory network. A common factor among these networks was the involvement of the precuneus and posterior cingulate cortex. Cognitive and subjective measures were taken as well, but yielded no significant treatment effects, emphasizing the sensitivity of RS-fMRI to pharmacological challenges. The results are consistent with the existence of an extensive serotonergic system relating to multiple brain functions with a possible key role for the precuneus and cingulate.

INTRODUCTION

The central serotonergic system plays an important modulatory role and affects diverse functions like cognition, mood, appetite, sleep and sensorimotor activity. Different classes of serotonin (5-hydroxytryptamine, 5-HT) receptors exist, and they are distributed throughout the whole brain, including the cortex, limbic areas, hypothalamus, basal ganglia, brain stem and cerebellum [48-50, 109, 110]. The selective serotonin reuptake inhibitor (SSRI) sertraline increases the concentration of synaptic serotonin and is commonly prescribed as a treatment for depression and anxiety disorders [52].

Functional brain imaging shows that SSRIs change brain activation and perfusion in limbic and prefrontal regions, which have been identified as important mediators in emotional processing. However, SSRIs also influence many other brain structures, including the precuneus, basal ganglia, brain stem, cerebellum, hypothalamus, temporal, parietal and occipital areas [111-117].

Understanding the mechanism of action of the extensive system of serotonergic neurons requires a method for studying large-scale network interactions instead of isolated brain regions [83]. The resting state functional magnetic resonance imaging (RS-fMRI) technique allows an integral non-invasive investigation of these network interactions, taking into account the brain's comprehensive neural circuit [7, 118].

The main focus of most RS-fMRI studies on SSRIs has been functional connectivity of the default mode network (DMN), which includes the posterior cingulate, precuneus and medial prefrontal, temporal and parietal regions. The DMN, one of the most consistent networks, is affected in multiple mental disorders, including depression [88]. SSRI administration shows a reduction in functional DMN connectivity, indicating normalization of patterns as seen in depression [82, 84-87]. Yet, SSRIs are expected to change functional connections in brain regions beyond the DMN too [83].

Here, we apply a technique of repeated measures RS-fMRI and an analysis of region-to-network connectivity to study whole brain treatment effects of an SSRI in healthy young volunteers. We have shown the sensitivity of this approach for various other pharmacological challenges [76, 78-81]. Given the widespread distribution of serotonergic receptors in the brain and the involvement of serotonin in many brain functions, we hypothesize that a single-dose of the SSRI sertraline will not only affect the DMN but various resting state brain networks, related to emotional, sensory, motor, cognitive and executive functioning.

MATERIALS AND METHODS

Subjects

Twelve healthy young volunteers (mean age 23.0 ± 2.8 , range 19-28; gender ratio 1:1; BMI 19-24 kg/m²) were recruited to participate in the study. All subjects underwent a thorough medical screening at the Centre for Human Drug Research (CHDR) to investigate whether they met the inclusion and exclusion criteria. They had a normal history of physical and mental health and were able to refrain from using nicotine and caffeine during study days. Other exclusion criteria included positive drug or alcohol screen on study days, regular excessive consumption of alcohol (>4 units/day), caffeine (>6 units/day) or cigarettes (>5 cigarettes/day), use of concomitant medication 2 weeks prior to study participation and involvement in an investigational drug trial 3 months prior to administration. The study was approved by the medical ethics committee of the Leiden University Medical Center (LUMC) and the scientific review board of the CHDR. Written informed consent was obtained from each subject prior to study participation.

Study design

This was a single center, double blind, placebo-controlled, crossover study with sertraline 75 mg. To cover the interval of maximum concentrations of sertraline (T_{max} : 5.5-9.5 h, $T_{1/2}$: 26 h), five RS-fMRI scans were acquired during study days, one at baseline and four after administering sertraline or placebo (at 3, 5, 7 and 9 h post dosing). Each scan was followed by performance of computerized cognitive tasks (taken twice at baseline) on the NeuroCart® test battery, developed by the CHDR for quantifying pharmacological effects on the central nervous system (CNS). By including multiple measurements during the T_{max} interval, this repeated measures profile increases the statistical power of the analysis. Currently, there are no formal power calculation methods that allow estimating the sample size for testing whole brain functional variations. Our sample size was selected based on previous studies [76, 78-80] that demonstrated sufficient power to detect significant effects in repeated measures designs with 12 subjects. Sertraline and placebo were administered orally as capsules, matched for size and weight. To reduce the most common side effect of sertraline (nausea and vomiting), drug treatment was combined with granisetron 2 mg tablets on both study days. Multiple blood samples were taken during the course of the day to define the pharmacokinetic (PK) profile of sertraline in serum, its active metabolite desmethylsertraline and concentrations of cortisol and prolactin. Washout period between the two study days was at least 10 days. An overview of the study design is provided in Figure 2.1.

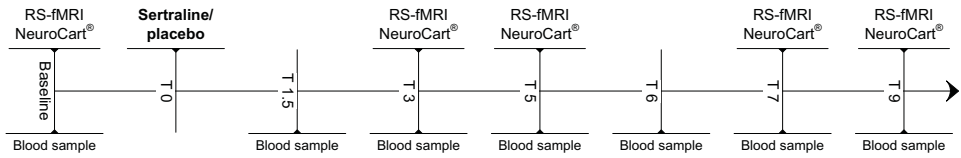


Figure 2.1. Schematic presentation of a study day. At baseline, one RS-fMRI scan was acquired, followed by the NeuroCart® CNS test battery (performed twice at baseline). After drug administration, four more RS-fMRI scans were acquired at time points T = 3, 5, 7 and 9 h post dosing, each time followed by the NeuroCart® test battery. During the day, seven blood samples were taken to measure the concentrations of (desmethyl) sertraline, cortisol and prolactin.

Blood sampling

Pharmacokinetics

Blood samples were collected in 4 mL serum tubes at baseline and 1.5, 3, 5, 6, 7 and 9 h post dosing, centrifuged (2000 g for 10 min) and stored at -40°C until analysis with liquid chromatography-tandem mass spectrometry (LC-MS/MS). PK parameters for sertraline and its active metabolite desmethylsertraline were calculated using a non-compartmental analysis. Maximum serum concentrations (C_{max}) and time of C_{max} (T_{max}) were obtained directly from the serum concentration data. The area under the serum concentration vs. time curve was calculated from time zero to the time of the last quantifiable serum measured concentration, which is equal to the last blood sample of the study day ($\text{AUC}_{0\text{-last}}$). The calculated PK parameters were not used for further analysis but investigated to validate the choice of time points of measurements.

Neuroendocrine variables

Blood samples were also obtained to determine cortisol and prolactin concentrations. Serum samples were taken in a 3.5 mL gel tube at baseline and 1.5, 3, 5, 6, 7 and 9 h post dosing, centrifuged (2000 g for 10 min) and stored at -40°C until analysis. Serum concentrations were quantitatively determined with electrochemiluminescence immunoassay. Cortisol and prolactin concentrations were subsequently used for statistical analysis using a mixed effects model with treatment, time, visit and treatment by time as fixed effects, subject, subject by treatment and subject by time as random effects and the average of the period baseline (pre-dose) values as covariate (SAS for Windows V9.1.3; SAS Institute, Inc., Cary, NC, USA). In the Results section, significant treatment effects (at $p < 0.05$) will be discussed.

NeuroCart® test battery

Each RS-fMRI scan was followed by functional CNS measures outside the scanner using the computerized NeuroCart® test battery measuring alertness, mood and calmness (Visual Analogue Scales (VAS) Bond & Lader), nausea (VAS Nausea), vigilance and visual motor performance

(Adaptive Tracking task), reaction time (Simple Reaction Time task), attention, short-term memory, psychomotor speed, task switching and inhibition (Symbol Digit Substitution Test and Stroop task), working memory (N-back task) and memory imprinting and retrieval plus social processing (Face Encoding and Recognition task) [95-103]. The Face Encoding and Recognition task was only performed twice during each day (at baseline and 7 h post dosing) because of limited different test versions. Duration of each series of NeuroCart® brain function tests was approximately 20 min (except for the baseline series when each task was executed twice within approximately 40 min). To minimize learning effects, training for the NeuroCart® tasks occurred during the screening visit within 3 weeks prior to the first study day.

Analysis

All post-dose repeatedly measured CNS endpoints were analyzed using a mixed effects model with treatment, time, visit and treatment by time as fixed effects, subject, subject by treatment and subject by time as random effects and the average of the period baseline (pre-dose) values as covariate (SAS for Windows V9.1.3; SAS Institute, Inc., Cary, NC, USA). As data of the Simple Reaction Time task were not normally distributed, these data were log-transformed before analysis and back transformed after analysis. The data of the Face Encoding and Recognition task were analyzed using a mixed effects model with treatment as fixed effect and subject as random effect and the baseline value as covariate. In the Results section, significant treatment effects (at $p < 0.05$) will be discussed.

Imaging

Scanning was performed at the LUMC on a Philips 3.0 Tesla Achieva MRI scanner (Philips Medical System, Best, The Netherlands) using a 32-channel head coil. During the RS-fMRI scans, all subjects were asked to close their eyes while staying awake. They were also instructed not to move their head during the scan. Instructions were given prior to each scan on both days. T1-weighted anatomical images were acquired once per visit. To facilitate registration to the anatomical image, each RS-fMRI scan was followed by a high-resolution T2*-weighted echo-planar scan. Duration was approximately 8 min for the RS-fMRI scan, 5 min for the anatomical scan and 30 s for the high-resolution scan. Heart rate and respiration signals were recorded during each scan.

RS-fMRI data were obtained with T2*-weighted echo-planar imaging (EPI) with the following scan parameters: 220 whole brain volumes, repetition time (TR) = 2180 ms; echo time (TE) = 30 ms; flip angle = 85°; field-of-view (FOV) = 220 x 220 x 130 mm; in-plane voxel resolution = 3.44 x 3.44 mm, slice thickness = 3.44 mm, including 10% interslice gap. The next parameters were used to collect T1-weighted anatomical images: TR = 9.7 ms; TE = 4.6 ms; flip angle = 8°; FOV = 224 x 177 x 168 mm; in-plane voxel resolution = 1.17 x 1.17 mm; slice thickness = 1.2 mm. Parameters of

high-resolution T2*-weighted EPI scans were set to: TR = 2200 ms; TE = 30 ms; flip angle = 80°; FOV = 220 x 220 x 168 mm; in-plane voxel resolution = 1.96 x 1.96 mm; slice thickness = 2.0 mm.

Analysis

All analyses were performed using the Functional Magnetic Resonance Imaging of the Brain (FMRIB) Software Library (FSL, Oxford, United Kingdom) version 5.0.4 [119-121]. Each individual functional EPI image was inspected, brain-extracted and corrected for geometrical displacements due to head movement with linear (affine) image registration [122, 123]. Images were temporally filtered (with a high pass filter of 150 s) and spatially smoothed (with a 6 mm full-width half-maximum Gaussian kernel). Thereafter, scans were co-registered with the brain extracted high resolution T2*-weighted EPI scans (with 6 degrees of freedom) and T1 weighted images (using the Boundary-Based-Registration method) [122, 124]. The T1-weighted scans were non-linearly registered to the MNI 152 standard space (the Montreal Neurological Institute, Montreal, QC, Canada) using FMRIB's Non-linear Image Registration Tool. Registration parameters were combined to transform fMRI scans into standard space.

After preprocessing, RS-fMRI networks were extracted from each individual RS-fMRI dataset (12 subjects x 2 days x 5 scans = 120 datasets) using a dual regression analysis [36, 125] based on 10 predefined standard network templates. Confound regressors of time series from white matter (measured from the center of the corpus callosum) and cerebrospinal fluid (measured from the center of lateral ventricles) as well as six motion parameters (the estimated translation along and rotation around the x, y and z axes) were included in this analysis to account for non-neuronal signal fluctuations [126]. The 10 standard templates (see Figure 2.2) have previously been identified using a data-driven approach [10] and comprise the following networks: three visual networks (consisting of medial, occipital pole, and lateral visual areas), DMN (medial parietal, bilateral inferior-lateral-parietal and ventromedial frontal cortex), cerebellar network, sensorimotor network (supplementary motor area, sensorimotor cortex, and secondary somatosensory cortex), auditory network (superior temporal gyrus, Heschl's gyrus, and posterior insular), executive control network (medial-frontal areas, including anterior cingulate and paracingulate) and two frontoparietal networks (frontoparietal areas left and right). With the dual regression method, spatial maps representing voxel-to-network connectivity were estimated for each dataset separately in two stages for use in within-group comparisons. First, the weighted network maps were used in a spatial regression into each dataset. This stage generated 12 time series per dataset that describe the average temporal course of signal fluctuations of the 10 networks plus 2 confound regressors (cerebrospinal fluid and white matter). The six motion parameters, as estimated during motion correction, were inserted into the output files of this first stage for further analysis. Next, these time series were entered in a temporal regression into the same dataset. This resulted in a spatial map per network per dataset with regression coefficients referring to the weight of each voxel being associated with the characteristic signal

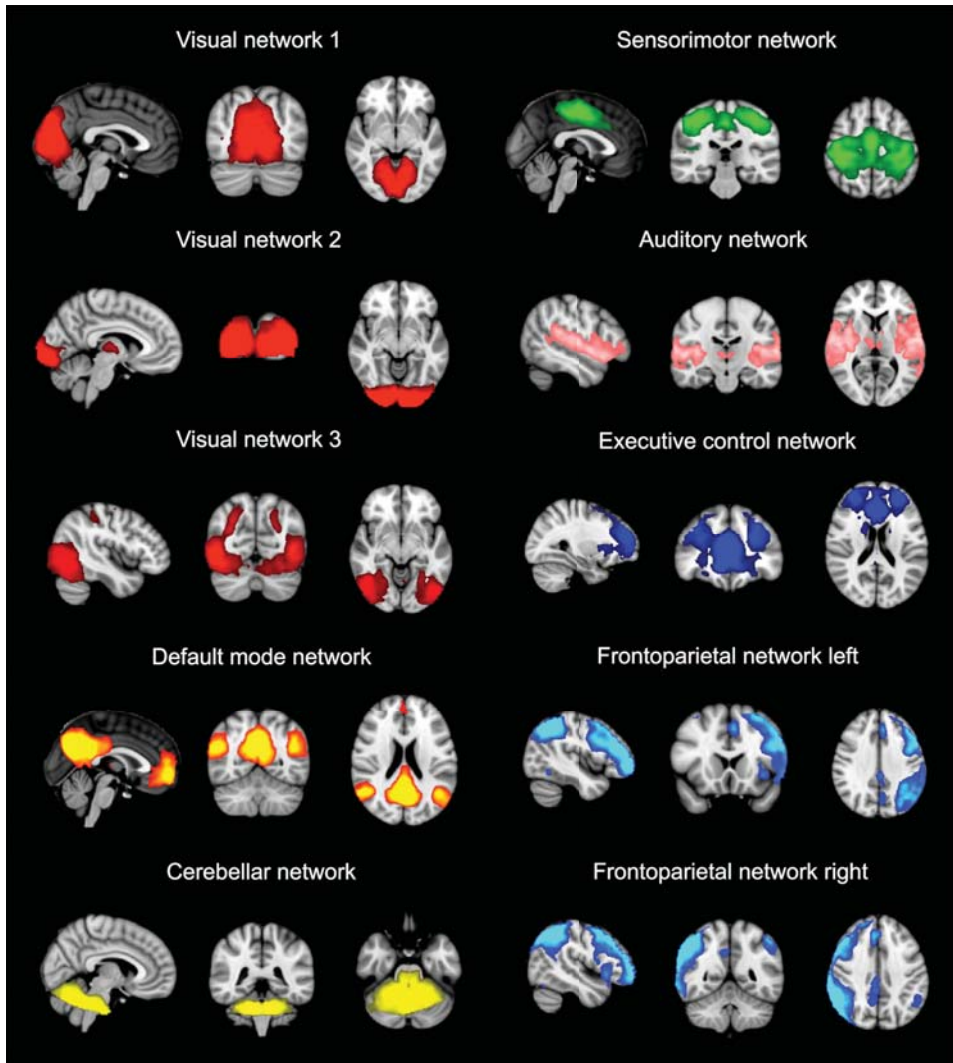


Figure 2.2. Ten functional resting state networks as identified by Smith et al. [10] in 36 healthy adults. To investigate sertraline effects, subject-wise spatial maps of these 10 networks were estimated using dual regression and entered in a mixed effects model for within-group comparisons ($p < 0.005$, corrected).

change of a specific network. The higher the value of the coefficient, the stronger the connectivity of this voxel with a given network. These individual statistical maps were subsequently used for higher level analysis.

Within-group comparisons for the contrast sertraline relative to placebo of voxelwise functional connectivity with each of the 10 functional networks were examined with a mixed effects general

linear model as used in our previous studies [76, 78, 80]. Average heart rate (beats/m) and respiration frequency (Hz) per RS-fMRI scan were added to the model as confound regressors, indicated as the most robust method to account for physiological variations [127]. In this model, treatment and time are used as fixed within-subject factors and subject as a random factor. More specifically, the treatment effect of sertraline vs. placebo was tested, with the subjects' means, and variance across time (each time point post dosing vs. baseline) modeled as covariates of no interest. Nonparametric permutation testing was used to estimate (with 5000 repeated permutations) for each network whether connectivity was significantly different on sertraline relative to placebo days. The resulting voxelwise probability map was corrected for the familywise error using threshold-free cluster enhancement and by Bonferroni correction for the 10 separately investigated networks (by examining the results at $p < 0.005$) [128, 129].

RESULTS

Pharmacokinetics

The T_{max} of serum sertraline varied between 2.90 and 6.92 h (mean T_{max} : 3.93 ± 1.34) and between 2.90 and 6.92 h (mean T_{max} : 4.01 ± 1.44) for desmethylsertraline. C_{max} for sertraline was between 14.40 and 52.80 ng/mL (mean C_{max} : 31.06 ± 11.84) and for desmethylsertraline between 4.50 and 17.10 ng/mL (mean C_{max} : 10.08 ± 3.84). AUC_{0-last} was between 78.17 and 305.60 ng*h/mL (mean AUC_{0-last} : 173.90 ± 69.62) for sertraline and between 5.16 and 98.30 ng*h/mL (mean AUC_{0-last} : 50.75 ± 27.65) for desmethylsertraline (see Figure 2.3 for individual and median sertraline PK time profiles).

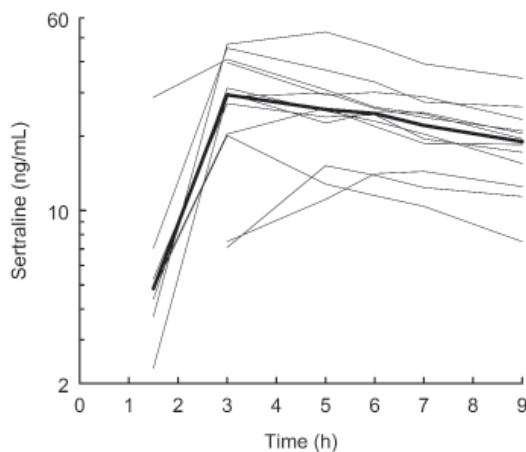


Figure 2.3. Median (bold line) and individual (thin lines) pharmacokinetic profiles for sertraline concentrations in nanograms per milliliter on semi-log scale. Observations below limit of quantification were dismissed.

Cortisol and prolactin

There was a significant treatment effect on concentrations of cortisol (with $F = (1, 10) 17.87, p < 0.01$). As shown in Figure 2.4, cortisol concentrations were increased after sertraline, relative to placebo. There was no significant treatment effect for prolactin concentrations.

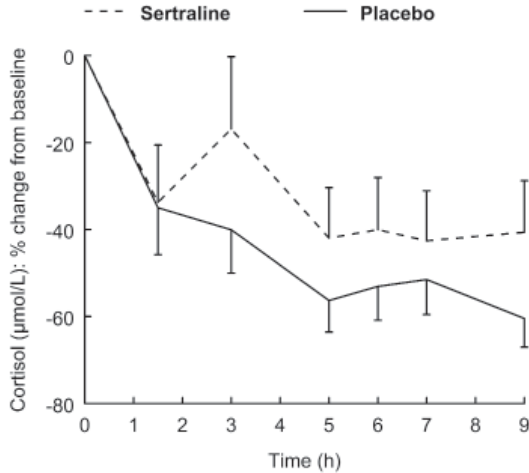


Figure 2.4. Least squares means percent change from baseline profiles of cortisol concentrations (with standard errors of the mean as error bars).

NeuroCart® test battery

There were no significant treatment effects on measures of cognitive performance. Non-significant trends were found for the VAS Calmness (with $F = (1, 8) 5.11, p = 0.054$: sertraline < placebo), the VAS Mood (with $F = (1, 8) 4.12, p = 0.076$: sertraline < placebo) and the VAS Nausea (with $F = (1, 10) 3.84, p = 0.078$: sertraline > placebo).

Imaging

Functional connectivity changes caused by sertraline were observed in relation to seven functional networks (see Figure 2.5 for statistical maps of the results; $p < 0.005$, corrected). The colors in Figure 2.5 match the colors of Figure 2.2 with regard to the defined networks. In Figure 2.2, the network that was investigated is shown, whereas in Figure 2.5, we show the regions in the brain that have altered connectivity with this network. Specifications of effects (cluster size and peak t -value of the clusters) are provided in Table 2.1. Compared to placebo, connections with the following networks were altered after administering sertraline:

Default mode network

Functional connectivity of the anterior cingulate cortex (ACC), posterior cingulate cortex (PCC), medial prefrontal cortex and precuneus (orange in Figure 2.5a) with the DMN (orange in Figure 2.2) was decreased after sertraline compared to placebo.

Executive control network

Functional connectivity of the limbic system (including the ACC, PCC, thalamus, amygdala and hippocampus), precuneus, midbrain and medial prefrontal cortex (blue in Figure 2.5b) with the executive control network (blue in Figure 2.2) was decreased after sertraline compared to placebo.

Visual networks

Functional connectivity of the occipital cortex, ACC, PCC, precuneus, medial prefrontal cortex and small parts of the cerebellum (red in Figure 2.5c) with the three visual networks (red in Figure 2.2) was decreased after sertraline compared to placebo.

Sensorimotor network

Functional connectivity of the ACC, PCC, precuneus, central gyri and supplementary motor cortex (green in Figure 2.5d) with the sensorimotor network (green in Figure 2.2) was decreased after sertraline compared to placebo.

Auditory network

Functional connectivity was increased between the precuneus and PCC (pink in Figure 2.5e) and the auditory network (pink in Figure 2.2) after sertraline compared to placebo.

Common regions

For each of these networks, treatment effects were found in two common areas: the precuneus and PCC. In Figure 2.6 these effects are shown for each network in their corresponding color with the precuneus and PCC depicted in pale brown. Regions of effect within the precuneus and PCC were chosen to visualize the time profiles of changes in connectivity in relation to the networks (Figure 2.6a-e).

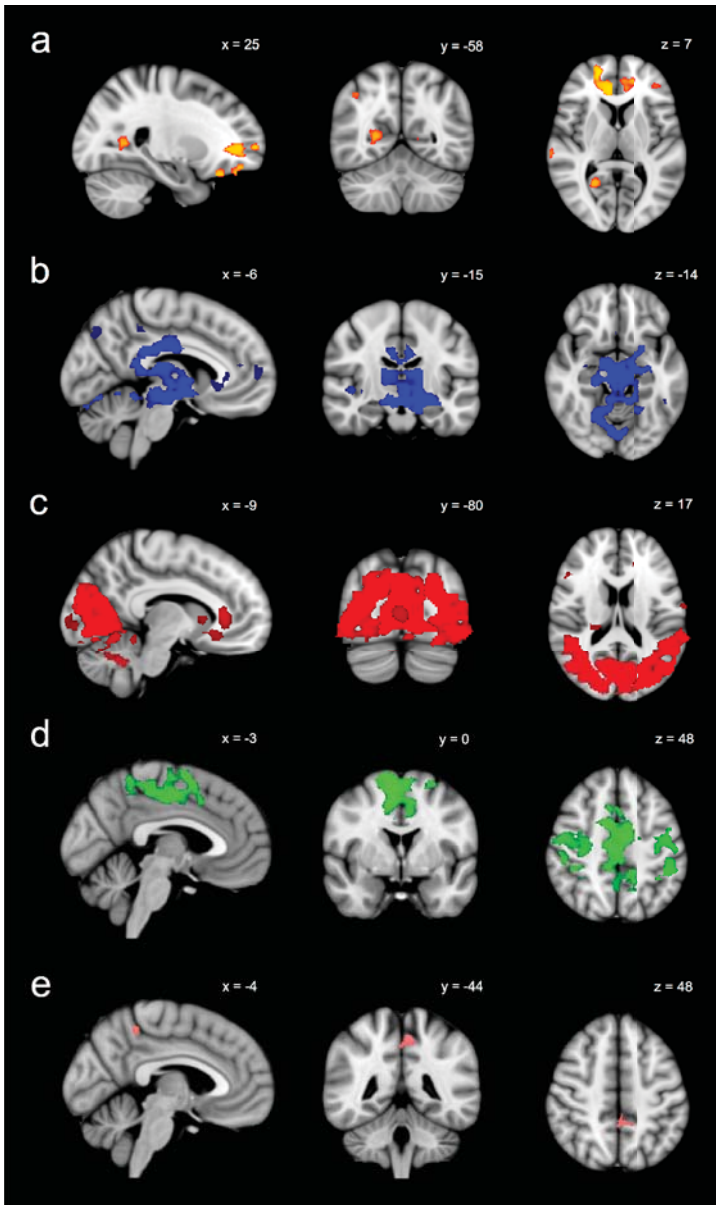


Figure 2.5. Spatial maps (with coordinates in mm) of sertraline-induced (a) decreases in functional connectivity between the ACC, PCC, precuneus and medial prefrontal cortex (orange) and the default mode network; (b) decreases in functional connectivity between the limbic system, precuneus, medial prefrontal cortex and midbrain (blue) and the executive control network; (c) decreases in functional connectivity between the occipital cortex, PCC, ACC, precuneus, medial prefrontal cortex and cerebellum (red) and the visual networks; (d) decreases in functional connectivity between the ACC, PCC, precuneus, central gyri and supplementary motor cortex (green) and the sensorimotor network; (e) increases in functional connectivity between the PCC and precuneus (pink) and the auditory network ($p < 0.005$, corrected). Coronal and axial slices are displayed in radiological convention (left = right).

Table 2.1. Overview of significant decreases and increases in functional connectivity as estimated with threshold-free cluster enhancement ($p < 0.005$, corrected)

Network	Region (Harvard-Oxford)	t*	x	y	z	Cluster size
Default mode network	B/M ACC, frontal pole (including frontal medial cortex, paracingulate gyrus)	5.28	16	42	-18	2703
	R inferior and middle frontal gyrus	5.33	46	26	32	1060
	R parahippocampal gyrus	4.74	-14	-10	-30	273
	L ACC, paracingulate gyrus	4.56	-12	46	4	193
	R PCC, precuneus cortex	5.31	24	-56	6	100
	R posterior superior temporal gyrus	4.89	66	-26	6	96
	R pre- and postcentral gyrus	3.96	36	-20	40	90
	R angular gyrus, posterior supramarginal gyrus	4.57	38	-50	34	83
	L frontal pole	4.86	-44	40	2	82
	B/M limbic system (including amygdala, hippocampus, thalamus), temporal pole, PCC, midbrain	6.24	52	12	-4	11381
Executive control network	L/M superior lateral occipital cortex, cuneal cortex, precuneus cortex	4.13	-18	-62	42	432
	M ACC, frontal medial cortex	4.4	-2	24	-2	295
	R PCC, precuneus cortex	4.77	16	-56	32	243
	L frontal pole (including frontal medial cortex, paracingulate gyrus)	4.65	-8	56	6	140
Visual network 1	B/M occipital cortex (including fusiform gyrus, lingual gyrus, intra- and supracalcarine cortex, cuneal cortex extending into precuneus cortex)	5.55	-18	-68	-4	6592
	B/M occipital cortex (including fusiform gyrus, lingual gyrus, calcarine cortex, cuneal cortex)	5.46	-2	-86	-12	1463
Visual network 2	B lateral occipital, frontal, temporal and parietal cortex, cerebellum, PCC, precuneus cortex, pre- and postcentral gyrus	5.78	20	-80	26	28546
	B ACC, paracingulate gyrus, subcallosal cortex, frontal medial cortex	5.05	34	42	-2	3757
Visual network 3	R ACC, PCC, precentral gyrus, (middle and superior) frontal gyrus	4.59	12	-10	38	331
	L precentral gyrus, (middle and superior) frontal gyrus	4.96	-30	2	46	111
Sensorimotor network	B/M ACC, PCC, precuneus cortex, supplementary motor area, pre- and postcentral gyrus	7.26	8	2	60	9262
	L ACC, paracingulate gyrus	4.2	-8	26	26	112
Auditory network	B PCC, precuneus cortex, pre- and postcentral gyrus	4.48	-6	-44	52	125

Abbreviations: L = left, R = right; B = bilateral, M = midline, ACC = anterior cingulate cortex, PCC = posterior cingulate cortex. Voxel dimension = 2 mm x 2 mm x 2 mm (voxel volume 0.008 mL). * = uncorrected peak t -value within cluster.

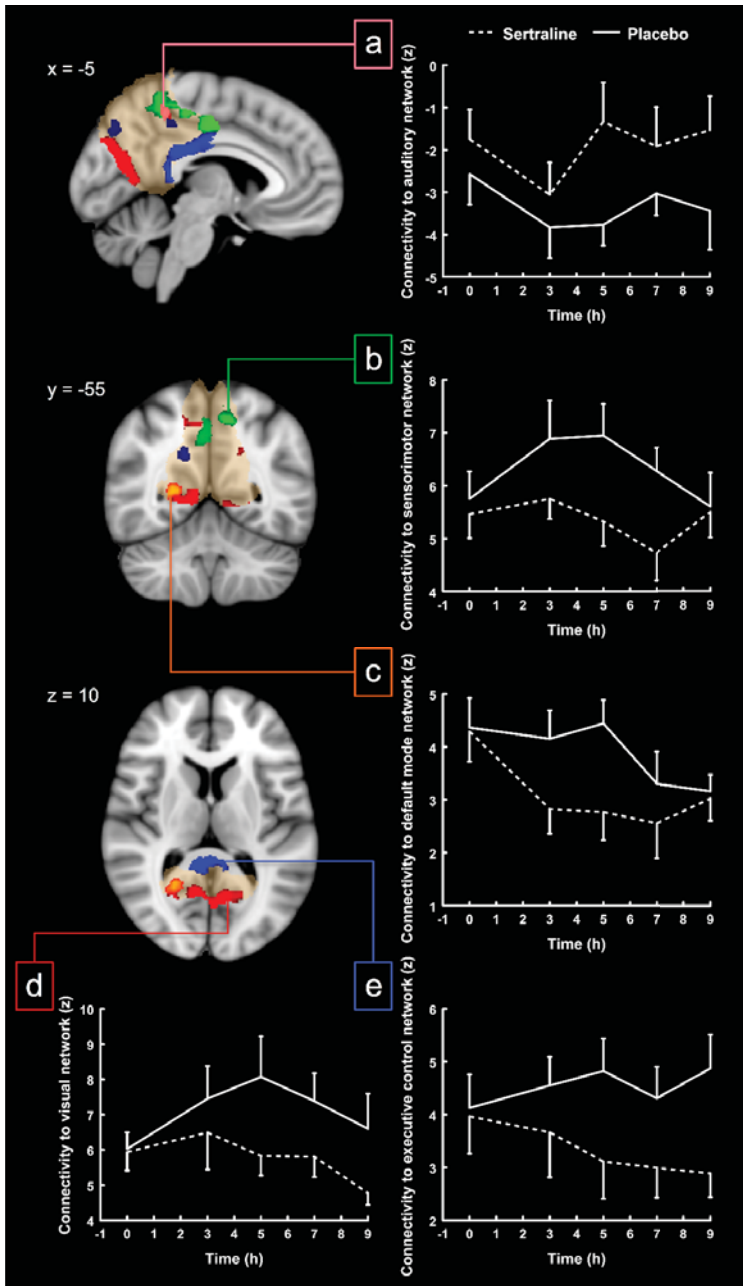


Figure 2.6. Alterations in functional connectivity after sertraline administration within the precuneus and PCC (shown in pale purple) for the different networks. Plots visualize the corresponding average time profiles of changes in functional connectivity for sertraline (dotted line) and placebo (continuous line) conditions for (a) the auditory network; (b) the sensorimotor network; (c) the default mode network; (d) the medial visual network; (e) the executive control network (z-values with standard errors of the mean as error bars). Coronal and axial slices are displayed in radiological convention (left = right).

DISCUSSION

Sertraline induced widespread alterations in functional connectivity with multiple resting state networks in the brain. In line with Schaefer et al. [83] these alterations were primarily decreases in connectivity. Effects in the DMN, executive control network and limbic-frontal circuitry are mostly in agreement with earlier RS-fMRI studies on SSRI effects [82, 84-87]. New findings were a lowering of connectivity within visual networks and alterations in functional connectivity of the sensorimotor and auditory network with the cingulate cortex and precuneus. The PK time profile was consistent with our repeated measures, taken at appropriate time points when the largest effects could be expected. Post hoc investigation of connectivity changes over time suggests that sertraline might sometimes suppress regular diurnal fluctuations, similar to the effect we found on cortisol. Consistent with other literature, cortisol concentrations were slightly higher after SSRI administration [104, 105], as opposed to a gradual decrease during placebo days. The paucity of effects on cognitive performance implies that RS-fMRI is highly sensitive and appropriate as a measure of a serotonergic challenge when compared to neuropsychological testing.

Default mode and executive control network

Connectivity within the DMN (precuneus, ACC, PCC and medial prefrontal cortex) was decreased after exposure to sertraline. Furthermore, administration of sertraline led to decreased connectivity between the executive control network and the limbic system (including cingulate cortex, amygdala, hippocampus and thalamus), medial prefrontal cortex and the midbrain. The midbrain's median and dorsal raphe nuclei are the major source of serotonin release to the cerebral cortex, especially to the forebrain [47, 109] and are therefore considered to play an important role in SSRI enhancement [130, 131]. The desirable effects of SSRIs on mood are hypothesized to be mainly due to improved functionality and regulation of 5-HT_{1A} (concentrated in the limbic system, especially the hippocampus, cortical areas as the cingulate and raphe nuclei) and 5-HT_{2A/C} (represented in the limbic system, cortex, basal ganglia and choroid plexus) receptors [47, 49, 52, 110, 132]. Inhibitory 5-HT_{1A} receptors have a higher affinity for 5-HT than excitatory 5-HT₂ receptors [133]. Consequently, the net result of elevation of serotonin is a reduction of serotonergic activity at low concentrations, followed by stimulation at higher levels. Furthermore, after acute SSRI administration, serotonin reuptake inhibition is attenuated by activation of 5-HT_{1A} autoreceptors in the raphe nuclei, causing inhibition of cell firing [134]. The relatively limited pharmacological effect of a single 75 mg dose of sertraline could explain the decrease in functional connectivity that we found in many parts of the brain. However, compared to our healthy subjects, it is likely that the sensitivity of 5-HT receptors differs in depressed patients and changes with prolonged antidepressant treatment [135]. The effects on both networks point to alterations in limbic and frontal brain areas. Together, these regions have been regarded as related to emotional

functioning and processing [136], with deficits in the fronto-limbic circuitry shown in depressed patients [137-139]. Administering SSRIs might correct dysfunction of the fronto-limbic pathways as seen in depression [140], thereby influencing emotional and motivational information processing and integration. Interestingly, we found changes in connectivity with the precuneus and PCC for all five networks, both part of the DMN and mentioned as playing a central role in self-consciousness and self-reference [141]. The majority of previous RS-fMRI studies point to increased connectivity in depression, particularly of cortical midline structures as the precuneus, ACC and PCC with prefrontal areas [88]. The deviant pattern of the overactivated DMN, supporting internal mentation and integration of experiences, might refer to rumination; heightened self-awareness and -preoccupation during rest [142-144]. The effects that we observed include the sub- and perigenual ACC which are particularly associated with rumination [142]. The posterior parts of the DMN have been proposed as specific regions where normalization of abnormal activity and functional connectivity takes place after SSRI treatment [84, 145, 146].

Visual, auditory and sensorimotor networks

In the cortex, the frontal lobe contains the highest density of 5-HT terminals, but the midbrain's raphe nuclei project to all other cortical areas as well. High cortical concentrations of serotonin have been found in the primary visual, auditory and somatosensory cortices of primates [147-150]. The relative predominance of high affinity 5-HT_{1A} vs. low affinity 5-HT₂ receptors has been demonstrated in the prefrontal cortex [132, 151] but also in the visual and motor cortex of rhesus monkeys [152]. Again, this might explain the observed decrease in functional connectivity of the visual and sensorimotor networks after administering sertraline. Evidence for functional involvement of serotonin in the human visual system comes from observations in users of ecstasy (or 3,4-methylenedioxy-N-methylamphetamine; MDMA). MDMA induces an acute release and reuptake inhibition of serotonin, followed by serotonin depletion in the visual cortex, which is associated with changes in visual orientation processing [153]. Moreover, the 5-HT neuronal activity pattern seems to correspond to and facilitate tonic motor output in animals [154]. We found decreased connectivity of the sensorimotor network with the central gyri (the sensorimotor region) and the supplementary motor area. Improvement of motor behavior after giving SSRIs has been shown with task-related fMRI studies, accompanied by enhancement of brain motor activity in the sensorimotor cortex and supplementary motor area [155, 156]. Connectivity of the sensorimotor network and visual networks with the precuneus and (para)cingulate cortex was decreased in our study. The cingulate motor areas operate in concert with the limbic system for spatial orientation and executing voluntary movement [157, 158]. The precuneus has been identified as a major association area guiding visuo-spatial imagery, execution and preparation of complex motor behavior and attentive tracking [159, 160]. Connectivity of the precuneus and cingulate cortex with the auditory network was altered as well, although this time it concerned an increase instead of a decrease in connectivity. This corresponds to reverse

findings in depression of Sundermann et al. [88], who observed hypoconnectivity in areas that belong to the auditory network (left temporal cortex, insula). SSRIs have been used for treatment of tinnitus, the perception of a phantom sound [161]. fMRI studies on resting state connectivity in tinnitus patients illustrate the interplay between tinnitus and the auditory network, the DMN and limbic areas [162-166]. For example, the connectivity pattern of the precuneus/PCC region was discovered as positively correlating with emotional distress as measured with the tinnitus handicap inventory [165].

NeuroCart® test battery

Compared to placebo, sertraline did not result in any significant treatment effects on neurocognitive tasks of the NeuroCart® battery. There was a trend towards increasing nausea, decreasing calmness and decreasing mood on the VAS. The small size of our sample might be an explanation for the absence of behavioral effects. However, we did detect significant and large-scale effects on resting state connectivity, indicating the suitability of this method as a marker of efficacy compared to cognitive measures. These results suggest that RS-fMRI could be a useful technique in early CNS drug development, which generally requires the use of sensitive methods in relatively small study groups. Performance tasks are known to show limited and inconsistent effects after single acute dosing of an SSRI in healthy subjects [167], although we did not include tests that are potentially more sensitive to SSRIs as EEG recordings, REM-sleep and flicker discrimination tests [167, 168]. In task-related fMRI paradigms it was shown that acute neural changes take place in the limbic system and prefrontal circuitry [169-172]. Despite the instant neural changes after administration of an SSRI, improvements in mood and cognition usually begin only after a few weeks [173, 174]. One explanation for this apparent discrepancy is the acute effect of SSRIs on emotional bias [175-178], which could increase positive information processing, thereby slowly contributing to resolution of the depression [179]. Since the Face Encoding and Recognition task involves eliciting emotions, it was expected that an SSRI would exert the strongest acute effect on this task. Contrary to previous literature, we did not find such an effect in this study.

Limitations

Sertraline can be considered as one of the most selective SSRIs. Nevertheless, it still modulates catecholaminergic neurotransmission to some extent and noradrenergic and dopaminergic influences on functional connectivity cannot be ruled out. Sertraline is especially known for a low relative selectivity for 5-HT over dopamine [180]. The most common side effect during sertraline study days was nausea, which was reported by 50% of the subjects and lasted between 1.5 and 5 h, although this was never severe enough to lead to vomiting. This coincides with a non-significant trend towards experienced nausea on the VAS. Granisetron was added to prevent

nausea and vomiting [181], which as a side effect of sertraline could have altered the network responses or reduced the tolerability of the procedures [182]. To balance the study, granisetron was also administered on placebo days. However, granisetron, being a very selective 5-HT₃ receptor antagonist, might have affected some central serotonergic effects of sertraline that are specifically related to 5-HT₃ functions [109]. Cortisol influences functional connectivity between the amygdala and medial prefrontal cortex, which might have confounded the results as well [183]. It is possible that the effects that were found in these areas are partially secondary to the small but significant increase in cortisol concentrations. Moreover, SSRIs potentially affect constriction of blood vessels [184] and as a consequence induce blood oxygen level dependent signal changes. This study cannot resolve the question whether observed fMRI effects reflect true neural changes or altered neurovascular coupling [185-187]. Yet, SSRIs do not typically influence the hemodynamic response [188] and in our study we did not find significant effects of sertraline on heart rate and respiration frequency, which would be considered the main source of causing vascular artifacts.

Conclusions and future perspectives

Using 10 different networks in a well-powered repeated measures design allowed us to confirm both earlier established hypotheses and to discover new, uninvestigated effects of SSRIs on resting state connectivity. The results verify that serotonergic tracts cover a substantial part of the brain and suggest that serotonin is implicated in processing emotional information, conscious coordination of motor behavior and higher-level perception of the environment, possibly with a central role for the precuneus and cingulate. Many network effects of sertraline showed a striking overlap with opposing connectivity changes that are reported in depression [88]. Confirmation of these outcomes will strengthen the confidence in this technique as a highly sensitive and specific method of drug investigation, which in the future may also be used to characterize new drugs under development.

Acknowledgements

This project was funded by the Netherlands Initiative Brain and Cognition (NIHC), a part of the Netherlands Organization for Scientific Research (NWO) (grant number 056-13-016), and Pfizer Inc. Erica Klaassen (CHDR), Jules Heuberger (CHDR) and Pieter Buur (LUMC) are acknowledged for their contribution to statistical analyses.

Chapter 3

Time related effects on functional brain connectivity after serotonergic and cholinergic neuromodulation

Published in Human Brain Mapping 2017; 38(1):308-325

Bernadet L. Klaassens^{a,b,c,d}, Serge A.R.B. Rombouts^{a,b,c}, Anderson M. Winkler^e, Helene C. van Gorsel^{b,c,d}, Jeroen van der Grond^b, Joop M.A. van Gerven^d

^aLeiden University, Institute of Psychology, Leiden, the Netherlands, ^bLeiden University Medical Center, Department of Radiology, Leiden, the Netherlands, ^cLeiden University, Leiden Institute for Brain and Cognition, Leiden, the Netherlands, ^dCentre for Human Drug Research, Leiden, the Netherlands, ^eOxford University, Oxford Centre for Functional MRI of the Brain, Oxford, United Kingdom

ABSTRACT

Psychopharmacological research, if properly designed, may offer insight into both timing and area of effect, increasing our understanding of the brain's neurotransmitter systems. For that purpose, the acute influence of the selective serotonin reuptake inhibitor citalopram (30 mg) and the acetylcholinesterase inhibitor galantamine (8 mg) was repeatedly measured in 12 healthy young volunteers with resting state functional magnetic resonance imaging (RS-fMRI). Eighteen RS-fMRI scans were acquired per subject during this randomized, double blind, placebo-controlled, crossover study. Within-group comparisons of voxelwise functional connectivity with 10 functional networks were examined ($p < 0.05$, FWE-corrected) using a non-parametric multivariate approach with cerebrospinal fluid, white matter, heart rate and baseline measurements as covariates. Although both compounds did not change cognitive performance on several tests, significant effects were found on connectivity with multiple resting state networks. Serotonergic stimulation primarily reduced connectivity with the sensorimotor network and structures that are related to self-referential mechanisms, whereas galantamine affected networks and regions that are more involved in learning, memory, and visual perception and processing. These results are consistent with the serotonergic and cholinergic trajectories and their functional relevance. In addition, this study demonstrates the power of using repeated measures after drug administration, which offers the chance to explore both combined and time specific effects.

INTRODUCTION

Drugs acting on serotonin (5-hydroxytryptamine; 5-HT) and acetylcholine (ACh) are known for their regulating influence on behavior and cognition. Selective serotonin reuptake inhibitors (SSRIs) are accepted for their mood altering properties and usually prescribed to treat depression and anxiety disorders [50, 109]. Acetylcholinesterase inhibitors (AChEIs) are found to be beneficial in neurodegenerative disorders (Alzheimer's disease (AD), dementia with Lewy bodies and Parkinson's disease) due to their effect on attention, learning and memory [63, 189].

The brain's serotonergic axonal pathways originate in the midbrain's medial and dorsal raphe nuclei. In the central nervous system (CNS), a particularly high density of 5-HT receptors is observed in the cerebral cortex, limbic structures, basal ganglia and brain stem regions [47, 190]. For ACh, the major source is the basal forebrain, with fibers diffusing to the cortex, amygdala and hippocampus [59]. The finding that specific neurotransmitters like 5-HT and ACh also act as neuromodulators, has led to the formation of distributed computational network models [191-193]. Consequently, studies of cholinergic or serotonergic drug effects also need to consider their extensive modulatory effects [194]. This is possible with resting state functional magnetic resonance imaging (RS-fMRI) in the context of pharmacological stimulation [7, 195].

Evidence is growing on the sensitivity of resting state networks, consisting of regions with coherent blood-oxygen-level-dependent fluctuations, to pharmacological challenges [76, 78-81]. These networks have consistently been found in healthy and clinical conditions, and are related to specific functions of the brain (i.e. motor, auditory, visual, emotional and executive function) [9, 10, 196, 197]. Disruptions of functional networks have been demonstrated in both depressed and demented patients, especially for the default mode network (DMN) [20, 88, 198]. Several studies point to normalization of DMN connectivity in depression after SSRI administration [82, 85-87]. Yet, there is also proof of more extensive effects of SSRIs on brain connectivity [83, 199]. In AD patients, cholinergic stimulation induces alterations in connectivity for DMN regions [89-91], as well as networks involved in attention, control and salience processing [200].

Characteristically, neuromodulators support the processing of sensory information, coordination of motor output and higher order cognitive functioning [201-203]. In line with the diverse and widespread patterns of effect of both transmitters we investigated the direct influence of the SSRI citalopram 30 mg and the AChEI galantamine 8 mg on various brain networks. Both RS-fMRI and functional (cognitive and neuroendocrine) responses were examined in 12 healthy young volunteers in a repeated measures fashion. Galantamine was hypothesized to mainly affect connectivity with brain structures that are involved in learning and memory mechanisms. Based on our previous study with the SSRI sertraline 75 mg, we expected to see widespread decreases in connectivity immediately after citalopram administration in the absence of cognitive change.

METHOD

Subjects

Twelve healthy young volunteers (mean age 22.1 ± 2.7 , range 18-27; gender ratio 1:1, BMI 21-28 kg/m²) were recruited to participate in the study. All subjects underwent a thorough medical screening at the Centre for Human Drug Research (CHDR) to investigate whether they met the inclusion and exclusion criteria. They had a normal history of physical and mental health and were able to refrain from using nicotine and caffeine during study days. Exclusion criteria included positive drug or alcohol screen on study days, regular excessive consumption of alcohol (>4 units/day), caffeine (>6 units/day) or cigarettes (>5 cigarettes/day), use of concomitant medication 2 weeks prior to study participation and involvement in an investigational drug trial 3 months prior to administration. The study was approved by the medical ethics committee of the Leiden University Medical Center (LUMC) and the scientific review board of the CHDR. Written informed consent was obtained from each subject prior to study participation.

Study design

This was a single center, double blind, placebo-controlled, crossover study with citalopram 30 mg and galantamine 8 mg. Each subject received citalopram, galantamine and placebo on three different occasions with a washout period in between of at least 7 days. Citalopram has an average time point of maximum concentration (T_{max}) of 2-4 h, with a half-life ($T_{1/2}$) of 36 h. For galantamine, $T_{max} = 1-2$ h and $T_{1/2} = 7-8$ h. To correct for the different pharmacokinetic (PK) profiles of the compounds, citalopram 20 mg was administered at $T = 0$ h, followed by a second dose of 10 mg at $T = 1$ h (if the first dose was tolerated and subjects did not become too nauseous). Galantamine was given as a single 8 mg dose at $T = 2$ h. Blinding was maintained by concomitant administration of double-dummy placebo's at all three time points. All subjects also received an unblinded dose of granisetron 2 mg at $T = -0.5$ h, to prevent the most common drug-induced adverse effects of nausea and vomiting.

Six RS-fMRI scans were acquired during study days, two at baseline and four after administering citalopram, galantamine or placebo (at $T = 2.5, 3.5, 4.5$ and 6 h post dosing). Each scan was followed by performance of computerized cognitive tasks (taken twice at baseline) on the NeuroCart® test battery, developed by the CHDR for quantifying pharmacological effects on the CNS [167, 204, 205]. By including multiple measurements during the T_{max} interval, this repeated measures profile increases the statistical power of the analysis and allows for identification of time related effects, associated with changing serum concentrations. Nine blood samples were taken during the course of the day to define the PK profile of citalopram, citalopram's active metabolite desmethylcitalopram, galantamine and concentrations of cortisol and prolactin [182, 206]. An overview of the study design is provided in Figure 3.1.

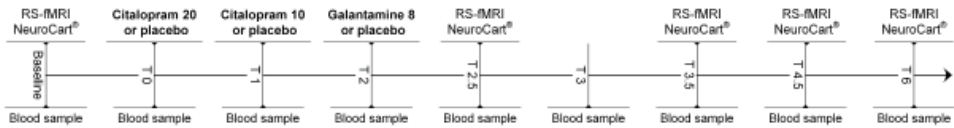


Figure 3.1. Schematic overview of a study day. Each subject received citalopram, galantamine and placebo on three different days. At baseline, two RS-fMRI scans were acquired, followed by the NeuroCart® CNS test battery. After drug administration, four more RS-fMRI scans were acquired at time points $T = 2.5, 3.5, 4.5$ and 6 h post dosing, each time followed by the NeuroCart® test battery. During the day, nine blood samples were taken to measure the concentrations of citalopram, desmethylcitalopram, galantamine, cortisol and prolactin. On each study day there were three moments of administration. The second administration only took place when subjects tolerated the first dose well (did not vomit or feel too nauseous):

Galantamine study day:	$T = 0$) placebo	$T = 1$) placebo	$T = 2$) galantamine 8 mg
Citalopram study day:	$T = 0$) citalopram 20 mg	$T = 1$) citalopram 10 mg	$T = 2$) placebo
Placebo study day:	$T = 0$) placebo	$T = 1$) placebo	$T = 2$) placebo

Blood sampling

Pharmacokinetics

Blood samples were collected in 4 mL EDTA plasma tubes at baseline and 1, 2, 2.5, 3, 3.5, 4.5 and 6 h post dosing, centrifuged (2000 g for 10 min) and stored at -40°C until analysis with liquid chromatography-tandem mass spectrometry (LC-MS/MS). PK parameters for citalopram, galantamine and citalopram's active metabolite desmethylcitalopram were calculated using a non-compartmental analysis. Maximum plasma concentrations (C_{max}) and time of C_{max} (T_{max}) were obtained directly from the plasma concentration data. The area under the plasma concentration vs. time curve was calculated from time zero to the time of the last quantifiable measured plasma concentration, which is equal to the last blood sample of the study day ($\text{AUC}_{0-\text{last}}$). The calculated PK parameters were not used for further analysis but investigated to validate the choice of time points of measurements.

Neuroendocrine variables

Blood samples were also obtained to determine cortisol and prolactin concentrations. Serum samples were taken in a 3.5 mL gel tube at baseline (twice) and 1, 2, 2.5, 3.5, 4.5 and 6 h post dosing, centrifuged (2000 g for 10 min) and stored at -40°C until analysis. Serum concentrations were quantitatively determined with electrochemiluminescence immunoassay. Cortisol and prolactin concentrations were subsequently used for statistical analysis using a mixed effects model with treatment, time, visit and treatment by time as fixed effects, subject, subject by treatment and subject by time as random effects and the average of the period baseline (pre-dose) values as covariate (SAS for Windows V9.4; SAS Institute, Inc., Cary, NC).

NeuroCart® test battery

Each RS-fMRI scan was followed by functional CNS measures outside the scanner using the computerized NeuroCart® test battery measuring alertness, mood and calmness (Visual Analogue Scales (VAS) Bond & Lader), nausea (VAS Nausea), vigilance and visual motor performance (Adaptive Tracking task), reaction time (Simple Reaction Time task), attention, short-term memory, psychomotor speed, task switching and inhibition (Symbol Digit Substitution Test and Stroop task), working memory (N-back task) and memory imprinting and retrieval (Visual Verbal Learning Test) [95-103]. The Visual Verbal Learning Test was only performed once during each day (at 3 and 4 h post dosing) as the test itself consists of different trials (imprinting and retrieval). Duration of each series of NeuroCart® brain function tests was approximately 20 min. To minimize learning effects, training for the NeuroCart® tasks occurred during the screening visit within 3 weeks prior to the first study day.

Analysis

All within period repeatedly measured CNS endpoints were analyzed using a mixed effects model with treatment, time, visit and treatment by time as fixed effects, subject, subject by treatment and subject by time as random effects and the average of the period baseline (pre-dose) values as covariate (SAS for Windows V9.4; SAS Institute, Inc., Cary, NC). As data of the Simple Reaction Time task were not normally distributed, these data were log-transformed before analysis and back transformed after analysis. The data of the Visual Verbal Learning test were analyzed using a mixed effects model with treatment and visit as fixed effects and subject as random effect. Treatment effects were considered significant at $p < 0.05$ (uncorrected).

Imaging

Scanning was performed at the LUMC on a Philips 3.0 Tesla Achieva MRI scanner (Philips Medical System, Best, The Netherlands) using a 32-channel head coil. During the RS-fMRI scans, all subjects were asked to close their eyes while staying awake. They were also instructed not to move their head during the scan. Instructions were given prior to each scan on all study days. T1-weighted anatomical images were acquired once per visit. To facilitate registration to the anatomical image, each RS-fMRI scan was followed by a high-resolution T2*-weighted echo-planar scan. Duration was approximately 8 min for the RS-fMRI scan, 5 min for the anatomical scan and 30 s for the high-resolution scan. Heart rate signals were recorded during each scan.

RS-fMRI data were obtained with T2*-weighted echo-planar imaging (EPI) with the following scan parameters: 220 whole brain volumes, repetition time (TR) = 2180 ms; echo time (TE) = 30 ms; flip angle = 85°; field-of-view (FOV) = 220 x 220 x 130 mm; in-plane voxel resolution = 3.44 x 3.44 mm, slice thickness = 3.44 mm, including 10% interslice gap. The next parameters were used to collect T1-weighted anatomical images: TR = 9.7 ms; TE = 4.6 ms; flip angle = 8°; FOV = 224 x 177

x 168 mm; in-plane voxel resolution = 1.17 x 1.17 mm; slice thickness = 1.2 mm. Parameters of high-resolution T2*-weighted EPI scans were set to: TR = 2200 ms; TE = 30 ms; flip angle = 80°; FOV = 220 x 220 x 168 mm; in-plane voxel resolution = 1.96 x 1.96 mm; slice thickness = 2.0 mm.

Analysis

All analyses were performed using the Functional Magnetic Resonance Imaging of the Brain (FMRIB) Software Library (FSL, Oxford, United Kingdom) version 5.0.7 [119-121]. Each individual functional EPI image was inspected, brain-extracted and corrected for geometrical displacements due to head movement with linear (affine) image registration [122, 123]. Images were spatially smoothed with a 6 mm full-width half-maximum Gaussian kernel and co-registered with the brain extracted high resolution T2*-weighted EPI scans (with 6 degrees of freedom) and T1 weighted images (using the Boundary-Based-Registration method) [122, 124]. The T1-weighted scans were non-linearly registered to the MNI 152 standard space (the Montreal Neurological Institute, Montreal, QC, Canada) using FMRIB's Non-linear Image Registration Tool. Registration parameters were estimated on non-smoothed data to transform fMRI scans into standard space. Automatic Removal of Motion Artifacts based on Independent Component Analysis (ICA-AROMA vs0.3-beta) was used to detect and remove motion related artifacts. ICA decomposes the data into independent components that are either noise related or pertain to functional networks. ICA-AROMA attempts to identify noise components by investigating its temporal and spatial properties and removes these components from the data that are classified as motion related. Registration was thereafter applied on the denoised functional data with registration parameters as derived from non-smoothed data. As recommended, high pass temporal filtering (with a high pass filter of 150 s) was applied after denoising the fMRI data with ICA-AROMA [207, 208].

RS-fMRI networks were thereafter extracted from each individual denoised RS-fMRI dataset (12 subjects x 3 days x 6 scans = 216 datasets) applying a dual regression analysis [36, 125] based on 10 predefined standard network templates as used in our previous research [199]. Confound regressors of time series from white matter (measured from the center of the corpus callosum) and cerebrospinal fluid (measured from the center of lateral ventricles) were included in this analysis to account for non-neuronal signal fluctuations [126]. The 10 standard templates have previously been identified using a data-driven approach [10] and comprise the following networks: three visual networks (consisting of medial, occipital pole, and lateral visual areas), DMN (medial parietal (precuneus and posterior cingulate), bilateral inferior-lateral-parietal and ventromedial frontal cortex), cerebellar network, sensorimotor network (supplementary motor area, sensorimotor cortex and secondary somatosensory cortex), auditory network (superior temporal gyrus, Heschl's gyrus and posterior insular), executive control network (medial-frontal areas, including anterior cingulate and paracingulate) and two frontoparietal networks (frontoparietal areas left and right). With the dual regression method, spatial maps representing voxel-to-network connectivity were estimated for each dataset separately in two stages for use in

within-group comparisons. First, the weighted network maps were simultaneously used in a spatial regression into each dataset. This stage generated 12 time series per dataset that describe the average temporal course of signal fluctuations of the 10 networks plus 2 confound regressors (cerebrospinal fluid and white matter). Next, this combination of time series was entered in a temporal regression into the same dataset. This resulted in a spatial map per network per dataset with regression coefficients referring to the weight of each voxel being associated with the characteristic signal change of a specific network. The higher the value of the coefficient, the stronger the connectivity of this voxel with a given network. These individual statistical maps were subsequently used for higher level analysis.

To infer treatment effects of citalopram and galantamine vs. placebo across time as well as for each time point separately we used non-parametric combination (NPC) as provided by FSL's Permutation Analysis for Linear Models tool (PALM vs65-alpha) [209, 210]. NPC is a multivariate method that offers the possibility to combine data of separate, possibly non-independent tests, such as our multiple time points, and investigate the presence of joint effects across time points, in a test that has fewer assumptions and is more powerful than repeated-measurements analysis of variance (ANOVA) or multivariate analysis of variance (MANOVA). NPC testing was used in two phases to estimate for each network whether connectivity was significantly different on drug relative to placebo days. First, tests were performed for each time point using 5000 synchronized permutations. More specifically, to investigate changes in voxelwise functional connectivity with each of the 10 functional networks, four t-tests (drug vs. placebo) were performed for all post-dose time points ($T = 2.5, 3.5, 4.5$ and 6 h), with average heart rate (beats/m) per RS-fMRI scan as confound regressor [127]. The average of the two baseline RS-fMRI scans was used as covariate as well, by adding the coefficient spatial map as a voxel-dependent regressor in the model. Second, tests for the four time points were combined non-parametrically via NPC using Fisher's combining function [211] and the same set of synchronized permutations as mentioned above. Threshold-free cluster enhancement was applied to the tests at each time point and after the combination, and the resulting voxelwise statistical maps were corrected for the familywise error rate using the distribution of the maximum statistic [128, 129]. Voxels were considered significant at p -values < 0.05 , corrected.

RESULTS

Pharmacokinetics

The time to reach maximum plasma concentrations (T_{max}) was highly variable for both citalopram and galantamine (see Figure 3.2 for individual and median PK time profiles). Maximum plasma concentrations of citalopram were reached between 1.93 and 6 h after the first dose (mean T_{max} : 2.99 ± 1.18) and between 2.48 and 6.05 h (mean T_{max} : 4.92 ± 1.33) for desmethylcitalopram.

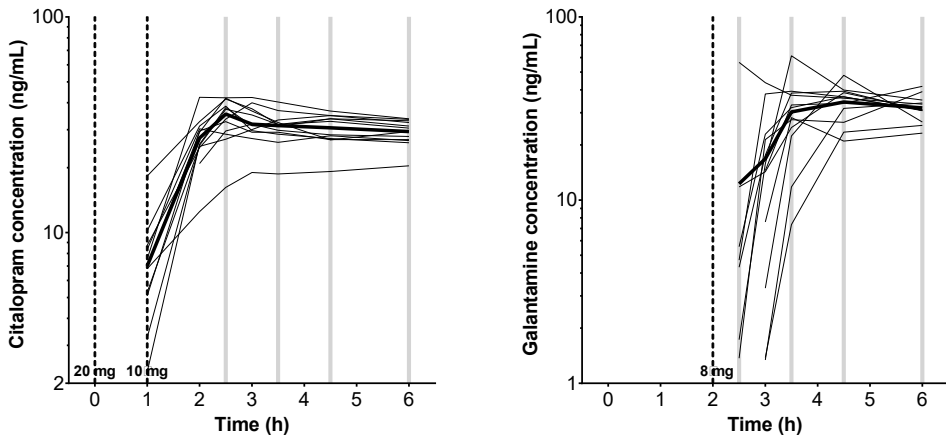


Figure 3.2. Median (bold line) and individual (thin lines) pharmacokinetic profiles for citalopram (left) and galantamine (right) concentrations in nanograms per milliliter on semi-log scale. Grey bars illustrate moments of RS-fMRI acquisition post drug administration. Observations below limit of quantification were dismissed.

C_{max} for citalopram was between 20.4 and 42.4 ng/mL (mean C_{max} : 35.8 ± 6.34) and between 1.45 and 4.7 ng/mL (mean C_{max} : 2.95 ± 1.07) for desmethylcitalopram. AUC_{0-last} was between 86.8 and 186 ng*h/mL (mean AUC_{0-last} : 146 ± 25.2) for citalopram and between 5.43 and 18.6 ng*h/mL (mean AUC_{0-last} : 11.7 ± 4.78) for desmethylcitalopram. Maximum plasma concentrations of galantamine were reached between 0.5 and 4 h (mean T_{max} : 2.67 ± 1.11). Consequently, maximum concentrations were reached between 2.5 and 6 h post zero point (mean T_{max} : 4.67 ± 1.11). C_{max} for galantamine was between 25.6 and 61.4 ng/mL (mean C_{max} : 40.7 ± 10.4). AUC_{0-last} was between 49.1 and 152 ng*h/mL (mean AUC_{0-last} : 95.1 ± 27.7).

Cortisol and prolactin

As shown in Figure 3.3a/b, concentrations of cortisol and prolactin increased after citalopram, relative to placebo ($p < 0.01$). There was no significant treatment effect of galantamine on either neuroendocrine hormone concentration.

NeuroCart® test battery

There were no significant treatment effects of citalopram and galantamine on measures of cognitive performance. Compared with placebo, galantamine increased the level of nausea as measured with the VAS Nausea ($p < 0.05$). Citalopram did not cause significant nausea (see Figure 3.3c). The effects of citalopram and galantamine on all cognitive and subjective NeuroCart® measures are summarized in Supplementary Table S3.1.

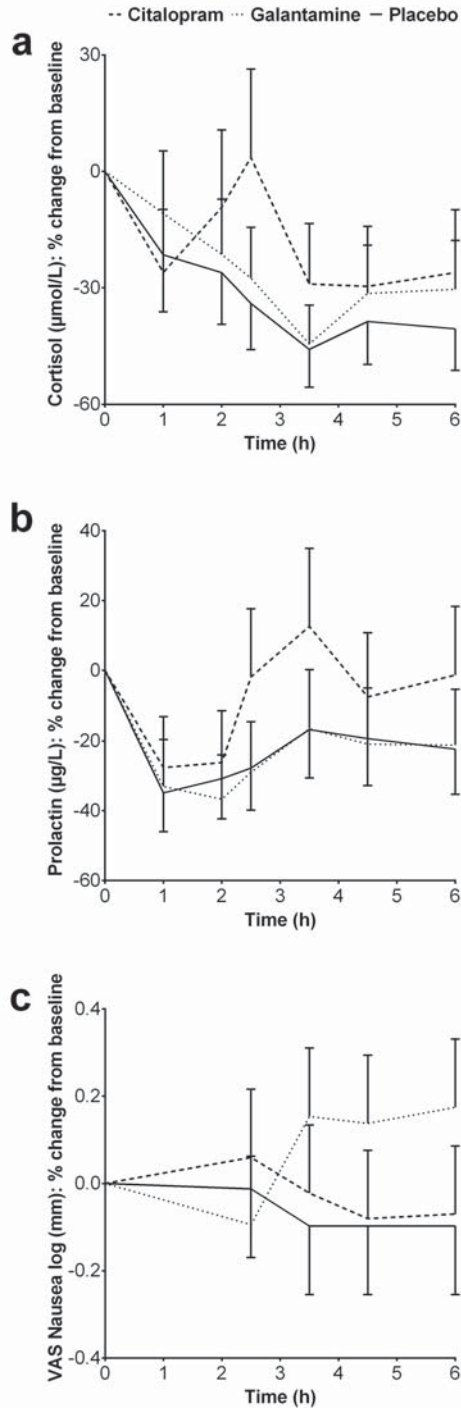


Figure 3.3. Least squares means percent change from baseline profiles of cortisol and prolactin concentrations and nausea as measured with the Visual Analogue Scales (with standard errors of the mean as error bars).

Imaging

Citalopram: combined test

Combining the data of all post-dose time points, there was a decrease in connectivity after administering citalopram compared with placebo (Figure 3.4a) between (1) the sensorimotor network and the pre- and postcentral gyri, supplementary motor area (SMA), precuneus, posterior and anterior cingulate cortex (PCC/ACC), medial prefrontal cortex and cerebellum, and (2) the right frontoparietal network and brain stem.

Citalopram: partial tests

Time specific effects of citalopram compared with placebo were explored by investigating changes in connectivity for each partial test (each time point post dosing) that contributed to the combined test (see Figure 3.4b).

At T = 2.5 h after citalopram administration there were no significant changes in connectivity.

At T = 3.5 h after citalopram administration there was a decrease in connectivity between the right frontoparietal network and the insula and Heschl's gyrus.

At T = 4.5 h after citalopram administration there was a decrease in connectivity between (1) the default mode network and the precuneus, PCC, ACC, cerebellum and left temporal lobe, (2) the sensorimotor network and the pre- and postcentral gyri, SMA, precuneus, PCC, ACC, medial prefrontal cortex, planum temporale and Heschl's gyrus, and (3) the right frontoparietal network and brain stem.

At T = 6 h after citalopram administration there was a decrease in connectivity between the executive control network and the middle and superior frontal gyrus.

Specifications of citalopram's combined and partial effects (sizes of significant regions and peak z-values) are provided in Table 3.1.

Galantamine: combined test

Combining the data of all post-dose time points, there was an increase in connectivity after administering galantamine compared with placebo (Figure 3.5a) between visual network 2 (occipital pole) and the left and right hippocampus, precuneus, thalamus, fusiform gyrus, precentral and superior frontal gyrus, PCC and cerebellum.

Galantamine: partial tests

Time specific effects of galantamine compared with placebo were explored by investigating changes in connectivity for each partial test (each time point post dosing) that contributed to the combined test (see Figure 3.5b).

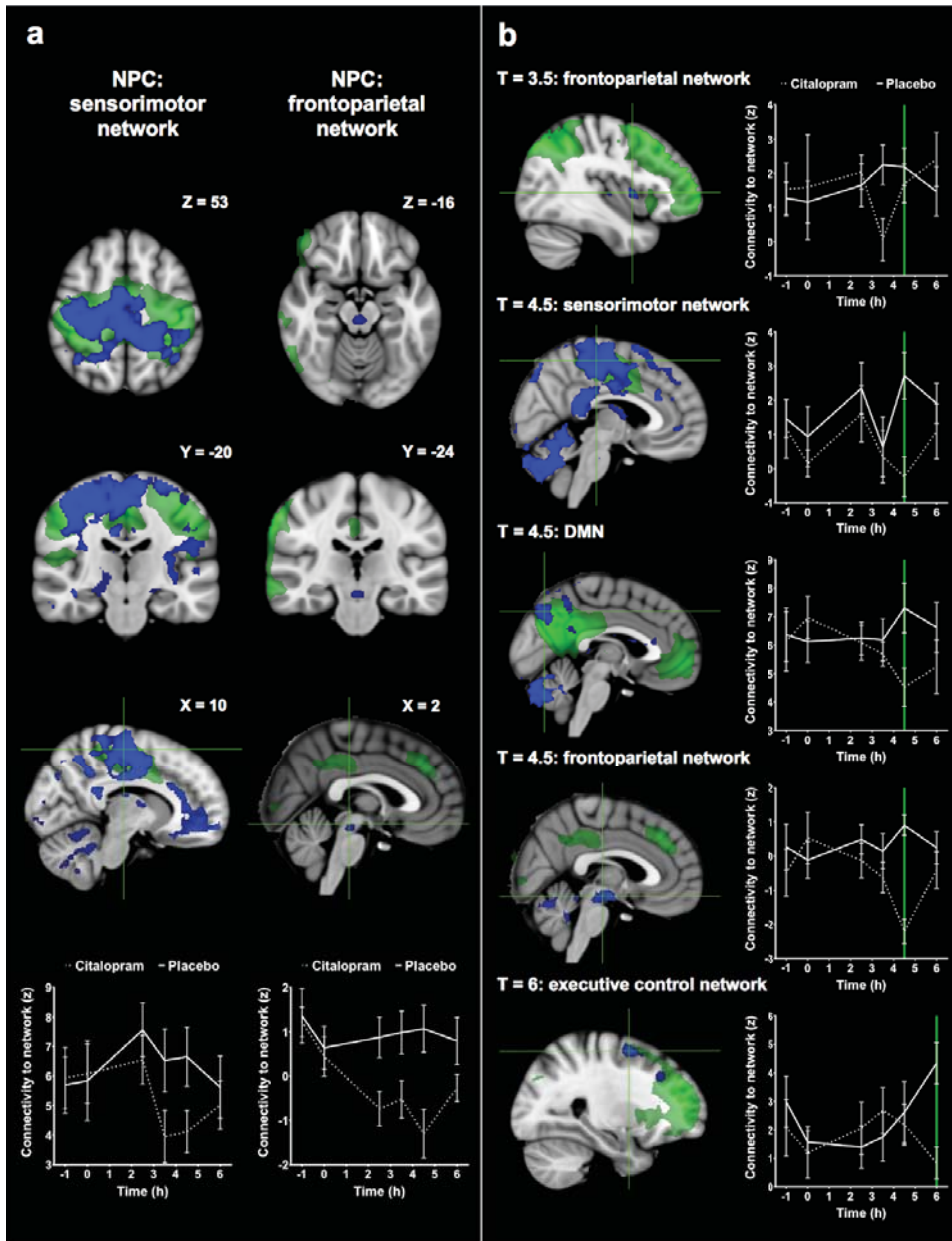


Figure 3.4. Statistical maps of citalopram induced decreases in functional connectivity. Networks are shown in green with decreases in connectivity with the network in blue (at $p < 0.05$, corrected). Figure (a) shows significant alterations in connectivity for all time points post dosing combined (with coordinates in mm). Figure (b) shows significant alterations in connectivity for each time point separately. Plots visualize the corresponding average time profiles of changes in functional connectivity for citalopram (dotted line) and placebo (continuous line) conditions (z-values with standard errors of the mean as error bars). Coronal and axial slices are displayed in radiological convention (left = right).

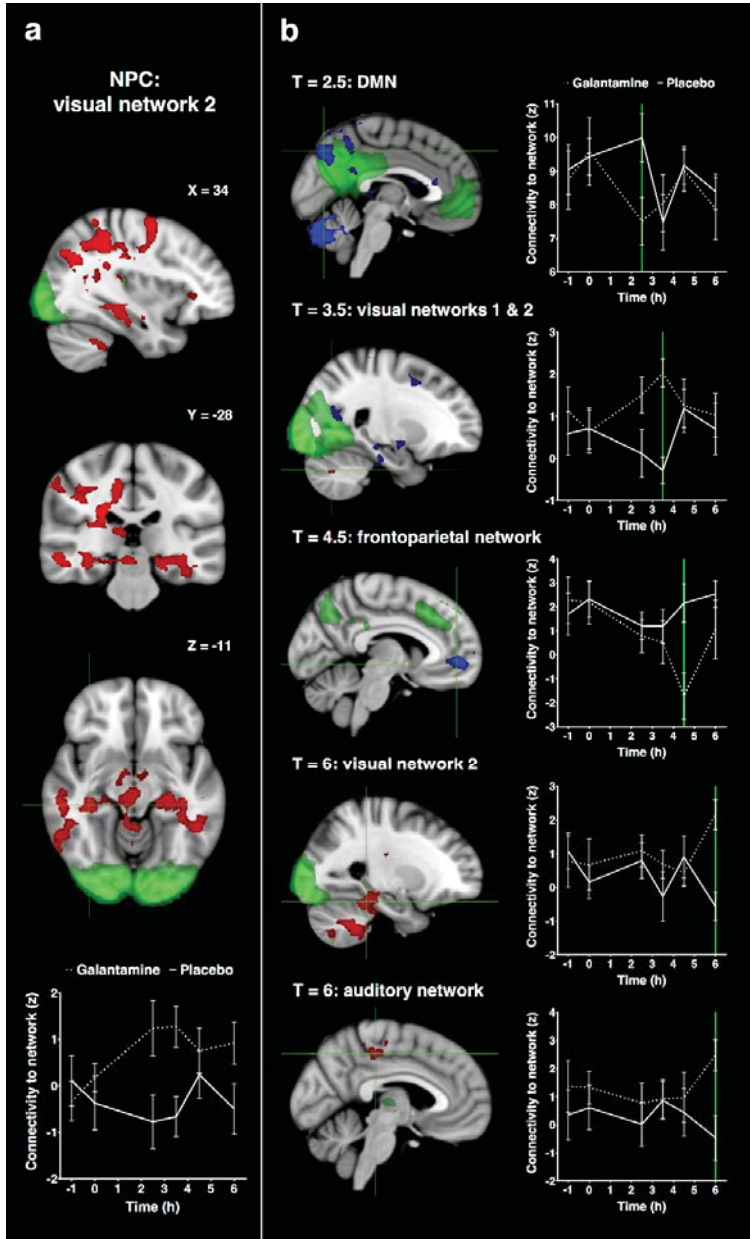


Figure 3.5. Statistical maps of galantamine induced increases and decreases in functional connectivity. Networks are shown in green with increases in connectivity with the network in red and decreases in connectivity in blue (at $p < 0.05$, corrected). Figure (a) shows significant alterations in connectivity for all time points post dosing combined (with coordinates in mm). Figure (b) shows significant alterations in connectivity for each time point separately. Plots visualize the corresponding average time profiles of changes in functional connectivity for galantamine (dotted line) and placebo (continuous line) conditions (z-values with standard errors of the mean as error bars). Coronal and axial slices are displayed in radiological convention (left = right).

Table 3.1. Overview of significant decreases in functional connectivity after citalopram as estimated with threshold-free cluster enhancement ($p < 0.05$, corrected)

Network	NPC/T	Region (Harvard-Oxford)	z^*	x	y	z	# voxels	
Sensorimotor network	NPC	L/R/M	ACC, PCC, precuneus, SMA, post- and precentral gyrus, medial and orbital frontal cortex	-22	50	-16	27308	
		L/R/M	Cerebellum	4.28	0	-72	-30	1696
	R	L/M	Lateral occipital cortex, inferior and superior division	4.20	-14	-92	20	585
		R/M	Cerebellum and temporal occipital fusiform cortex	3.92	36	-78	-22	530
	L	R/M	Occipital pole and lingual gyrus	3.28	8	-96	-6	92
Sensorimotor network	T = 4.5	L	Superior frontal gyrus	3.25	-18	32	28	91
		L/R/M	ACC, PCC, precuneus, SMA, brain stem, post- and precentral gyrus, orbital frontal cortex and cerebellum, lateral occipital cortex, inferior and superior division	5.03	-14	-92	20	46242
	L	Insular cortex, temporal and frontal opercular cortex	4.91	-38	16	-4	498	
	M	Thalamus	4.72	2	-12	18	212	
	M	Brain stem	4.42	2	-26	-16	55	
Frontoparietal network right	NPC	M	Brain stem	5.22	40	4	41	
		R	Insular and central opercular cortex	4.53	40	-16	4	11
Frontoparietal network right	T = 3.5	R	Insular cortex and Heschl's gyrus	4.43	8	-44	-18	1655
		L	Brain stem and cerebellum	3.72	-26	8	-14	45
Default mode network	T = 4.5	L	Frontal orbital cortex	3.78	-32	-44	28	34
		L	Parietal opercular cortex	5.14	-22	-78	-24	5374
	L/R	Cerebellum	4.56	-36	-58	28	2407	
	L/M	Precuneus, PCC, hippocampus, temporal and supramarginal gyrus	4.40	-28	-82	8	134	
	L	Lateral occipital cortex, inferior and superior division	4.63	42	16	20	302	
Executive control network	T = 6	R	Precentral gyrus, inferior and middle frontal gyrus	4.48	28	2	58	213
		R	Superior and middle frontal gyrus	3.91	56	-70	-4	187
	R	Lateral occipital cortex, inferior and superior division	4.07	54	-44	-24	37	
	R	Inferior temporal gyrus	5.21	36	-36	20	19	
	R	Parietal operculum cortex	4.18	42	0	32	15	

Abbreviations: L = left, R = right, M = midline, ACC = anterior cingulate cortex, PCC = posterior cingulate cortex, SMA = supplementary motor area. Voxel dimension = 2 mm x 2 mm x 2 mm (voxel volume 0.008 mL). * = standardized z-value of the uncorrected peak Fisher- (NPC) or t-statistic (partial tests) within regions.

At T = 2.5 h after galantamine administration there was a decrease in connectivity between the default mode network and precuneus, PCC and calcarine cortex.

At T = 3.5 h after galantamine administration there was (1) a decrease in connectivity between visual network 1 (medial visual areas) and the right hippocampus, PCC and ACC, and (2) an increase in connectivity between visual network 2 (occipital pole) and the cerebellum.

At T = 4.5 h after galantamine administration there was a decrease in connectivity between the left frontoparietal network and the medial prefrontal cortex, precuneus, PCC and ACC.

At T = 6 h after galantamine administration there was an increase in connectivity between (1) visual network 2 (occipital pole) and the hippocampus, brain stem, cerebellum and fusiform cortex, and (2) the auditory network and PCC, precuneus, and pre- and postcentral gyri.

Specifications of galantamine's combined and partial effects (sizes of significant regions and peak z-values) are provided in Table 3.2.

DISCUSSION

Single-dose SSRI and AChEI administration is usually not sufficient to alter cognitive and behavioral states in depression or dementia [167, 212-215]. Pharmacological research and development is therefore often restricted to clinical trials that last for weeks or even months. However, considering the acute elevations of synaptic neurotransmitters, it is expected that changes will already take place on a neural level, well before this results in improved performance and clinical outcome. In our study, both agents altered resting state functional connectivity within our time frame of measurements. The results of our study replicate the finding that SSRIs can have an immediate and widespread diminishing impact on interactions of the healthy neural system [83, 171, 199]. In conjunction with other SSRIs, citalopram had clear neuroendocrine effects [216], but did not induce cognitive or subjective changes as measured with the NeuroCart® battery. Network effects of galantamine were more discrete and variable over time. The relatively low dose and highly variable PK properties of this drug in our study and an unexpected delay in onset of galantamine's T_{max} which may in hindsight be related to a food interaction with lunch, may have obscured the detection of more subtle fMRI effects and time-related changes. Galantamine increased nausea but did not alter cognitive or behavioral states.

Citalopram

In congruence with both task-related [171, 217] and resting-state fMRI paradigms with SSRIs [83, 199], citalopram rapidly lowered connectivity in several cortical and subcortical regions. This

Table 3.2. Overview of significant decreases (↓) and increases (↑) in functional connectivity after galantamine as estimated with threshold-free cluster enhancement ($p < 0.05$, corrected)

Network	NPC/T	Region (Harvard-Oxford)	z*	x	y	z	# voxels	
Visual network 2 (↑)	NPC	L/R/M	4.84	2	-62	-26	10765	
		Hippocampus, thalamus, precuneus, PCC, lateral occipital cortex, brain stem, fusiform gyrus, superior frontal gyrus, precentral gyrus and cerebellum						
		L/M	4.21	8	-48	-44	1249	
		M	3.10	-8	-40	54	147	
		R	4.09	34	32	0	31	
Default mode network (↓)	T = 2.5	R	3.56	48	14	14	25	
		R	3.40	50	10	-2	16	
		R/M	4.36	10	-58	26	210	
		R	4.34	40	-72	28	74	
		M	3.70	4	-54	2	15	
Visual network 1 (↓)	T = 3.5	M	4.41	8	22	18	246	
		R	3.64	14	-56	16	210	
		R	4.06	48	-26	0	105	
		R/M	3.65	14	8	38	93	
		L	3.46	-18	-46	-12	91	
Visual network 2 (↑)	T = 3.5	R	4.54	18	2	-8	76	
		R	4.79	24	-66	-36	14	
		Cerebellum						

Table 3.2 continues on next page

Table 3.2. *Continued*

Network	NPC/T	Region (Harvard-Oxford)	z*	x	y	z	# voxels	
Visual network 2 (†)	T = 6	L/R/M	5.01	8	-48	-44	4876	
		Hippocampus, parahippocampal gyrus, cerebellum, brain stem, temporal occipital fusiform cortex and inferior temporal gyrus						
		R	4.24	28	-62	52	677	
		R	3.85	32	-8	38	470	
		R	4.32	14	-24	44	372	
Frontoparietal network left (‡)	T = 4.5	L	3.66	-18	-68	52	152	
		R	3.62	42	-76	30	146	
		L/R/M	5.25	-2	52	-2	630	
Auditory network (†)	T = 6	R	4.12	16	-50	12	110	
		R	4.53	12	-30	-16	44	
		R	3.44	36	-42	-10	14	
		L/M	4.83	-4	-32	48	188	
		L	4.65	-46	-28	50	23	

Abbreviations: L = left, R = right, M = midline, ACC = anterior cingulate cortex, PCC = posterior cingulate cortex. Voxel dimension = 2 mm x 2 mm x 2 mm (voxel volume 0.008 mL). * = standardized z-value of the uncorrected peak Fisher- (NPC) or t-statistic (partial tests) within regions.

is consistent with the numerous afferent and efferent serotonergic fibers originating from the brain stem's raphe nuclei [218]. Compared with our recent results on the SSRI sertraline [199], there was considerable overlap between the two SSRIs in direction (decreased connectivity) and regions (ACC, PCC, precuneus, prefrontal cortex, midbrain and motor cortex) of effect, especially with respect to other pharmacological compounds that usually show more restricted responses [76, 78, 80]. Part of these findings is in line with RS-fMRI studies in depressed patients who exhibit hyperconnectivity of cortical midline structures (ACC, PCC, precuneus and medial prefrontal regions) that are related to emotion regulation and modulated by serotonin transmission [88, 219]. It has been hypothesized that this increase in connectivity in depression is representative of disruptions in self-consciousness and rumination of negative thoughts [142, 144]. An explanation of the overall inhibitory effect of acute SSRI exposure is the relative predominance of inhibitory 5-HT₁ vs. stimulatory 5-HT₂ receptor subtypes [133] that has been demonstrated throughout the cortex [110, 132, 151, 152]. Most outstanding was the citalopram induced decrease in connectivity with the sensorimotor network, mainly due to alterations at T = 4.5 h. Citalopram also increased cortisol and prolactin levels, most noticeable at one time point as well (T = 2.5 h for cortisol and T = 3.5 h for prolactin). Although this took place before appearance of the largest alterations in connectivity, it postulates an apex in the pharmacodynamic effect of citalopram. Equal SSRI effects for the sensorimotor network (decreased connectivity with the sensorimotor region, supplementary motor area, precuneus and cingulate cortex) have been found earlier [199]. The primary motor and somatosensory cortex are both characterized by a high 5-HT axon density [220] and serotonin is recognized to be important for motor behavior in animals and humans [221, 222]. This is demonstrated by enhanced motor area activity during improved motor performance after SSRI administration [155, 156]. The precuneus and cingulate cortex are presumed to support voluntary and complex motor control [157, 159] and seem to play a central role in SSRI enhancement [199]. While the effect was more focal, connectivity between the midbrain and right fronto-parietal network was decreased as well. This matches observations that acute blockade of serotonin reuptake activates 5-HT_{1A} autoreceptors in the midbrain's median and dorsal raphe nuclei [47, 109, 134], in turn leading to reduced 5-HT release in particularly the forebrain [130, 223].

Nevertheless, comparing effects of citalopram and sertraline, we did not find alterations in relation to exact identical functional networks. No differences have been found on the antidepressant efficacy of both SSRIs [224, 225], although sertraline induces more gastrointestinal side effects than citalopram [224, 225]. This corresponds to our finding that sertraline significantly increased the level of nausea, whereas this did not occur in our current study group. Citalopram is also known as the most selective SSRI; sertraline has more affinity for dopamine, noradrenaline and σ -receptors than citalopram [180], which in turn modulate N-methyl-D-aspartate and glutamate receptors as well [226]. Citalopram, on the other hand, has a high affinity on histamine H₁ receptors [180]. It is possible that these properties may account for differences in network

changes between the two SSRIs [81, 227]. However, it is yet to be established what the value is of specific network vs. region effects in connectivity analyses. Considering the resemblance in direction and location of effect we presume that sertraline and citalopram induce quite comparable connectivity alterations.

Galantamine

The cholinergic system is mostly related to aging and aging related diseases, as cholinergic malfunction, especially in the hippocampus, cortex, the entorhinal area, the ventral striatum, and the basal forebrain, plays a key role in associated functional degeneration [228, 229]. Combining fMRI data of all time points, we found an increase in connectivity with the visual network which was mostly associated with effects on T = 6 h. The medial and lateral cholinergic pathways, originating from Meynert's basal nucleus, supply a large portion of the brain and merge in the posterior occipital lobe [230]. In dementia and schizophrenia, it is hypothesized that cholinergic dysregulation is responsible for psychotic manifestations and AChEIs have been successfully used for treatment of visual hallucinations [231, 232]. ACh release in the primary visual cortex is increased during visual stimulation pointing to ACh as influencing visual processing and learning mechanisms [233, 234]. It has been proposed that cholinergic enhancement facilitates bottom-up visual attention and perception by increasing activity in the extrastriate cortex [235, 236]. More importantly, galantamine altered connectivity with areas that are highly relevant in learning and memory: the left and right hippocampus and thalamus. Changes in cholinergic markers such as choline acetyltransferase, acetylcholinesterase and muscarinic and nicotinic acetylcholine receptor availability in hippocampal regions is typical for AD and normal aging [229]. In patients with AD, hippocampal volume loss appears to slow down during treatment with donepezil [237] and cholinergic enhancement even improved visual and verbal episodic memory and long-term visual episodic recall in healthy young subjects, memory domains that are specifically related to hippocampal functioning [238]. Cholinergic treatment aided the processing of novel faces in AD patients, which was accompanied by normalization in the fusiform gyrus [239, 240], where we found connectivity changes as well. In addition, acute exposure to cholinergic stimulation increased activation in occipital and hippocampal regions of patients with AD and mild cognitive impairment (MCI) during a visual memory task [241, 242]. The thalamus, considered to be a gate for sensory information, contains various nuclei that receive excitatory cholinergic input [243], including the lateral geniculate nucleus that has feedback connections with the primary visual cortex [244, 245]. Results for this network are compatible with previous studies [246, 247], indicating that cholinergic enhancement benefits memory performance and visual stimulation orientation by selective perceptual processing.

Repeated measures

Collecting multiple scans per day increases the power of the statistical test and decreases individual variability, which reduces the need for large sample sizes. The observed variation in connectivity on placebo days emphasizes the importance of a placebo-controlled design with repeated measures, providing insight into potential diurnal fluctuations. Furthermore, it offers possibilities to investigate effects on different time points and relate these effects to other pharmacodynamic and PK profiles. NPC groups the data of all time points to test one joint null hypothesis without the necessity to explicitly model their dependence [209, 210], ending up with effects among them that are statistically most robust. In addition, univariate partial tests allow for inference per time point. For citalopram, it might have been sufficient to acquire scans at one time point ($T = 4.5$ h). However, it is largely impossible to predict beforehand at which specific moment we can expect the most stable and 'real' drug effect, since the peak effect does not appear to coincide directly with the observed T_{\max} in plasma and neuroendocrine responses. Effects at other time points may not reach significance but still contribute to the net result. The combined outcome therefore tends to be more reliable and powerful in defining pharmacological effects that are variable over time, as it will grasp the strongest effects without the risk of missing out on important information [211]. This does not imply that the partial (time specific) effects are meaningless. A decrease in connectivity at $T = 4.5$ h between the default mode network and precuneus, PCC and ACC is in line with earlier results [82, 85-87, 199] and in agreement with opposite features in depression, which is characterized by increased connectivity of DMN components [88]. Especially the posterior part of the DMN, where citalopram effects were most prevalent, has been implicated in SSRI efficacy in depression [84, 145]. Furthermore, consistent with an increased cerebellar-DMN connectivity in depression [88], citalopram reduced connectivity between the DMN and cerebellum. The cerebellum is primarily known for its service in motor control, illustrating our findings for the sensorimotor network, but influences mood regulation as well [248, 249].

In contrast to citalopram, the effects of galantamine were more focal, less related to a specific network or point in time and less uniform with regard to direction of effect. This heterogeneity in effect possibly reflects the large kinetic variability in this study. Although the variation in timing of T_{\max} did not clearly differ between citalopram and galantamine, the variance of galantamine's C_{\max} (ranging from 25.6 to 61.4 ng/mL) was high compared with citalopram and desmethylcitalopram. Since the combined effect mainly depended on the last time point it is possible that the impact of galantamine does not follow a time course that equals the PK profile or that effects might have become larger and more stable later in time. This is congruent with the unanticipated delay in onset of galantamine's T_{\max} in our study group, resulting in a less powerful aggregation of data, in which especially the value of measurements at $T = 2.5$ is questionable. Although galantamine is known for a T_{\max} of 1-2 h after dosing, the mean T_{\max} in our sample was 2.67 h (4.67 h after zero point), whereas citalopram, known for a T_{\max} between 2 and 4 h, did reach its maximum

concentration at 2.99 h post dosing. Furthermore, the relatively low dose and variable kinetic time profile of galantamine might have contributed to the absence of a larger response on functional connectivity and neuroendocrine parameters. A larger sample size, a higher dose of galantamine (16-32 mg), and earlier drug administration might have reduced this variability in response. The outcomes of our partial tests reveal additional information beyond the combined approach as well. There is a tendency towards diminished DMN activity in normal aging, MCI and dementia, pointing to reduced integrity of structures that are vulnerable to atrophy, beta amyloid deposition and reduced glucose metabolism [20]. Studies that are performed on the resting state fMRI response to cholinergic interventions are restricted to AD patients and mainly indicate an increase in connectivity with DMN areas [89-91]. In another study, no effect on the DMN was found in both APOE $\epsilon 4$ carriers and non-carriers [200]. Acute exposure to cholinergic stimulation decreased DMN connectivity with the precuneus and occipital cortex in our study group at T = 2.5 h. This direction of effect might be the consequence of investigating cholinergic responses in healthy young adults instead of subjects with impaired cholinergic systems. It is possible that when neural cholinergic processes are still intact, ceiling effects may prevent further activation and excessive stimulation may actually impair optimal connectivity. Moreover, these studies all used AChEI treatment for several weeks, instead of our single-dose administration. More research is needed to unravel differential cholinergic responses among specific populations and treatment designs.

Limitations

Agents that enhance the cholinergic and serotonergic system commonly elicit gastrointestinal adverse events, which is attributable to their peripheral influences [250, 251]. In order to prevent these adverse effects, we administered granisetron on both drug- and placebo study days before study drug administration. RS-fMRI effects of selective 5-HT₃ receptor antagonists as granisetron are lacking, but need to be taken into consideration when interpreting the results [109]. However, intolerance to our intensive study procedures would have been undesirable [181] and vomiting might have altered brain connectivity as well. To reduce nausea, we also decided to administer citalopram in two doses, and to skip the second dose in case of tolerability issues. For citalopram, our measures were adequate, and all subjects received both doses without significant nausea. For the same reasons, a relatively low dose of galantamine was chosen. However, increased nausea was present after administering galantamine compared with placebo, primarily at the end of the day, which may also have influenced some of the observed network effects but justifies our decision to limit the dose of galantamine. This also emphasizes the mismatch of our repeated measurements and galantamine's absorption rate. Despite our attempt to equalize the PK responses of citalopram and galantamine during the course of the day, both drugs did not reach their maximum concentration at the same time point, which hampers comparability. Currently, no accepted methods are available to include individual drug concentrations in the

network analysis. Further, fMRI effects, especially in pharmacological research, are potentially the result of vasodilation, and hence to changes in neurovascular coupling instead of true neural activity [185, 186]. Although SSRIs do not typically alter the hemodynamic response [188], AChEIs could increase vessel tone by contraction of the smooth muscles of blood vessels [252, 253]. Yet, there was no significant treatment effect of either drug on heart rate frequency, which minimizes the probability of cardiac artifacts. Besides, vessel dilation would more likely alter connections throughout the entire brain instead of inducing the network-specific effects that we observed. Future studies with appropriate protocols are needed to specify these processes more accurately.

Summary

This study provides further support for RS-fMRI as a sensitive method for investigating instant neural processes after pharmacological challenges. The results on the SSRI citalopram and AChEI galantamine identify their neuromodulating role in cognitive and sensory systems. Citalopram altered connectivity with networks and regions that are mostly implied in sensorimotor functioning and self-reference, whereas the results of galantamine show acetylcholine's relation to visual processing and learning mechanisms. Our findings also encourage the use of repeated measurements after single-dose administration, leading to a more powerful and reliable picture of pharmacological effects. Results may have been partially obscured by the variability of individual PK characteristics, which was larger than expected. A future challenge therefore is to develop appropriate statistical models (PK/PD-modeling) to investigate concentration-dependent modulation of resting state functional connectivity.

Acknowledgements

Erica S. Klaassen and Jasper Stevens (CHDR) are acknowledged for their contribution to statistical analyses.

Supplementary Table S3.1: Summary of treatment effects of citalopram and galantamine on the NeuroCart® cognitive test battery

Parameter	Least Squares Means			Treatment			Contrasts		
	Placebo	Citalopram	Galantamine	p-value	Citalopram vs. placebo	Galantamine vs. placebo	Citalopram vs. galantamine		
VAS Alertness (mm)	49.3	48.3	47.3	0.329	-0.9 (-3.7, 1.8) <i>p</i> = 0.485	-2.0 (-4.6, 0.7) <i>p</i> = 0.141	1.0 (-1.7, 3.7) <i>p</i> = 0.443		
VAS Calmness (mm)	52.9	51.5	52.9	0.326	-1.4 (-3.7, 0.9) <i>p</i> = 0.217	0.0 (-2.3, 2.4) <i>p</i> = 0.976	-1.4 (-3.6, 0.8) <i>p</i> = 0.188		
VAS Mood (mm)	53.5	51.2	52.3	0.169	-2.3 (-4.7, 0.1) <i>p</i> = 0.063 ²	-1.2 (-3.7, 1.2) <i>p</i> = 0.310	-1.1 (-3.5, 1.3) <i>p</i> = 0.359		
VAS Nausea log (mm)	0.32	0.37	0.49	0.084	0.048 (-0.104, 0.200) <i>p</i> = 0.519	0.169 (0.015, 0.323) <i>p</i> = 0.033¹	-1.21 (-2.72, 0.030) <i>p</i> = 0.109		
Adaptive tracking (%)	24.7	23.4	23.4	0.219	-1.32 (-3.09, 0.46) <i>p</i> = 0.137	-1.34 (-3.11, 0.43) <i>p</i> = 0.129	0.02 (-1.75, 1.80) <i>p</i> = 0.977		
Simple reaction time task (s)	265.16	275.04	268.09	0.265	3.7% (-1.0%, 8.7%) <i>p</i> = 0.117	1.1% (-3.5%, 5.9%) <i>p</i> = 0.627	2.6% (-2.1%, 7.5%) <i>p</i> = 0.264		
Stroop mean RT Incongruent-Congruent (ms)	62.2	85.4	69.9	0.433	23.2 (-14.6, 61.0) <i>p</i> = 0.214	7.7 (-30.4, 45.8) <i>p</i> = 0.678	15.5 (-21.2, 52.2) <i>p</i> = 0.387		
Stroop Correct Congruent-Incongruent	0.1	0.3	0.1	0.573	0.2 (-0.3, 0.6) <i>p</i> = 0.444	-0.0 (-0.5, 0.4) <i>p</i> = 0.830	0.2 (-0.2, 0.7) <i>p</i> = 0.318		
SDST Correct Responses	63.3	63.1	63.1	0.762	-0.2 (-0.8, 0.4) <i>p</i> = 0.517	-0.2 (-0.8, 0.4) <i>p</i> = 0.553	-0.0 (-0.7, 0.6) <i>p</i> = 0.928		
SDST Average Reaction Time (ms)	1468.53	1541.28	1538.40	0.093	72.75 (-1.60, 147.1) <i>p</i> = 0.055 ²	69.87 (-4.50, 144.2) <i>p</i> = 0.064 ²	2.88 (-71.5, 77.25) <i>p</i> = 0.935		
N-back mean RT 0 back (ms)	401	403	394	0.654	2 (-19, 23) <i>p</i> = 0.838	-7 (-29, 15) <i>p</i> = 0.497	9 (-13, 31) <i>p</i> = 0.384		
N-back mean RT 1 back (ms)	432	431	416	0.266	-1 (-22, 21) <i>p</i> = 0.930	-15 (-37, 6) <i>p</i> = 0.152	14 (-7, 36) <i>p</i> = 0.173		
N-back mean RT 2 back (ms)	510	517	504	0.832	7 (-37, 51) <i>p</i> = 0.732	-5 (-49, 39) <i>p</i> = 0.797	13 (-31, 57) <i>p</i> = 0.551		
N-back correct:incorrect/total 0 back	0.95	0.96	0.95	0.812	0.01 (-0.03, 0.05) <i>p</i> = 0.602	-0.00 (-0.04, 0.04) <i>p</i> = 0.956	0.01 (-0.03, 0.05) <i>p</i> = 0.564		
N-back correct:incorrect/total 1 back	0.96	0.96	0.95	0.583	0.00 (-0.04, 0.05) <i>p</i> = 0.895	-0.02 (-0.06, 0.03) <i>p</i> = 0.422	0.02 (-0.02, 0.06) <i>p</i> = 0.345		
N-back correct:incorrect/total 2 back	0.92	0.91	0.92	0.913	-0.01 (-0.06, 0.04) <i>p</i> = 0.719	0.00 (-0.05, 0.05) <i>p</i> = 0.997	-0.01 (-0.06, 0.04) <i>p</i> = 0.709		
WLT Recall 1 correct	11.4	10.7	12	0.484	-0.8 (-3.0, 1.5) <i>p</i> = 0.499	0.6 (-1.7, 2.9) <i>p</i> = 0.598	-1.3 (-3.6, 0.9) <i>p</i> = 0.235		
WLT Recall 2 correct	16.9	16.8	16.8	0.993	-0.1 (-1.8, 1.6) <i>p</i> = 0.920	-0.1 (-1.8, 1.6) <i>p</i> = 0.920	-0.0 (-1.7, 1.7) <i>p</i> = 1.000		
WLT Recall 3 correct	19.8	19.9	19.6	0.944	0.1 (-2.1, 2.2) <i>p</i> = 0.936	-0.2 (-2.4, 1.9) <i>p</i> = 0.809	0.3 (-1.8, 2.5) <i>p</i> = 0.748		
WLT Delayed Recall correct	18.4	17.0	18.1	0.329	-1.4 (-3.4, 0.6) <i>p</i> = 0.158	-0.3 (-2.3, 1.7) <i>p</i> = 0.734	-1.1 (-3.1, 0.9) <i>p</i> = 0.275		
WLT Delayed Recognition correct	25.7	26.2	26.9	0.506	0.6 (-1.6, 2.8) <i>p</i> = 0.586	1.3 (-0.9, 3.4) <i>p</i> = 0.249	-0.7 (-2.9, 1.5) <i>p</i> = 0.534		
WLT Delayed Recognition RT correct (ms)	894.3	860.8	836.3	0.241	-33.6 (-103, 35.9) <i>p</i> = 0.326	-58.0 (-128, 11.5) <i>p</i> = 0.097 ²	24.4 (-45.1, 93.9) <i>p</i> = 0.472		

Abbreviations: VAS = Visual Analogue Scale; SDST: Symbol Digit Substitution Test; WLT = Visual Verbal Learning Test; RT = reaction time. ¹Significant at *p* < 0.05; ²non-significant trend (0.05 < *p* < 1.0).



Part II

Functional brain connectivity and
neuromodulation in older age and
Alzheimer's disease



Chapter 4

Diminished posterior precuneus connectivity with the default mode network differentiates normal aging from Alzheimer's disease

Published in Frontiers in Aging Neuroscience 2017; 9:1-13

Bernadet L. Klaassens^{a,b,c,d}, Joop M.A. van Gerven^d, Jeroen van der Grond^b, Frank de Vos^{a,b,c}, Christiane Möller^{a,b,c}, Serge A.R.B. Rombouts^{a,b,c}

^aLeiden University, Institute of Psychology, Leiden, the Netherlands, ^bLeiden University Medical Center, Department of Radiology, Leiden, the Netherlands, ^cLeiden University, Leiden Institute for Brain and Cognition, Leiden, the Netherlands, ^dCentre for Human Drug Research, Leiden, the Netherlands

ABSTRACT

Both normal aging and Alzheimer's disease (AD) have been associated with a reduction in functional brain connectivity. It is unknown how connectivity patterns due to aging and AD compare. Here, we investigate functional brain connectivity in 12 young adults (mean age 22.8 ± 2.8), 12 older adults (mean age 73.1 ± 5.2) and 12 AD patients (mean age 74.0 ± 5.2 ; mean MMSE 22.3 ± 2.5). Participants were scanned during 6 different sessions with resting state functional magnetic resonance imaging (RS-fMRI), resulting in 72 scans per group. Voxelwise connectivity with 10 functional networks was compared between groups ($p < 0.05$, corrected). Normal aging was characterized by widespread decreases in connectivity with multiple brain networks, whereas AD only affected connectivity between the default mode network (DMN) and precuneus. The preponderance of effects was associated with regional gray matter volume. Our findings indicate that aging has a major effect on functional brain interactions throughout the entire brain, whereas AD is distinguished by additional diminished posterior DMN-precuneus coherence.

INTRODUCTION

When age progresses, the brain is subjected to many changes that are related to deterioration of sensory, motor and intellectual functioning [254-256]. In Alzheimer's disease (AD), a gradual worsening in memory and other cognitive domains occurs, accompanied by a notable reduction in independency and daily life functioning [15]. This age and dementia related decline in function is likely to be associated with a loss of integrity of large-scale brain networks [5]. Accordingly, functional network connectivity as measured with functional magnetic resonance imaging (fMRI) is diminished in normal aging and AD [20, 38, 257-260].

The default mode network (DMN) has been preferentially studied, as its core regions (precuneus, posterior cingulate cortex) are relevant for episodic memory retrieval [261, 262] and susceptible to accumulation of β -amyloid [263] in older adults and patients with AD. Both aging and AD are most prominently characterized by a reduction in DMN connectivity [20, 37, 38, 261, 264-268].

There are also indications for connectivity change in other brain networks in aging [28, 39-42, 269-271] and AD [22-26]. However, this has been studied less well and results tend to be mixed. For example, contradicting results have been found for the visual system in older adults [28, 39, 41, 269, 271].

Although previous work suggests overlap and differences in functional connectivity patterns in normal aging and AD, it has not yet been investigated how changes due to older age relate to changes as seen in AD. Here, we compare voxelwise connectivity between young and older adults and between older adults and patients with AD with 10 standard functional networks as obtained by imaging 36 subjects at rest [10]. Since aging and AD are primarily characterized by gray matter atrophy [272], it is encouraged to evaluate whether group differences in connectivity are explained by underlying gray matter loss [273]. We therefore present our results with and without correction for regional gray matter volume.

METHODS

Subjects and design

We included 12 young subjects, 12 older adults and 12 AD patients in this single center study (see Table 4.1 for demographics and Supplementary Figure S4.1 for additional background information on cognitive performance on the computerized NeuroCart® test battery). The clinical diagnosis of probable AD was established according to the revised criteria of the National Institute of Neurological and Communicative Disorders and Stroke and the Alzheimer's Disease and Related Disorders Association (NINCDS-ADRDA) [15], including clinical and neuropsychological assessment. All AD patients participating in this study were recently diagnosed and had mild to

Table 4.1. Demographics of young and older adults and AD patients

	Young adults	Older adults	AD patients
n	12	12	12
Age (mean \pm SD)	22.8 \pm 2.8	73.1 \pm 5.2	74.0 \pm 5.2
Age range	18-27	64-79	65-81
Male/female	6/6	6/6	6/6
MMSE (mean \pm SD)	29.9 \pm 0.3	29.3 \pm 0.9	22.3 \pm 2.5

moderate cognitive deficits with a Mini Mental State Examination (MMSE) score of at least 18 [274]. Furthermore, they were assessed by a physician (i.e. neurologist, geriatrician) as mentally capable of understanding the implications of study participation.

All subjects underwent a thorough medical screening to investigate whether they met the inclusion and exclusion criteria. They had a normal history of physical health and were able to refrain from using nicotine and caffeine during study days. Exclusion criteria included positive drug or alcohol screen on study days, regular excessive consumption of alcohol (>4 units/day), caffeine (>6 units/day) or cigarettes (>5 cigarettes/day) and use of benzodiazepines, selective serotonin reuptake inhibitors, cholinesterase inhibitors, monoamine oxidase inhibitors or other medication that is likely to alter resting state connectivity. The study was approved by the medical ethics committee of the Leiden University Medical Center (LUMC). Written informed consent was obtained from each subject prior to study participation. To compensate for the small sample sizes and increase the statistical power, six resting state fMRI (RS-fMRI) scans were analyzed per subject, giving 72 RS-fMRI scan series per group. Subjects were scanned two times (with 1 h in between) on three different occasions within 2 weeks. These data concern the baseline measurements that were acquired as part of a project in which the same subjects were measured before and after an intervention. The results of this intervention study will be published elsewhere.

Imaging

“Scanning was performed at the LUMC on a Philips 3.0 Tesla Achieva MRI scanner (Philips Medical System, Best, The Netherlands) using a 32-channel head coil. During the RS-fMRI scans, all subjects were asked to close their eyes while staying awake. They were also instructed not to move their head during the scan. Instructions were given prior to each scan on all study days. T1-weighted anatomical images were acquired once per visit. To facilitate registration to the anatomical image, each RS-fMRI scan was followed by a high-resolution T2*-weighted echo-planar scan. Duration was approximately 8 min for the RS-fMRI scan, 5 min for the anatomical scan and 30 s for the high-resolution scan.

RS-fMRI data were obtained with T2*-weighted echo-planar imaging (EPI) with the following scan parameters: 220 whole brain volumes, repetition time (TR) = 2180 ms; echo time (TE) = 30 ms; flip angle = 85°; field-of-view (FOV) = 220 x 220 x 130 mm; in-plane voxel resolution = 3.44 x 3.44 mm, slice thickness = 3.44 mm, including 10% interslice gap. The next parameters were used to collect T1-weighted anatomical images: TR = 9.7 ms; TE = 4.6 ms; flip angle = 8°; FOV = 224 x 177 x 168 mm; in-plane voxel resolution = 1.17 x 1.17 mm; slice thickness = 1.2 mm. Parameters of high-resolution T2*-weighted EPI scans were set to: TR = 2200 ms; TE = 30 ms; flip angle = 80°; FOV = 220 x 220 x 168 mm; in-plane voxel resolution = 1.96 x 1.96 mm; slice thickness = 2.0 mm." [275, p. 311].

Functional connectivity analysis

Data preprocessing

All analyses were performed using the Functional Magnetic Resonance Imaging of the Brain (FMRIB) Software Library (FSL, Oxford, United Kingdom) version 5.0.7 [119-121]. "Each individual functional EPI image was inspected, brain-extracted and corrected for geometrical displacements due to head movement with linear (affine) image registration [122]. Images were spatially smoothed with a 6 mm full-width half-maximum Gaussian kernel. Registration parameters for non-smoothed data were estimated to transform fMRI scans into standard space and co-registered with the brain extracted high resolution T2*-weighted EPI scans (with 6 degrees of freedom) and T1 weighted images (using the Boundary-Based-Registration method) [124]. The T1-weighted scans were non-linearly registered to the MNI 152 standard space (the Montreal Neurological Institute, Montreal, QC, Canada) using FMRIB's Non-linear Image Registration Tool. Registration parameters were estimated on non-smoothed data to transform fMRI scans into standard space. Automatic Removal Of Motion Artifacts based on Independent Component Analysis (ICA-AROMA vs0.3-beta) was used to detect and remove motion-related artifacts. ICA decomposes the data into independent components that are either noise-related or pertain to functional networks. ICA-AROMA attempts to identify noise components by investigating its temporal and spatial properties and removes these components from the data that are classified as motion-related. Registration was thereafter applied on the denoised functional data with registration as derived from non-smoothed data. As recommended, high pass temporal filtering (with a high pass filter of 150 s) was applied after denoising the fMRI data with ICA-AROMA [207, 208]." [275, p. 311].

Estimation of network connectivity

RS-fMRI networks were thereafter extracted from each individual denoised RS-fMRI dataset (12 subjects x 3 groups x 6 scans = 216 datasets) applying a dual regression analysis [36, 125] based on 10 predefined standard network templates as used in our previous research [199, p. 442]: "These standard templates have previously been identified using a data-driven

approach [10] and comprise the following networks: three visual networks (consisting of medial, occipital pole, and lateral visual areas), DMN (medial parietal, bilateral inferior-lateral-parietal and ventromedial frontal cortex), cerebellar network, sensorimotor network (supplementary motor area, sensorimotor cortex and secondary somatosensory cortex), auditory network (superior temporal gyrus, Heschl's gyrus and posterior insular), executive control network (medial-frontal areas, including anterior cingulate and paracingulate) and two frontoparietal networks (frontoparietal areas left and right). In addition, time series of white matter (measured from the center of the corpus callosum) and cerebrospinal fluid (measured from the center of lateral ventricles) were included as confound regressors in this analysis to account for non-neuronal signal fluctuations [126]. With the dual regression method, spatial maps representing voxel-to-network connectivity were estimated for each dataset separately in two stages for use in group comparisons. First, the weighted network maps were used in a spatial regression into each dataset. This stage generated 12 time series per dataset that describe the average temporal course of signal fluctuations of the 10 networks plus 2 confound regressors (cerebrospinal fluid and white matter). Next, these time series were entered in a temporal regression into the same dataset. This resulted in a spatial map per network per dataset with regression coefficients referring to the weight of each voxel being associated with the characteristic signal change of a specific network. The higher the value of the coefficient, the stronger the connectivity of this voxel with a given network. These individual statistical maps were subsequently used for higher level analysis."

Higher level analysis

To investigate whether voxel wise functional connectivity with each of the 10 functional networks differed between groups, ANOVA F-tests were performed on four contrasts of interest (young > older adults, older > young adults, older adults > AD patients and AD patients > older adults). Networks with a significant outcome were followed by post-hoc unpaired two-sample t-tests to investigate the four contrasts separately. These tests were performed with and without correction for gray matter (GM) volume. For correction, a voxelwise partial volume estimate map of GM, as calculated from T1-weighted images with FMRIB's Automated Segmentation Tool (FAST) [276], was added as nuisance regressor. As the results of this analysis may depend on the selection of the 10 functional networks derived from 36 healthy adults (mean age 28.5) as spatial regressors [10], we also explored a number of data driven extracted networks with Independent Component Analysis using FSL's MELODIC vs3.14. Of 70 extracted networks, the 20 networks that correlated highest with the 10 networks of Smith et al. [10] were chosen for group analyses in order to compare these with the results of the 10 functional networks. Therefore, these 20 networks were entered in a dual regression analysis to obtain spatial connectivity maps per network per dataset followed by higher level analysis as described below.

To test for differences in connectivity between young and older adults and between AD patients and older adults across the six repeated measures per subject we used non-parametric

combination (NPC) as provided by FSL's Permutation Analysis for Linear Models tool (PALM vs94-alpha) [129, 209, 210]. NPC is a multivariate method that offers the possibility to combine data of separate, possibly non-independent tests, such as our repeated measures (six scans per subject), and investigate the presence of joint effects across them, in a test that has fewer assumptions and is more powerful than repeated-measurements analysis of variance (ANOVA) or multivariate analysis of variance (MANOVA). To measure these joint effects (combining the six scans per subject to one composite variable), NPC testing first performs an independent test for each repeated measure using 5000 synchronized permutations. These tests are then combined non-parametrically via NPC using Fisher's combining function [211] and the same set of synchronized permutations. A liberal mask was used to investigate voxels of gray and white matter within the MNI template, excluding voxels belonging to cerebrospinal fluid. Threshold-free cluster enhancement was applied to each independent test and after the combination, and the resulting voxelwise statistical maps were corrected for the familywise error rate using the distribution of the maximum statistic [128, 129]. Voxels were considered significant at p -values < 0.05 , corrected.

RESULTS

Significant F-test results pointed to differences in connectivity in AD patients vs. elderly controls and in older vs. young adults for all networks, except the cerebellar network.

Resting state connectivity without correction for GM volume

Differences in resting state functional connectivity were most apparent between young and older adults (see Figure 4.1A). For all functional networks, except the cerebellar network, connectivity was decreased in the older compared to the young adults, involving most cortical and subcortical regions. AD patients and elderly controls differed in connectivity with the DMN, that showed lower connectivity with the precuneus in AD patients compared to older adults (see Figure 4.2A). None of the networks showed higher connectivity in the older as opposed to young adults or in AD patients as opposed to the elderly controls. Specifications of effects (sizes of significant regions and peak z -values) are provided in Table 4.2. These results using 10 pre-defined networks as spatial regressors were largely similar to the results using independent component analysis to extract 70 networks from the current data, of which 20 were used as spatial regressors (see methods).

Figure 4.3 shows connectivity for all three groups, where Figure 4.3A corresponds to the mean connectivity of significant voxels across all networks in Figure 4.1A (young vs. older adults). This illustrates that the average connectivity in these regions is significantly different between young and older adults but not between elderly controls and AD patients. Figure 4.3A corresponds

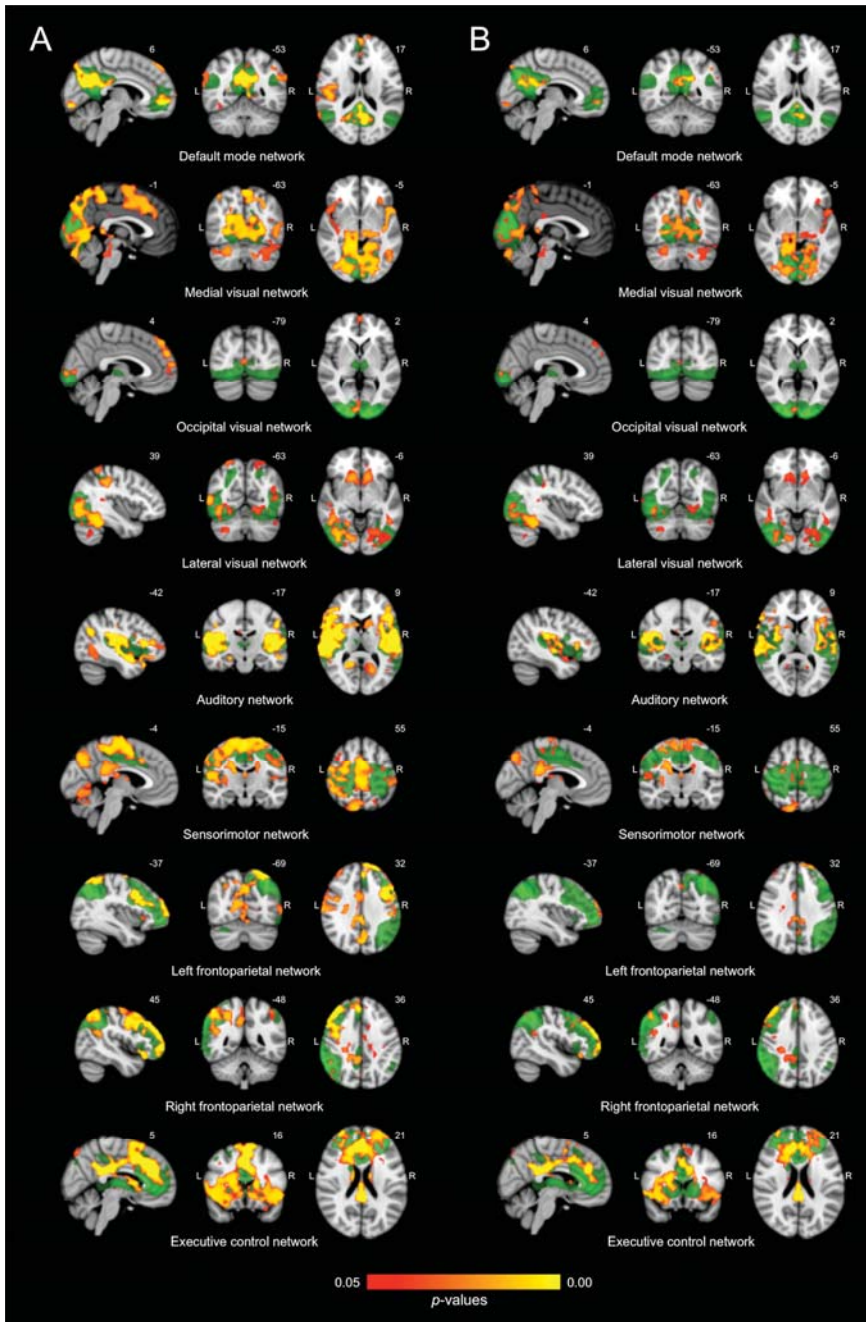


Figure 4.1. Differences in network connectivity between young and older adults. (A) Reduced functional connectivity in older compared to young adults between the default mode network, three visual networks, the auditory network, the sensorimotor network, the left and right frontoparietal network and the executive control network (shown in green) and regions as shown in red-yellow (at $p < 0.05$, corrected). (B) Reduced functional connectivity in older compared to young adults when including regional gray matter volume as regressor.

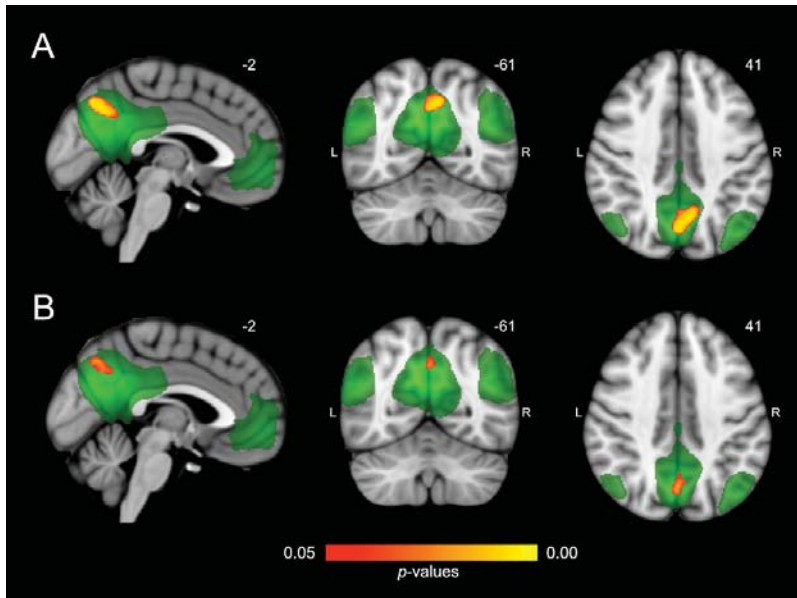


Figure 4.2. Differences in network connectivity between AD patients and elderly controls. (A) Reduced functional connectivity in AD patients compared to elderly controls between the default mode network (shown in green) and the precuneus (shown in red-yellow at $p < 0.05$, corrected). (B) Reduced functional connectivity in AD patients compared to elderly controls when including regional gray matter volume as regressor.

to the mean connectivity of significant voxels for the DMN in Figure 4.2A (elderly controls vs. AD patients). This illustrates that the average connectivity in this region (posterior precuneus) is significantly different between AD patients and elderly controls but not between young and older adults.

Resting state connectivity after regional correction for GM volume

After correction for regional GM volume, differences in resting state functional connectivity between young and older adults were less profound with a reduction in the number of significant voxels of 58.9% (see Figure 4.1B). Reduced connectivity with the same functional networks in the group of older compared to young adults mainly involved midline regions (posterior and anterior cingulate cortex, precuneus), occipital, temporal and frontal areas. The difference between elderly controls and AD patients was more restricted after correction as well (reduction of 65.8% in the number of significant voxels) but still involved a decrease in connectivity of the DMN with the precuneus in AD patients (see Figure 4.2B). Specifications of effects (sizes of significant regions and peak z -values) are provided in Table 4.3.

Table 4.2. Overview of significant differences in functional connectivity without gray matter correction as estimated with threshold-free cluster enhancement ($p < 0.05$, corrected)

Network	Contrast	Region (Harvard-Oxford)	z*	x	y	z	# voxels	
Default mode network	Older < young adults	L/R/M	9.60	0	-42	20	7814	
		Precuneus, PCC, ACC, cuneal cortex, lingual gyrus, supracalcarine cortex, lateral occipital cortex, parahippocampal gyrus, hippocampus						
	M	M	9.27	4	56	-6	2600	
		Frontal pole, frontal medial cortex, ACC, paracingulate gyrus						
		R	6.95	50	-20	12	2382	
		Middle and superior temporal gyrus, parietal operculum cortex, central opercular cortex, insular cortex, Heschl's gyrus, pre- and postcentral gyrus						
		R	7.04	-38	-70	54	1436	
		Lateral occipital cortex						
		R	7.60	56	-8	-26	561	
		L	6.97	-58	-34	-8	328	
L	7.43	-58	-10	-18	299			
R	5.48	20	-40	-14	154			
R	5.71	50	20	-22	102			
R	Temporal pole							
Default mode network	AD patients < controls	M	7.39	0	-70	44	415	
	Precuneus, PCC							
Executive control network	Older < young adults	L/R/M	10.90	0	-28	28	21857	
		Frontal pole, ACC, PCC, precuneus, thalamus, putamen, SMA, post- and precentral gyrus, temporal pole, frontal orbital cortex, superior frontal gyrus						
	M	M	6.84	8	-78	52	735	
		Precuneus, lateral occipital cortex						
		R	5.94	42	-82	4	323	
		Lateral occipital cortex, occipital fusiform gyrus						
		R	5.65	40	-54	-36	153	
		Cerebellum						
		R	5.48	-12	-36	46	103	
		Pre- and postcentral gyrus, precuneus, PCC						
Sensorimotor network	Older < young adults	L/R/M	7.66	64	-10	42	32668	
		PCC, precuneus, lingual gyrus, paracingulate gyrus, pre- and postcentral gyrus, SMA, central opercular cortex, caudate, thalamus						
R	6.18	38	46	32	442			
Frontal pole, middle frontal gyrus								

Table 4.2 continues on next page

Table 4.2. Continued

Network	Contrast	Region (Harvard-Oxford)	z*	x	y	z	# voxels
Visual network 1	Older < young adults	L/R/M	7.81	14	-42	-6	35606
		Intracalcarine cortex, supracalcarine cortex, occipital pole, precuneus, cerebellum, PCC, pre- and postcentral gyrus, brain stem, thalamus, parahippocampal gyrus, planum temporale, Heschl's gyrus, middle and inferior temporal gyrus					
		R	8.88	38	48	28	869
Visual network 2	Older < young adults	M	6.75	2	56	32	1143
		M	7.62	8	-94	6	258
Visual network 3	Older < young adults	R	6.86	46	-32	40	8644
		Supramarginal gyrus, pre- and postcentral gyrus, superior and middle temporal gyrus, temporal occipital fusiform cortex,					
		L	7.55	-18	-94	4	4065
Auditory network	Older < young adults	L/R/M	7.35	16	22	-6	1160
		Putamen, accumbens, frontal orbitol and medial cortex					
		L	6.62	-30	-50	72	838
		L/R/M	8.69	66	-30	20	31540
		Heschl's gyrus, planum polare, supracalcarine cortex, caudate, putamen, hippocampus, parahippocampal gyrus, precuneus, middle and superior temporal gyrus, insular cortex, inferior and middle frontal gyrus					
M	6.85	12	-76	56	1082		
R	7.73	46	-48	54	399		
M	7.00	8	-8	26	138		
Precuneus, lateral occipital cortex							
Superior parietal lobule, angular gyrus							
PCC, ACC							

Table 4.2 continues on next page

Table 4.2. *Continued*

Network	Contrast	Region (Harvard-Oxford)	z*	X	Y	Z	# voxels
Frontoparietal network R	Older < young adults	R	8.80	38	50	23	9850
		R/M	8.13	48	-52	52	5209
		L	5.72	-58	-2	2	621
		M	5.82	-14	-84	-26	549
		M	6.43	-42	-50	54	451
		M	4.98	-22	-36	36	182
		R	4.83	62	-26	-12	142
Frontoparietal network L	Older < young adults	L/R/M	5.73	60	-20	12	136
		L/R/M	8.83	-4	34	62	17586
		R	5.73	42	8	24	2362
		M	7.16	-66	-54	-2	1460
		R	6.65	42	48	26	1052
		M	6.30	-30	20	-26	455

Abbreviations: L = left, R = right, M = midline, ACC = anterior cingulate cortex, PCC = posterior cingulate cortex, SMA = supplementary motor area. Voxel dimension = 2 mm x 2 mm x 2 mm (voxel volume 0.008 mL). * = standardized z-score of the uncorrected peak Fisher- (NPC) within regions (for regions with > 100 voxels).

Table 4.3. Overview of significant differences in functional connectivity with gray matter correction as estimated with threshold-free cluster enhancement ($p < 0.05$, corrected)

Network	Contrast	Region (Harvard-Oxford)	z*	x	y	z	# voxels
Default mode network	Older < young adults	M PCC, precuneus, lingual gyrus	7.92	-2	-40	20	3214
		L Lateral occipital cortex	8.08	-48	-58	42	244
		L Lateral occipital cortex	6.31	-42	-64	58	113
Default mode network	AD patients < controls	M Precuneus, PCC	7.52	0	-70	44	142
Executive control network	Older < young adults	L/R/M Frontal pole, middle frontal gyrus, ACC, PCC, precuneus, thalamus, SMA	10.70	0	-28	28	14548
Sensorimotor network		M Lateral occipital cortex, precuneus	5.94	10	-78	50	161
	Older < young adults	L/R/M PCC, precuneus, lingual gyrus, paracingulate gyrus, pre- and postcentral gyrus, SMA, central opercular cortex, caudate, thalamus	7.40	4	-38	24	12667
Visual network 1		L Postcentral gyrus	7.83	-62	-12	46	525
	Older < young adults	L/R/M Precuneus, PCC, lateral occipital cortex, precentral gyrus, supramarginal gyrus, lingual gyrus, parahippocampal gyrus, hippocampus, thalamus	7.42	24	-54	-2	16775
Visual network 2		L Frontal pole	7.68	-34	50	30	664
	Older < young adults	R Frontal pole	8.21	36	48	28	205
Visual network 3		M Frontal pole, superior frontal gyrus	6.66	6	48	46	167
	Older < young adults	M Occipital pole	7.86	8	-94	6	103
	Older < young adults	R Temporal occipital fusiform cortex, lateral occipital cortex, cerebellum	7.37	44	-42	-16	3016
		L Temporal occipital fusiform cortex, inferior temporal gyrus, cerebellum	6.18	-46	-54	-24	1207
		L Occipital pole	7.49	-18	-94	4	1013
		R Supramarginal gyrus	5.82	52	-26	32	289
		L Subcallosal cortex, medial frontal cortex	6.66	-10	26	-6	270
		R Cerebellum	5.74	32	-58	-42	250

Table 4.3 continues on next page

Table 4.3. Continued

Network	Contrast	Region (Harvard-Oxford)	z*	x	y	z	# voxels
Auditory network		R Frontal orbital cortex	6.27	16	24	-8	242
		L Supramarginal gyrus	5.60	-58	-36	34	151
	Older < young adults	R Superior temporal gyrus, planum temporale, Heschl's gyrus, supramarginal gyrus, insular cortex, inferior frontal gyrus	7.58	66	-30	10	7741
		L Parietal operculum cortex, Heschl's gyrus, supramarginal gyrus, insular cortex, middle and inferior temporal gyrus	7.86	-54	-26	16	6219
		L Lingual gyrus, PCC, parahippocampal gyrus	5.55	-22	-62	-2	603
		R Lingual gyrus, precuneus, PCC, parahippocampal gyrus	5.55	22	-44	-4	471
Frontoparietal network R		M Precuneus, lateral occipital cortex	6.34	0	-74	50	361
		M PCC, ACC	7.04	8	-8	26	134
	Older < young adults	R Temporal occipital fusiform cortex	4.62	36	-46	-20	100
		R Frontal pole, middle frontal gyrus	8.54	42	50	28	3948
		R/M Postcentral gyrus, PCC, precuneus, superior parietal lobule	5.5	36	-26	42	1153
		R Angular gyrus	6.56	50	-48	50	505
Frontoparietal network L		R Temporal pole, inferior frontal gyrus	8.21	54	18	-10	353
		R/M Lateral occipital cortex, precuneus	5.71	10	-76	56	104
	Older < young adults	M Precuneus, PCC, caudate, thalamus	5.97	0	-62	42	1115
		L Frontal pole	6.74	-20	66	16	1070
		R Frontal pole	6.44	42	48	26	277
		R Occipital pole	6.71	10	-92	-4	228
	L Inferior temporal gyrus, temporal occipital fusiform cortex	6.44	-48	-56	-12	194	
	M ACC	5.91	6	2	32	134	
		L Lateral occipital cortex, superior division	7.01	-28	-74	56	122

Abbreviations: L = left, R = right, M = midline, ACC = anterior cingulate cortex, PCC = posterior cingulate cortex, SMA = supplementary motor area. Voxel dimension = 2 mm x 2 mm x 2 mm (voxel volume 0.008 mL). * = standardized z-value of the uncorrected peak Fisher- (NPC) within regions (for regions with > 100 voxels).

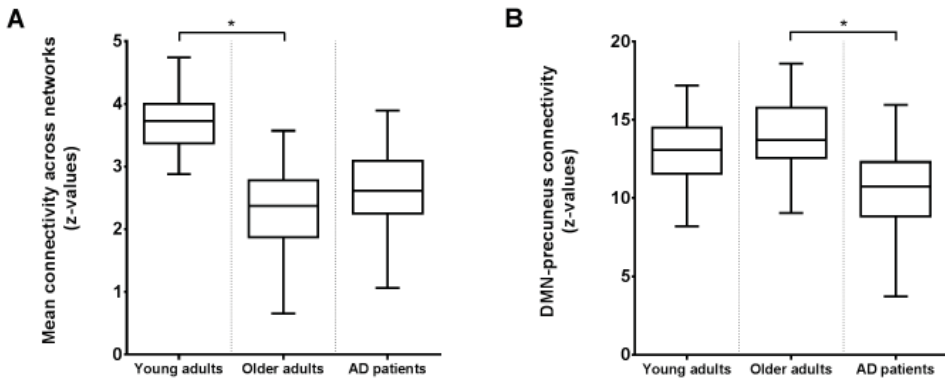


Figure 4.3. Boxplots of the average functional connectivity (z-values) in young and older adults and AD patients between (A) regions and networks as shown in Figure 4.1A with reduced connectivity in elderly compared to young subjects; (B) the precuneus and DMN as shown in Figure 4.2A with reduced connectivity in AD patients compared to elderly controls. Asterisks indicate a significant difference between groups (at $p < 0.05$, corrected).

DISCUSSION

We investigated how functional brain connectivity patterns in aging relate to connectivity as seen in AD. Brain connectivity as measured with RS-fMRI was most profoundly different between young and older adults. In contrast to the widespread disruptions in connectivity due to normal aging, the only altered network in the group of AD patients was the DMN, showing a decline in connectivity with the precuneus. This connotes that on top of reductions due to normal aging, there was an additional decrease in connectivity between the DMN and precuneus in our AD sample. A comparable effect (reduced precuneus-DMN connectivity) was found in our older adults compared to young subjects, even after GM volume control, indicating that both aging and, to a greater extent, AD compromise DMN-precuneus connectivity. The precuneus area that showed differences between groups did not exactly overlap for both comparisons. This is illustrated by Figure 4.3B, showing that DMN-precuneus connectivity for this specific part of the precuneus significantly differs between AD patients and older control adults but not between older and young adults. In AD patients vs. elderly controls, the effect was located more posteriorly than for the older vs. young subjects. Correspondingly, it is especially the posterior part of the precuneus that seems to be implicated in episodic memory retrieval [159]. However, considering the small sample size and possible disease specific reorganization of cortical boundaries [277], this lack of overlap does not conclusively point to AD-specific connectivity alterations.

Although there are some indications for connectivity change in frontoparietal, executive [22], visual sensory, cerebellum/basal ganglia [23], dorsal attention, sensory-motor, control and salience [24, 26] networks, the most consistent and frequent finding in AD is a reduction in DMN

connectivity [20, 261, 267, 268]. Brier et al. [24] showed that more networks become affected with increasing disease severity, which might declare the lack of alterations in networks beyond the DMN in our mild AD group. The relevance of the DMN in AD is explained by its core regions (precuneus, posterior cingulate cortex) being the target of β -amyloid deposition, one of the hallmarks of dementia [263, 278]. The precuneus comprises a central region of the DMN [279], with the highest metabolic response during rest [280] and strong connections with adjacent and remote regions [281]. Altered connectivity with the precuneus in AD patients has frequently been observed [23, 26, 198, 282-286]. The precuneus seems to play a significant role in episodic memory retrieval, self-consciousness and visual-spatial imagery [159, 160] and structural and task-related functional MRI studies have shown its association with memory problems and visual-spatial symptoms in AD [287-289]. Involvement of the precuneus in early AD has also been demonstrated by inflated uptake of Pittsburgh compound B (^{11}C PIB) in this area during positron emission tomography (PET), indicating increased levels of beta amyloid compared to nondemented subjects [290]. Studies that investigated pharmacological effects in AD show the importance of precuneus connectivity in AD as well. Memantine, an N-methyl-d-aspartate (NMDA) receptor antagonist and galantamine, a cholinesterase inhibitor, both used for treatment of early AD symptoms, increased resting-state functional connectivity between the DMN and precuneus in AD [92, 291], pointing to a normalizing effect of these compounds on AD symptomatology.

In contrast to the restricted DMN-precuneus disconnections in AD, aging effects on connectivity were extensive, involving multiple networks and regions. These findings indicate that functional network coherence is more sensitive to aging than AD. Reduced connectivity in the older adults was demonstrated for networks that pertain to language, attention, visual, auditory, motor and executive functioning as well as the DMN. The widespread decreases in connectivity in the older adults compared to the young group may be representative of age-related cognitive, sensory and motor decline. Hearing, vision and balance-gait problems arise and a gradual decrease in processing speed, episodic and working memory takes place during the process of normal aging [254-256]. The effects for the sensorimotor and frontoparietal networks are in line with studies of Allen et al. [41], Andrews-Hanna et al. [28], Tomasi and Volkow [42] and Wu et al. [40, 270], showing an age-related decrease of connectivity between and within motor and attention networks. The cognitive function of the DMN is not fully understood, but diminished connectivity of this network is likely accompanied by a general disturbance in switching to higher-order cognitive processes as (autobiographical) episodic memory, introspection and attention [292, 293]. The reduced coherence of DMN regions might reflect an inability to shift from a task-negative to a task-positive mode and hence hinder cognitive performance. This is concordant with results of Andrews-Hanna et al. [28] and Damoiseaux et al. [37], who demonstrated that alterations of the DMN in elderly subjects were associated with memory, executive functioning and processing speed.

It is questionable whether group differences in connectivity are fully or partly explained by reductions in GM volume. Although exact causal mechanisms are not completely clear, connectivity alterations are possibly representative of structural atrophy [18]. A global decrease in GM has been found with advancing age, affecting frontal, parietal, temporal and occipital cortices, precuneus, anterior cingulate, insula, cerebellum, pre- and postcentral gyri [294-296]. It has been proposed that ignoring structural information in voxelwise analyses could bias interpretation of functional outcomes [273], as apparent functional differences might be solely the consequence of anatomical variation. However, consistent with our outcome, it has also been demonstrated that age-related differences in functional connectivity cannot merely be explained by local decreases in GM volume [26, 37, 39, 297]. When we added voxelwise GM volume maps as confound regressor to account for its possible mediating effect, a substantial portion of results (41.1%), involving equal networks, was maintained. For those areas, GM partial volume fraction is expected to be homogeneous among groups and functional effects are strong enough to persist after correction. Although the earliest atrophy in Alzheimer's disease (AD) occurs in medial temporal structures as the hippocampus [298, 299], the precuneus has also been discovered as an area where atrophy appears in AD patients [287, 300, 301]. The observed difference between AD patients and elderly controls partly survived correction for GM volume (34.2%), suggesting that this finding is related to differences in cortical volume as well. More important, as the remaining effect on connectivity was unrelated to local structural differences, reduced DMN-precuneus connectivity might be an indicator of AD.

The small sample size ($n = 12$ per group) is an obvious limitation of our study as this reduces the power of the statistical analyses. It is possible that with a larger sample size, the DMN-precuneus connectivity change would show more overlap between the two group comparisons. However, we collected six RS-fMRI scans per subject, leading to a dataset of 72 scans per group. In addition to a gain in power, this offered us the possibility of investigating intrasubject as well as intersubject variation. The difference in effect for both group comparisons may partially be explained by higher within and between subject variance at older age and in AD [302, 303]. An exploration of the average connectivity (in z-values) across networks and voxels per scan did not show prominent differences in connectivity variance between the three groups (young subjects: mean = 4.12, variance^{between} = 0.90 and variance^{within} = 0.86; older adults: mean = 4.37, variance^{between} = 1.63 and variance^{within} = 1.29; AD patients, mean = 4.28, variance^{between} = 0.86 and variance^{within} = 1.26), largely ruling out this possibility. Further, although all older adults were intensively screened before study participation, no information on AD-associated biomarkers was available. As alterations in brain connectivity might also be due to beta-amyloid deposition in older people without AD [304, 305], the healthy elderly subjects in this study might unexpectedly include subjects in a preclinical AD stage, leading to AD- instead of age-related connectivity change.

In conclusion, differences in functional connectivity between young and older adults are more extensive than differences between AD patients and controls. We found reduced connectivity throughout the entire brain in older compared to young adults, which is potentially reflective of a normative decline in sensory, motor and cognitive function during senescence. In AD patients vs. elderly controls, the detected effect was restricted to further diminished connectivity of the DMN with the precuneus. Although the majority of these connections was associated with regional brain volume, effects were maintained for all networks after correction for GM volume. Our findings imply that posterior precuneus-DMN disconnections may act as a marker of AD pathology.

Author contributions

JvG, SR, and JvdG: Substantial contributions to the conception or design of the work, data acquisition. JvG, SR, JvdG, and Fd: Data analysis. JvG, SR, JvdG, Fd, and CM: Interpretation of data, drafting, and critical revision of the work for important intellectual content. All authors have approved the final version of the work and agree to be accountable for all aspects of the work in ensuring that questions related to the accuracy or integrity of any part of the work are appropriately investigated and resolved.

Funding

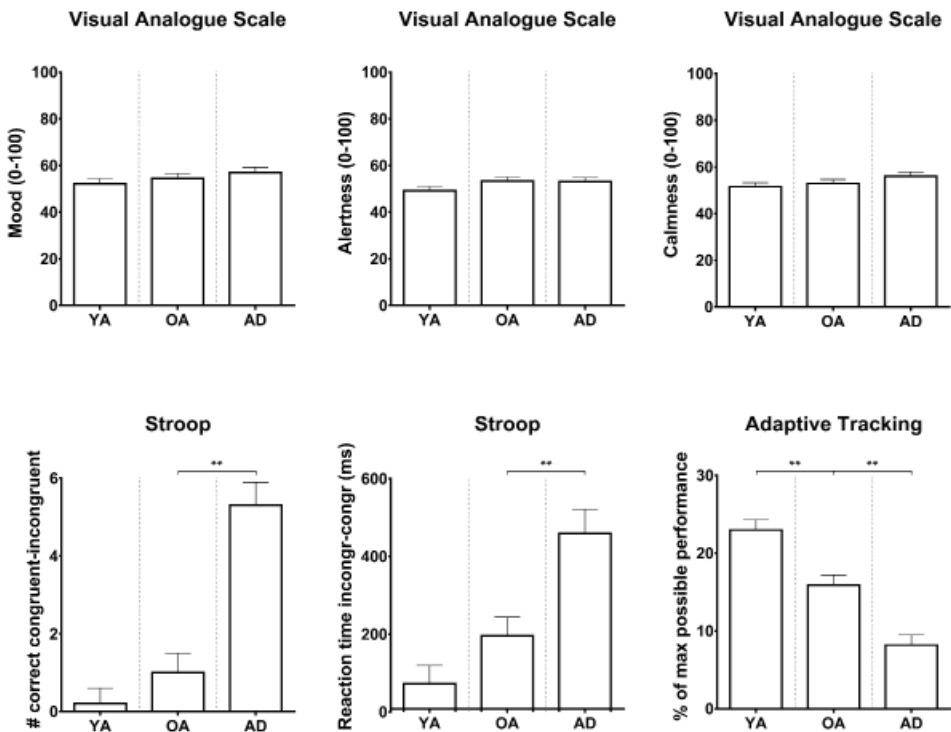
This study was funded by the Netherlands Initiative Brain and Cognition (NIHC), a part of the Netherlands Organization for Scientific Research (NWO) (grant number 056-13-016). SR is supported by a VICI grant from NWO (grant number 016-130-677).

Acknowledgements

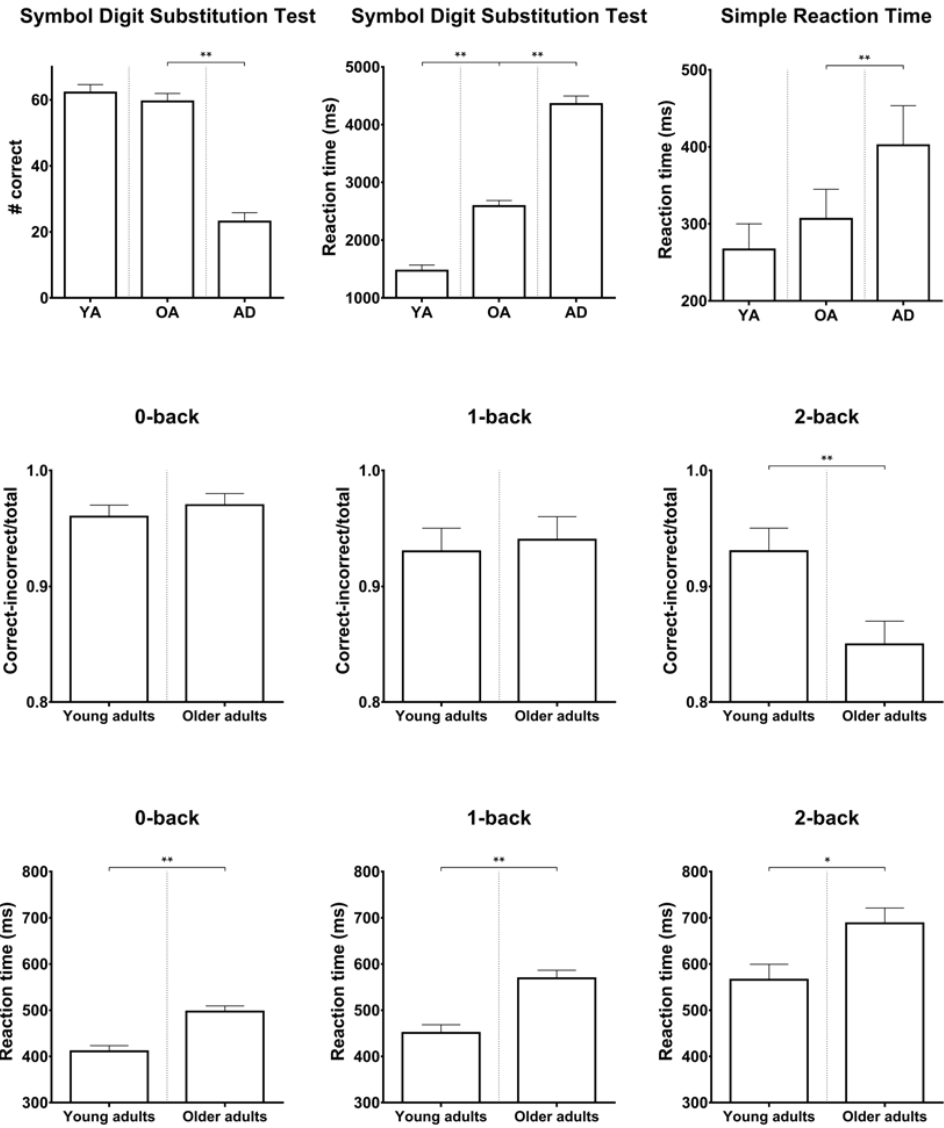
We are thankful for the assistance of the Alrijne Hospital Leiden, Alzheimer Nederland and GGZ Rivierduinen Leiden in the recruitment of AD patients. Erica Klaassen (Centre for Human Drug Research) is acknowledged for her contribution to statistical analyses.

SUPPLEMENTARY MATERIAL

All subjects performed cognitive tasks on a computerized NeuroCart® test battery measuring alertness, mood and calmness (Visual Analogue Scales (VAS) Bond & Lader), vigilance and visual motor performance (Adaptive Tracking task), reaction time (Simple Reaction Time task), attention, short-term memory, psychomotor speed, task switching and inhibition (Symbol Digit Substitution Test and Stroop task), working memory (N-back task) [95-98, 100-103]. All repeatedly measured NeuroCart® endpoints were analyzed using a mixed effects model with group, time and group by time as fixed effects, subject, subject by group and subject by time as random effects (SAS for Windows V9.1.3; SAS Institute, Inc., Cary, NC, USA). As data of the Simple Reaction Time task were not normally distributed, these data were log-transformed before analysis and back transformed after analysis. Group comparisons for the cognitive and subjective tests showed differences between the young and elderly subjects and between the elderly and AD patients for memory function, learning, attention and visuomotor skill. An overview of the results on performance tasks is provided in Supplementary Figure S4.1.



Supplementary Figure S4.1. Bar graphs of least squares means of performance on the NeuroCart® cognitive test battery with standard error of the means as error bars. Abbreviations: YA = young adults; OA = older adults; AD = patients with Alzheimer's disease; * = significant at $p < 0.05$; ** = significant at $p < 0.01$. Note: the N-back task for AD patients is an adapted (easier) version. It was therefore not possible to compare performance between AD patients and elderly controls. *Figure continues on next page.*



Supplementary Figure S4.1. *Continued.*

Chapter 5

Serotonergic and cholinergic modulation of functional brain connectivity: a comparison between young and older adults

Published in NeuroImage 2018; 169:312-322

Bernadet L. Klaassens^{a,b,c,d}, Joop M.A. van Gerven^d, Erica S. Klaassen^d, Jeroen van der Grond^b, Serge A.R.B. Rombouts^{a,b,c}

^aLeiden University, Institute of Psychology, Leiden, the Netherlands, ^bLeiden University Medical Center, Department of Radiology, Leiden, the Netherlands, ^cLeiden University, Leiden Institute for Brain and Cognition, Leiden, the Netherlands, ^dCentre for Human Drug Research, Leiden, the Netherlands

ABSTRACT

Aging is accompanied by changes in neurotransmission. To advance our understanding of how aging modifies specific neural circuitries, we examined serotonergic and cholinergic stimulation with resting state functional magnetic resonance imaging (RS-fMRI) in young and older adults. The instant response to the selective serotonin reuptake inhibitor citalopram (30 mg) and the acetylcholinesterase inhibitor galantamine (8 mg) was measured in 12 young and 17 older volunteers during a randomized, double blind, placebo-controlled, crossover study. A powerful dataset consisting of 522 RS-fMRI scans was obtained by acquiring multiple scans per subject before and after drug administration. Group x treatment interaction effects on voxelwise connectivity with ten functional networks were investigated ($p < 0.05$, FWE-corrected) using a non-parametric multivariate analysis technique with cerebrospinal fluid, white matter, heart rate and baseline measurements as covariates. Both groups showed a decrease in sensorimotor network connectivity after citalopram administration. The comparable findings after citalopram intake are possibly due to relatively similar serotonergic systems in the young and older subjects. Galantamine altered connectivity between the occipital visual network and regions that are implicated in learning and memory in the young subjects. The lack of a cholinergic response in the elderly might relate to the well-known association between cognitive and cholinergic deterioration at older age.

INTRODUCTION

During the process of aging, there is a decline in brain function [255]. Reduced synaptic plasticity, transmitter release and receptor availability in the central nervous system (CNS) might affect cognitive and behavioral performance [44, 306]. Impaired cholinergic transmission has been associated with age-related disruptions in attention and memory storage and retrieval, [53, 307-309], whereas serotonin (5-hydroxytryptamine; 5-HT) dysregulation may contribute to the increased prevalence of depressive symptoms in the elderly [45, 47, 310].

Magnetic resonance imaging (MRI) of resting state functional connectivity cannot be used to measure neurotransmission directly, but is commonly applied to improve insight into neurotransmitter function by studying brain networks after a pharmacological intervention [76, 79, 118, 311-313]. With regard to aging, the effects of serotonergic and cholinergic challenges on brain connectivity are especially relevant as compounds acting on these systems are used to treat depression and dementia [50, 189].

Acute or short-term dosing of drugs that prevent the presynaptic reuptake of serotonin seems to counteract the observed increased connectivity patterns in depression [88], showing reduced connectivity with several cortical and subcortical areas in healthy and depressed young subjects [82-87, 199, 275]. Cholinesterase inhibitors (AChEIs) cause connectivity enhancement of regions that are important for learning, memory and executive control after long-term treatment in patients with Alzheimer's disease [89-93] and immediately after administration in young subjects [275].

Despite evidence of cholinergic and serotonergic alterations with aging, it is unknown how the corresponding connectivity pathways are altered at older age. There is little proof of differentiated effects of selective serotonin reuptake inhibitors (SSRIs) and AChEIs on subjective and cognitive measures between healthy young and older subjects [167, 215, 314]. However, during senescence 5-HT receptor density declines [315] and the cholinergic system has been suggested to have diminished and more variable responsiveness [309, 316]. Given a negative association of aging with neuromodulation and brain function, we anticipate that effects of the SSRI citalopram and the AChEI galantamine on resting state connectivity are more constrained in older compared to young subjects.

MATERIALS AND METHODS

Subjects

Twelve healthy young volunteers (mean age 22.8 ± 2.8 ; age range 18-27; 6 female/6 male; body mass index range 21-28 kg/m²) and 17 healthy older adults (mean age 71.2 ± 6.1 ; age range 61-

79; 9 female/8 male; body mass index range 22-31 kg/m²) were included in the study. All subjects underwent a thorough medical screening at the Centre for Human Drug Research (CHDR) to investigate whether they met the inclusion and exclusion criteria. They had a normal history of physical and mental health and were able to refrain from using nicotine and caffeine during study days. Exclusion criteria included a positive drug or alcohol test on study days, regular excessive consumption of alcohol (>4 units/day), caffeine (>6 units/day) or cigarettes (>5 cigarettes/day), use of concomitant medication 2 weeks prior to study participation and involvement in an investigational drug trial 3 months prior to administration. The study was approved by the medical ethics committee of the Leiden University Medical Center (LUMC). Written informed consent was obtained from each subject prior to study participation.

Study design

Part of the data, showing drug effects in young adults, have been described previously [275]. This was a single center, double blind, placebo-controlled, crossover study with citalopram 30 mg and galantamine 8 mg. Citalopram has an average time point of maximum concentration (T_{max}) of 2-4 h, with a half-life ($T_{1/2}$) of 36 h. For galantamine, T_{max} = 1-2 h and $T_{1/2}$ = 7-8 h. To correct for the different pharmacokinetic (PK) profiles and obtain all pharmacodynamic measures within an equal time frame at around the T_{max} of both compounds, citalopram was administered earlier than galantamine. In addition, since a lower dose of SSRIs is recommended in elderly compared to young subjects [317], it was decided to retain the opportunity of administering a lower dose of citalopram in elderly than in young subjects. Therefore, citalopram 20 mg was administered at $T = 0$ h, followed by a second dose of 10 mg at $T = 1$ h (only if the first dose was tolerated). Galantamine was given as a single 8 mg dose at $T = 2$ h. Blinding was maintained by concomitant administration of double-dummy placebo's at all three time points. All subjects also received an unblinded dose of granisetron 2 mg at $T = -0.5$ h, to prevent the most common drug-induced adverse effects of nausea and vomiting.

Six resting state fMRI (RS-fMRI) scans were acquired during study days, two at baseline and four after administering citalopram, galantamine or placebo (at $T = 2.5, 3.5, 4.5$ and 6 h). Each scan was followed by performance of computerized cognitive tasks (taken twice at baseline) on the NeuroCart® test battery, developed by the CHDR for quantifying pharmacological effects on the CNS [167, 204, 205]. By including multiple measurements during the T_{max} interval, this repeated measures profile increases the statistical power of the analysis and allows for identification of time related effects, associated with changing drug concentrations related to absorption, distribution, metabolism and excretion. Nine blood samples were taken during the course of the day to define the PK profile of citalopram, citalopram's active metabolite desmethylcitalopram, galantamine and concentrations of cortisol and prolactin [182, 206]. Washout period between study days was at least 7 days. An overview of the study design is provided in Figure 5.1.

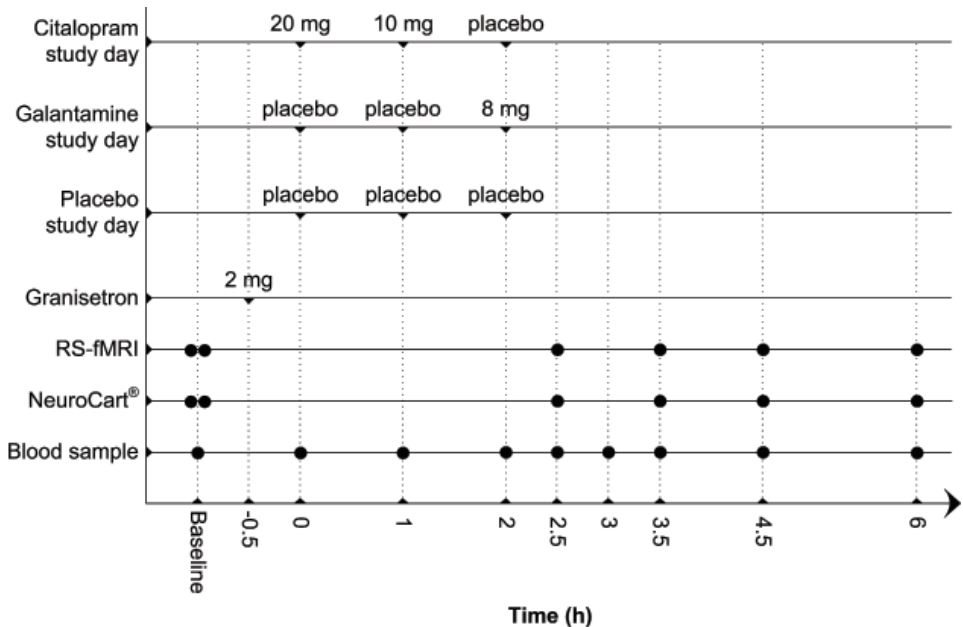


Figure 5.1. Schematic overview of the study design. Each subject received citalopram, galantamine and placebo on three different study days. On each study day there were three moments of administration. The second administration only took place when subjects tolerated the first dose well (did not vomit or feel too nauseous). At baseline, two RS-fMRI scans were acquired, followed by the NeuroCart® test battery. On all study days, subjects received 2 mg of granisetron 30 min before drug administration, to prevent for possible side effects of citalopram and/or galantamine. After drug administration, four RS-fMRI scans were acquired at time points T = 2.5, 3.5, 4.5 and 6 h post dosing, each time followed by the NeuroCart® test battery. During the day, nine blood samples were taken to measure the concentrations of citalopram, desmethylcitalopram, galantamine, cortisol and prolactin.

Outcome measures

Pharmacokinetics

Pharmacokinetic parameters for citalopram, galantamine and citalopram's active metabolite desmethylcitalopram were calculated using a non-compartmental analysis to validate the choice of time points of pharmacodynamic endpoints and, in case of equal absorption rates, increase confidence in pharmacodynamic outcomes (RS-fMRI, NeuroCart®, neuroendocrine measures). Blood samples were collected in 4 mL EDTA plasma tubes at baseline and 1, 2, 2.5, 3, 3.5, 4.5 and 6 h post dosing, centrifuged (2000 g for 10 min) and stored at -40°C until analysis with liquid chromatography-tandem mass spectrometry (LC-MS/MS).

Neuroendocrine variables

Blood samples were also obtained to determine cortisol and prolactin concentrations. Serum samples were taken in a 3.5 mL gel tube at baseline (twice) and 1, 2, 2.5, 3.5, 4.5 and 6 h post

dosing, centrifuged (2000 g for 10 min) and stored at -40°C until analysis. Serum concentrations were quantitatively determined with electrochemiluminescence immunoassay.

NeuroCart® test battery

Each RS-fMRI scan was followed by functional CNS measures outside the scanner using the computerized NeuroCart® test battery measuring alertness, mood and calmness (Visual Analogue Scales (VAS) Bond & Lader), nausea (VAS Nausea), vigilance and visual motor performance (Adaptive Tracking task), reaction time (Simple Reaction Time task), attention, short-term memory, psychomotor speed, task switching and inhibition (Symbol Digit Substitution Test and Stroop task), working memory (N-back task) and memory imprinting and retrieval (Visual Verbal Learning Test) [95-103]. The Visual Verbal Learning Test was only performed once during each day (at 3 and 4 h post dosing) as the test itself consists of different trials (imprinting and retrieval). Duration of each series of NeuroCart® brain function tests was approximately 20 min. To minimize learning effects, training for the NeuroCart® tasks occurred during the screening visit within 3 weeks prior to the first study day.

MR imaging

Scanning was performed at the LUMC on a Philips 3.0 Tesla Achieva MRI scanner (Philips Medical System, Best, The Netherlands) using a 32-channel head coil. During the RS-fMRI scans, all subjects were asked to close their eyes while staying awake. Instructions were given prior to each scan on all study days. T1-weighted anatomical images were acquired once per visit. To facilitate registration to the anatomical image, each RS-fMRI scan was followed by a high-resolution T2*-weighted echo-planar scan.

RS-fMRI data were obtained with T2*-weighted echo-planar imaging (EPI) with the following scan parameters: 220 whole brain volumes, repetition time (TR) = 2180 ms; echo time (TE) = 30 ms; flip angle = 85°; field-of-view (FOV) = 220 x 220 x 130 mm; in-plane voxel resolution = 3.44 x 3.44 mm, slice thickness = 3.44 mm, including 10% interslice gap; acquisition time 8 min. For 3D T1-weighted MRI the following parameters were used: TR = 9.7 ms; TE = 4.6 ms; flip angle = 8°; FOV = 224 x 177 x 168 mm; in-plane voxel resolution = 1.17 x 1.17 mm; slice thickness = 1.2 mm; acquisition time 5 min. Parameters of high-resolution T2*-weighted EPI scans were set to: TR = 2200 ms; TE = 30 ms; flip angle = 80°; FOV = 220 x 220 x 168 mm; in-plane voxel resolution = 1.96 x 1.96 mm; slice thickness = 2.0 mm; acquisition time 30 s.

Statistical analysis

Pharmacokinetics

Maximum plasma concentrations (C_{\max}) and time of C_{\max} (T_{\max}) were obtained directly from the plasma concentration data. The area under the plasma concentration vs. time curve was

calculated from time zero to the time of the last quantifiable measured plasma concentration (AUC_{0-last}). To investigate differences between groups, PK parameters were analyzed using a mixed effects model with group as fixed effect (SAS for Windows V9.4; SAS Institute, Inc., Cary, NC, USA).

Neuroendocrine variables

Treatment (drug vs. placebo) x group (young vs. older subjects) interaction effects on cortisol and prolactin concentrations were investigated using a mixed effects model with treatment, time, group, visit, treatment by time, treatment by group and treatment by group by time as fixed effects, subject, subject by treatment and subject by time as random effects and the average of the period baseline (pre-dose) values as covariate (SAS for Windows V9.4; SAS Institute, Inc., Cary, NC, USA). The data were not normally distributed and therefore log-transformed before analysis and back transformed after analysis.

NeuroCart® test battery

All post-dose repeatedly measured NeuroCart® measures were analyzed using the same mixed effects model as for neuroendocrine variables. As data of the Simple Reaction Time task were not normally distributed, these data were log-transformed before analysis and back transformed after analysis. The data of the Visual Verbal Learning Test were analyzed using a mixed effects model with treatment, group, visit and treatment by group as fixed effects and subject as random effect.

MR imaging

All analyses were performed using the Functional Magnetic Resonance Imaging of the Brain (fMRIB) Software Library (FSL, Oxford, United Kingdom) version 5.0.7 [119-121].

Data preprocessing

Each individual functional EPI image was inspected, brain-extracted and corrected for geometrical displacements due to head movement with linear (affine) image registration [122, 123]. Images were spatially smoothed with a 6 mm full-width half-maximum Gaussian kernel. Registration parameters for non-smoothed data were estimated to transform fMRI scans into standard space and co-registered with the brain extracted high resolution T2*-weighted EPI scans (with 6 degrees of freedom) and T1 weighted images (using the Boundary-Based-Registration method) [124]. The T1-weighted scans were non-linearly registered to the MNI 152 standard space (the Montreal Neurological Institute, Montreal, QC, Canada) using fMRIB's Non-linear Image Registration Tool. Registration parameters were estimated on non-smoothed data to transform fMRI scans into standard space after Automatic Removal of Motion Artifacts based on Independent Component Analysis (ICA-AROMA vs0.3-beta). ICA-AROMA attempts to identify and remove motion related noise components by investigating its temporal and spatial properties. As recommended, high

pass temporal filtering (with a high pass filter of 150 s) was applied after denoising the fMRI data with ICA-AROMA [207, 208].

Estimation of network connectivity

RS-fMRI networks were extracted from each individual denoised RS-fMRI dataset (29 subjects x 3 days x 6 scans = 522 datasets) with a dual regression analysis [36, 125] based on 10 predefined standard network templates as used in our previous research [199, 275]. These standard templates have been identified using a data-driven approach [10] and comprise the following networks: three visual networks (consisting of medial, occipital pole, and lateral visual areas), default mode network, cerebellar network, sensorimotor network, auditory network, executive control network and two frontoparietal networks (left and right). Time series of white matter (measured from the center of the corpus callosum) and cerebrospinal fluid (measured from the center of lateral ventricles) were added as confound regressors in this analysis to account for non-neuronal signal fluctuations [126]. With the dual regression method, spatial maps representing voxel-to-network connectivity were estimated for each dataset separately in two stages and used for higher level analysis. First, the weighted network maps were used in a spatial regression into each dataset. This stage generated 12 time series per dataset that describe the average temporal course of signal fluctuations of the 10 networks plus 2 confound regressors (cerebrospinal fluid and white matter). Next, these time series were entered in a temporal regression into the same dataset. This resulted in a spatial map per network per dataset with regression coefficients referring to the weight of each voxel being associated with the characteristic signal change of a specific network. The higher the value of the coefficient, the stronger the connectivity of this voxel with a given network.

Higher level analysis

To investigate group x treatment interaction effects of citalopram and galantamine we used non-parametric combination (NPC) as provided by FSL's Permutation Analysis for Linear Models tool (PALM vs94-alpha) [129, 209, 210]. NPC is a multivariate method that offers the possibility to combine data of separate, possibly non-independent tests, such as our multiple time points, and investigate the presence of joint effects across time points, in a test that has fewer assumptions and is more powerful than repeated-measurements analysis of variance (ANOVA) or multivariate analysis of variance (MANOVA). NPC testing was used in two phases to estimate for each network whether drug vs. placebo effects on connectivity were significantly different between young and older subjects.

First, tests were performed for each post-dose time point ($T = 2.5, 3.5, 4.5$ and 6 h) separately, using 1000 synchronized permutations, followed by the fit of a generalized Pareto distribution to the tail of the approximation distribution, thus refining the p -values at the tail further than otherwise possible with a small number of permutations [318]. To investigate group x treatment

interaction effects on voxelwise functional connectivity with each of the 10 functional networks, four two-sample t-tests (young adults: drug - placebo vs. older adults: drug - placebo) were performed, one per time point, with average heart rate (beats/m) per RS-fMRI scan as confound regressor [127]. The average of the two baseline RS-fMRI scans was used as covariate as well, by adding the coefficient spatial map as a voxel-dependent regressor in the model. This will control for the confounding influence of possibly systematic individual differences and age-related differences at baseline level as recently analyzed and described in Klaassens et al. [319]. The same method was applied for additional investigation of treatment effects (drug vs. placebo) within the group of older adults as was previously done for the group of young adults [275]. To that end, four one-sample t-tests (drug vs. placebo) were performed for all post-dose time points ($T = 2.5, 3.5, 4.5$ and 6 h), with average heart rate (beats/m) per RS-fMRI scan and the average of the two baseline RS-fMRI scans as covariates.

Second, to analyze effects across time, the tests for the four time points were combined non-parametrically via NPC using Fisher's combining function [211] and the same set of synchronized permutations as mentioned above. A liberal mask was used to investigate voxels within the MNI template, excluding voxels belonging to cerebrospinal fluid. Threshold-free cluster enhancement was applied to the tests at each time point and after the combination, and the resulting voxelwise statistical maps were corrected for the familywise error rate using the distribution of the maximum statistic [128, 129]. Voxels were considered significant at p -values < 0.05 , corrected.

RESULTS

Pharmacokinetics

Table 5.1 provides an overview of the PK parameters in young and older subjects, and the statistical outcomes of group analyses. In comparison to the young subjects, the T_{\max} of galantamine occurred significantly later in the older adults ($p < 0.001$). There were no further pharmacokinetic differences between young and older subjects. Figure 5.2 shows individual and median PK time profiles.

Cortisol and prolactin

There was a significant group x treatment interaction effect of citalopram and galantamine on cortisol ($p < 0.05$). In comparison to the young subjects, the increase in cortisol was significantly larger in the older adults after citalopram and galantamine, relative to placebo. There was no significant group x treatment interaction effect on prolactin. In both groups, there was an increase in prolactin after citalopram vs. placebo ($p < 0.005$). Galantamine did not affect the level of prolactin. See Figure 5.3 for cortisol and prolactin levels in young and older subjects.

Table 5.1. Pharmacokinetics of citalopram, desmethylcitalopram and galantamine in young and older adults

PK parameters	Citalopram		Desmethylcitalopram		Galantamine		Contrasts (p-value)
	Mean ± SD		Mean ± SD		Mean ± SD		
	Young adults	Older adults	Young adults	Older adults	Young adults	Older adults	
T_{max}	3.0 ± 1.2	3.4 ± 1.1	4.9 ± 1.3	4.0 ± 1.3	2.7 ± 1.1	4.5 ± 1.1	< 0.001
C_{max}	35.8 ± 6.3	41.8 ± 11.7	3.0 ± 1.1	3.5 ± 1.8	40.7 ± 10.4	41.8 ± 12.2	0.811
AUC_{0-list}	146.0 ± 25.2	165.0 ± 43.6	11.7 ± 4.8	13.3 ± 7.1	95.1 ± 27.7	104 ± 40.2	0.494

Abbreviations: PK = pharmacokinetic; T_{max} = time point (h) of maximum concentration; C_{max} = maximum concentration (ng/mL); AUC_{0-list} = area under the plasma concentration vs. time curve (ng*h/mL).

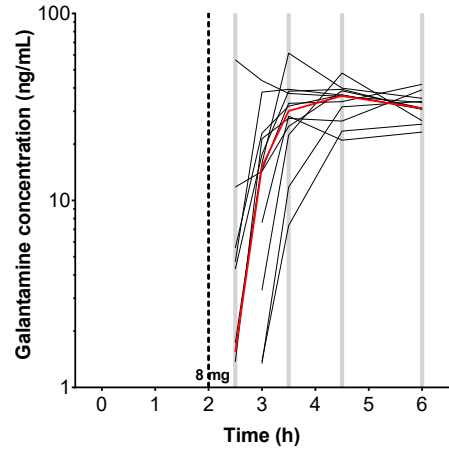
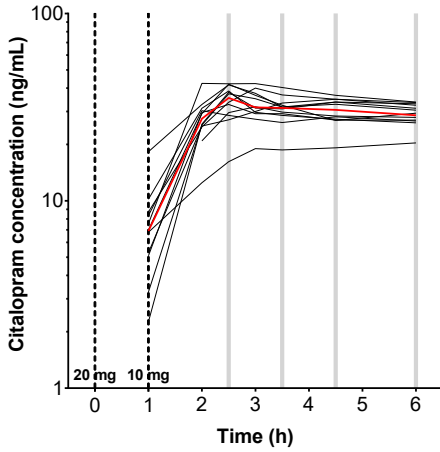
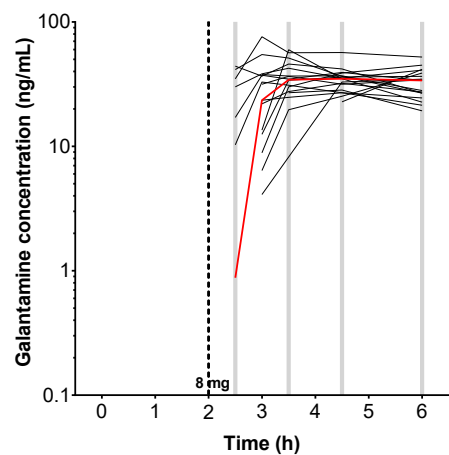
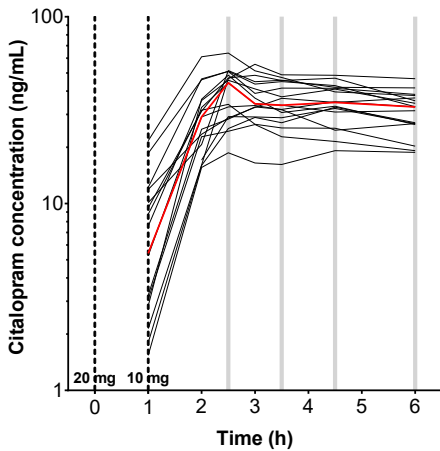
A Young adults**B Older adults**

Figure 5.2. Median (red line) and individual (black lines) pharmacokinetic profiles for citalopram (left) and galantamine (right) concentrations in nanograms per milliliter on semi-log scale in young (A) and older (B) subjects. Grey bars illustrate moments of RS-fMRI acquisition post drug administration. Observations below limit of quantification were dismissed.

NeuroCart® test battery

Supplementary Table S5.1 provides an overview of all NeuroCart® results. There were no convincing significant group x treatment interaction effects after galantamine or citalopram vs. placebo on any NeuroCart® measure.

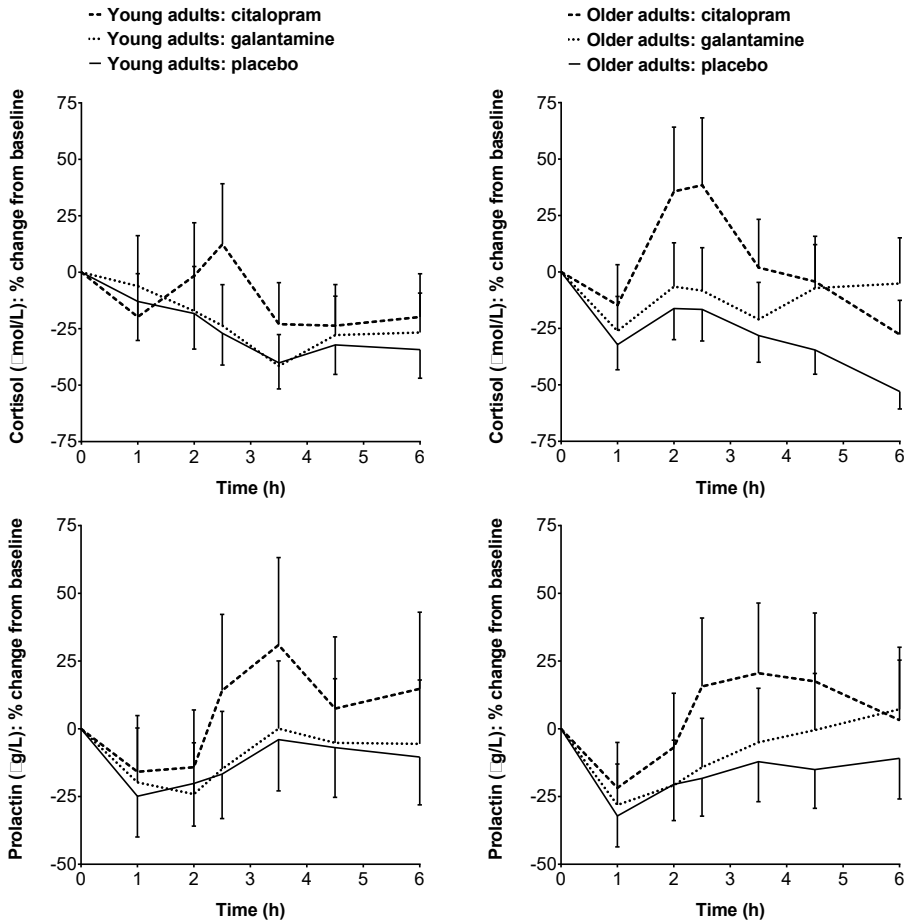


Figure 5.3. Least squares means percent change from baseline profiles of cortisol and prolactin concentrations (with standard errors of the mean as error bars) in young (left) and older (right) subjects.

Functional connectivity

Serotonergic effects

There was no group \times treatment interaction effect of citalopram on functional network connectivity. We did find main treatment effects of citalopram on connectivity with the sensorimotor network in both groups. Within the young subjects, citalopram decreased connectivity between the sensorimotor network and supplementary motor area, pre- and postcentral gyrus, anterior and posterior cingulate cortex (ACC and PCC), precuneus, medial and orbital prefrontal cortex, and cerebellum. Within the older adults, citalopram decreased connectivity between the sensorimotor network and supplementary motor area, pre- and postcentral gyrus, ACC, PCC, cingulate gyrus, precuneus, superior frontal gyrus and frontal orbital cortex (Figure 5.4). Specifications and extent of significant citalopram effects are summarized in Table 5.2.

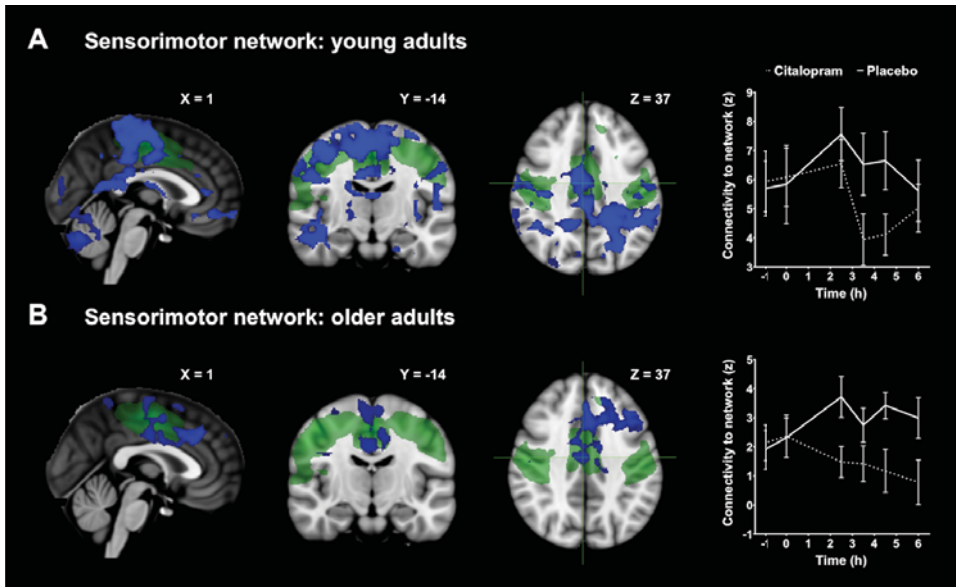


Figure 5.4. Decreased connectivity in young (A) and older subjects (B) after citalopram vs. placebo was observed between the sensorimotor network (shown in green) and regions as shown in blue. Plots visualize the corresponding average time profiles of changes in functional connectivity for citalopram (dotted line) and placebo (continuous line) conditions (z-values with standard errors of the mean as error bars). Coronal and axial slices are displayed in radiological convention (left = right).

Cholinergic effects

An interaction effect of galantamine was found for one visual network (occipital pole). An increase in connectivity after galantamine vs. placebo was significantly larger in the young compared to the older adults between the occipital visual network and the precuneus, PCC, postcentral-, angular- and supramarginal gyrus (Figure 5.5). Galantamine led to increased connectivity between the occipital visual network and the left and right hippocampus, precuneus, thalamus, fusiform gyrus, precentral and superior frontal gyrus, PCC and cerebellum in the young subjects, whereas no significant treatment effect of galantamine on this network was detected in the group of older adults. Specifications and extent of significant galantamine effects are summarized in Table 5.3.

DISCUSSION

To study the influence of older age on neurotransmitter pathways, we investigated differences in functional network responsiveness to single-dose serotonergic and cholinergic stimulation between young and older adults, independent of between-group variation in brain connectivity at baseline [319]. We found a significantly weaker pharmacological effect of galantamine on

Table 5.2. Overview of significant citalopram effects on functional connectivity as estimated with threshold-free cluster enhancement ($p < 0.05$, corrected)

Network effect	Region (Harvard-Oxford)	z^*	x	y	z	# voxels
Sensorimotor network (Young adults: drug < placebo)	L/R/M ACC, PCC, precuneus, SMA, pre- and postcentral gyrus, medial and orbital frontal cortex, cerebellum	5.23	-22	50	-16	36214
	L Inferior temporal gyrus, inferior and temporooccipital part	3.65	-50	-46	-12	153
	L Occipital fusiform gyrus	3.58	-40	-74	-18	94
	L Cerebellum	4.03	-28	-42	-32	52
Sensorimotor network (Older adults: drug < placebo)	L/R/M SMA, superior and middle frontal gyrus, ACC, PCC, paracingulate gyrus	4.27	-36	26	40	4076
	L/R/M Precuneus, postcentral gyrus, posterior cingulate gyrus, superior parietal lobule	3.52	0	-48	64	467
	L Temporal pole, frontal orbital cortex	4.54	-46	14	-18	368
	R Pre- en postcentral gyrus	3.34	34	-10	30	258
	R Occipital fusiform gyrus	4.29	30	-64	-16	204
	R Precentral gyrus	2.76	32	-12	68	41
	R Occipital fusiform gyrus	3.65	24	-78	-18	32
	R Middle frontal gyrus, frontal pole	3.43	28	36	34	30
	R Occipital fusiform gyrus	3.43	16	-82	-26	18
	R Precentral gyrus	3.33	20	-36	42	15

Abbreviations: L = left, R = right, M = midline, ACC = anterior cingulate cortex, PCC = posterior cingulate cortex, SMA = supplementary motor area. Voxel dimension = 2 mm x 2 mm x 2 mm (voxel volume 0.008 mL). * = standardized z-value of the uncorrected peak Fisher-statistic (NPC) within regions (with # voxels > 10).

Table 5.3. Overview of significant galantamine effects on functional connectivity as estimated with threshold-free cluster enhancement ($p < 0.05$, corrected)

Network effect	Region (Harvard-Oxford)	z^*	x	y	z	# voxels		
Occipital visual network (group x treatment interaction effect)	R/M	Precuneus, PCC, pre- and postcentral gyrus, posterior cingulate gyrus, posterior supramarginal gyrus, superior parietal lobule	4.15	10	-36	44	1218	
	R	Lateral occipital cortex, superior division	3.83	28	-62	26	224	
	R	Frontal pole	5.13	38	50	28	94	
	R	Cerebellum	4.05	20	-68	-32	79	
	R	Middle and superior frontal gyrus	4.25	34	0	56	57	
	M	Cerebellum	3.78	4	-68	-24	55	
	R	Cerebellum	3.80	20	-54	-34	52	
	R	Lateral occipital cortex, superior division	3.99	18	-60	54	29	
	Occipital visual network (Young adults: drug > placebo)	L/R/M	Hippocampus, thalamus, amygdala, precuneus, PCC, lateral occipital cortex, brain stem, fusiform gyrus, superior and middle frontal gyrus, superior temporal gyrus, pre- and postcentral gyrus and cerebellum	4.86	2	-62	-26	15341
		L	Precuneus, posterior cingulate gyrus	3.15	-16	-52	20	75
L		Temporal pole	3.41	-58	10	-10	18	
R		Inferior frontal gyrus	3.81	48	14	14	17	
L		Lateral occipital cortex, superior division	3.98	-46	-70	26	12	
L		Central opercular cortex, insular cortex	3.11	-46	4	-4	12	

Abbreviations: L = left, R = right, M = midline, PCC = posterior cingulate cortex. Voxel dimension = 2 mm x 2 mm x 2 mm (voxel volume 0.008 mL). * = standardized z-value of the uncorrected peak Fisher-statistic (NPC) within regions (with # voxels > 10).

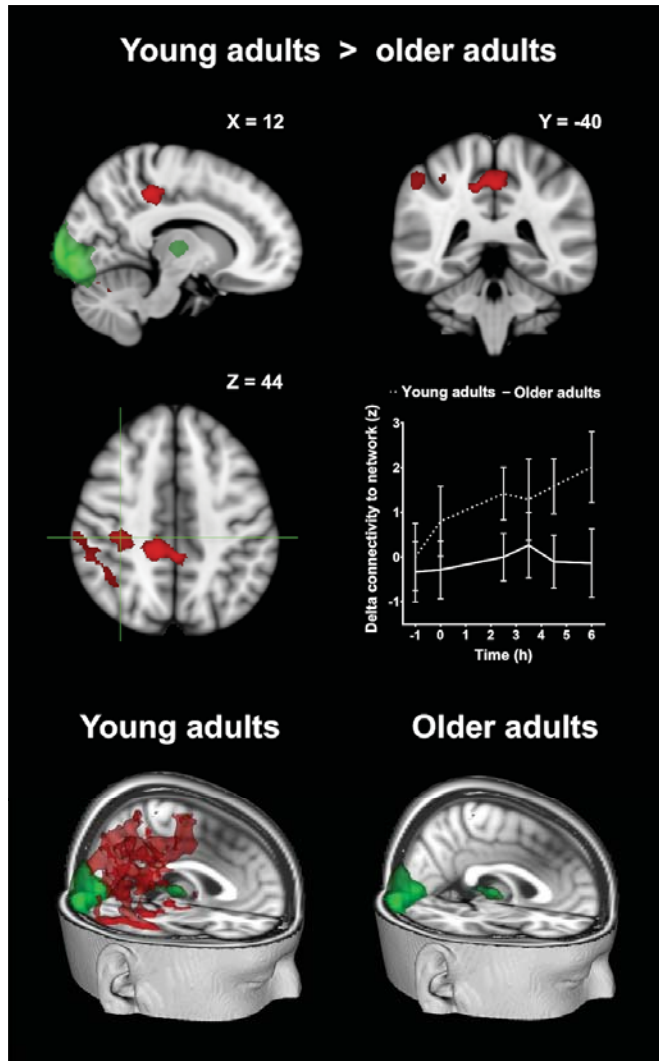


Figure 5.5. A larger effect on connectivity in young compared to older adults after galantamine vs. placebo between the occipital visual network (shown in green) and regions shown in red (top). The plot visualizes the corresponding average time profiles of changes in functional connectivity per group for galantamine - placebo conditions (delta z-values with standard errors of the mean as error bars). The 3D images (bottom) show main galantamine effects per group. Coronal and axial slices are displayed in radiological convention (left = right).

functional integrity of the occipital visual network in the older compared to the young subjects. Since the effects of AChEIs depend on intact cholinergic synapses, this finding might represent the general tendency towards diminished cholinergic function in the elderly [53, 309]. In contrast, older age had no impact on the response to the SSRI citalopram, which induced a strong decrease in connectivity with the sensorimotor network within both groups.

Citalopram

Reduced connections between multiple regions after citalopram administration is consistent with previous SSRI research in healthy young individuals [83, 199]. Although these effects seemed less pronounced in the older adults compared to young subjects, there was no significant difference in effect between the two groups on all networks. As an altered serotonergic system in the elderly has most often been associated with a higher incidence of depression and sleep disorders [45, 310], one explanation for this lack of differences is that there was no evidence for any abnormality of mood, anxiety or sleep in both groups as assessed during screening. The most prominent finding in both samples was a decrease in connectivity between the sensorimotor network and sensorimotor regions, precuneus, ACC and PCC (Figure 5.4). Similar findings have been detected in healthy young subjects with the SSRI sertraline, in which, amongst other networks, sensorimotor network connectivity with the ACC, PCC, precuneus, central gyri and supplementary motor cortex was decreased after single-dose administration [199]. Aging has been shown to alter motor network connectivity, possibly representing deteriorated motor ability in the elderly [40, 270] and leading to the somewhat smaller response in older compared to young subjects. However, in favor of a rather unaffected serotonergic system in our healthy group of elderly, we did not find significantly different changes in sensorimotor connectivity in the much younger subjects. This relative sparing of serotonergic network responsiveness in elderly subjects suggests that the reduced effects of galantamine are indicative of a selective age-related cholinergic decline. Citalopram caused a decrease in connectivity of cortical midline structures as the precuneus, ACC, PCC and prefrontal areas, related to self-referential mechanisms and emotion regulation, which is in line with opposite observations in (non-elderly) depressed patients [88] and indicates that SSRIs might reverse abnormalities in functional connectivity as seen in depression. The effects on sensorimotor connectivity also denote the well-known involvement of 5-HT pathways in motor behavior [320]. For example, an (uncommon) side effect of SSRIs is the observance of movement disorders (e.g. muscle twitches), possibly due to direct adverse effects on motor neurons or enhancement of serotonergic input on dopaminergic pathways [222, 321, 322]. In the young subjects, citalopram also reduced connectivity between the midbrain and left frontoparietal network [275]. This effect was restricted to a discrete region, and a comparable response could not be detected in the older adults, despite the lack of significant differences between groups on this network.

Additional measures of cognitive functioning and neuroendocrine responses were investigated to confirm the presence of neuropharmacological effects and improve the understanding of underlying changes in brain connectivity. There was no difference between young and older adults in effect of citalopram on performance on the NeuroCart® test battery. Single-dose SSRI administration does not seem to alter behavioral states in young and older subjects differently [167, 314]. Acute SSRI effects in healthy subjects of all ages are limited and variable and our protocol did not include more sensitive measures of SSRI modulation as EEG recordings, REM-

sleep and flicker discrimination tests [167]. Since SSRIs are mainly used as a treatment for depression and anxiety disorders [50, 109], the most likely change in our study would have taken place on mood, alertness or calmness as measured with the VAS. However, such improvements are usually only noticeable after a mood-specific behavioral challenge [176, 177, 323] or after a few weeks [173, 174], and accordingly we did not find these effects. The fact that citalopram had pharmacological effects in both age groups is demonstrated by increasing levels of cortisol and prolactin. Neuroendocrine fluctuations can be regarded as indirect measures of the 5-HT system state [216] and a larger increase in cortisol level in the older compared to young adults might be indicative of some serotonergic disturbances that accompany the process of normal aging. However, this interpretation is complicated by the fact that elevated cortisol has been shown to reduce amygdala-medial prefrontal cortex connectivity [183, 324], which in turn seems to be related to baseline cortisol levels. As cortisol was slightly but not significantly lower at baseline in the elderly, this might lead to a stronger drug effect on cortisol and network connectivity in older compared to young adults. There are multiple factors that can cause a decrease in clearance of antidepressants in the elderly [317, 325]. But most of these affect the terminal part of the concentration-time curve and exposure during multiple dosing. The duration of our study was limited, and our elderly subjects were relatively healthy. Consequently, no differences in pharmacokinetic profiles were observed between groups, ensuring comparable exposure in both age groups over the observation period, with similar and limited variability. Because elderly are known to have an increased expectancy for SSRI-related side effects [317], we wanted to provide them with the opportunity to take a lower dose of 20 instead of 30 mg of citalopram, by skipping the second 10 mg if necessary. However, all young and older subjects were administered the total dose of 30 mg without vomiting or experiencing nausea as measured with the VAS. This might also be due to the 2 mg of granisetron, given 30 minutes prior to drug administration on all three study days. Granisetron was added to suppress nausea and vomiting, which could otherwise adversely affect study procedures or alter network effects. Yet, it cannot be excluded that the selective 5-HT₃ receptor agonist granisetron might have also altered specific functional responses [109].

Galantamine

Whereas galantamine increased brain connectivity in the young subjects with one visual network (Figure 5.5), we could not detect any effects of galantamine on resting state connectivity in older adults. The cholinergic system is chiefly associated with an age- and dementia-related decline in memory, learning and attention with evidence pointing to cholinergic dysfunction in the hippocampus, cortex, the entorhinal area, the ventral striatum and the basal forebrain [228, 229]. In our young subjects, galantamine altered connectivity with the hippocampus, thalamus and the fusiform gyrus, areas that are involved in learning and memory [326-328]. ACh release in the primary visual cortex seems to be relevant for visual processing and learning [233, 234].

The findings in the young group are therefore consistent with studies that show an essential role for cholinergic enhancement in visual attention [235, 236], visual episodic memory and recall [238, 241, 242], processing of novel faces [239, 240], perceptual processing during working memory [246] and visual orientation [247]. The absence of effect in the elderly might point to attenuated activity of the cholinergic system, which accompanies the process of normal aging [329]. The sensitivity of the cholinergic system to aging is emphasized by the detection of clear and very similar serotonergic effects on connectivity in both young and older adults. An age-appropriate decline in cognitive function was also observed in our older group compared to the young subjects by investigating the difference in NeuroCart® performance at baseline level (before pharmacological stimulation), as presented in Klaassens et al. [319]. The elderly performed worse on several tests (% correct on the Adaptive Tracking task, reaction time on the Symbol Digit Substitution Test, 0-back, 1-back and 2-back task, and number of correct responses on the 2-back task), relating to decreased attentional, memory and processing speed capacities. Our observations of reduced connectivity alterations after galantamine in the older adults seem to confirm the cholinergic hypothesis of cognitive decline during aging [53].

Galantamine's mean T_{max} in the elderly (mean T_{max} : 4.52 ± 1.08) occurred significantly later than the mean T_{max} in the young subjects (mean T_{max} : 2.67 ± 1.11). This delay in pharmacokinetics might have caused small shifts in the time course of effects, although it is unlikely that this affected the overall response over the duration of the experiment, which was the basis for all principal analyses and comparisons. Since the T_{max} of galantamine was within the time frame of measurements for both groups, analyzing a combination of data points would be minimally influenced by different PK timing profiles. As the level and variability of plasma concentrations, as determined by C_{max} and AUC_{0-last} in the elderly was generally similar to those in the younger group, it is implausible that galantamine effects were obscured by pharmacokinetic dispersion. Moreover, the rise in plasma cortisol after galantamine was larger in elderly than in young subjects, which was particularly noticeable at $T = 2$ and $T = 2.5$. Because galantamine has been shown to increase cortisol [106], this indicates that galantamine was absorbed well enough in the older adults to induce pharmacodynamic effects. Nevertheless, as described earlier this finding may partly influence the observed network effects [183, 324]. In addition, despite the administration of granisetron, an increase in nausea, a typical side effect of AChEIs [330], after galantamine in both groups provides further support for sufficient drug concentrations in the older adults. AChEIs are commonly used to treat cognitive symptoms of Alzheimer's disease [331] and in healthy subjects there is little evidence for neuroenhancement with this drug [73]. A few studies have been performed on AChEI efficacy in subjects without cognitive disturbances, with inconclusive and contradicting results in both young and elderly subjects [73, 215, 238, 332, 333]. Two measures of the delayed recognition subtest of the Visual Verbal Learning Test, the number of correct responses and reaction time, showed a difference between young and older subjects with $p < 0.05$. However, the number of included NeuroCart® tests was large and

the effects were not clearly related to drug levels. Therefore, this marginal result might likely be due to chance, suggesting that AChEI challenges do not affect cognitive performance differently between young and older subjects.

Conclusions

The outcomes of this study illustrate the use of resting state connectivity to investigate different neurotransmitter systems, and how these selectively change with age. The SSRI citalopram affected sensorimotor network connectivity in both young and older adults, demonstrating that SSRIs consistently reduce the functional integrity of regions that are related to motor function and self-reference, regardless of age. The effect of the AChEI galantamine was restricted to the young subjects, who showed a response that indicates the contribution of acetylcholine to perceptual processing and learning mechanisms. We did not observe any network effects in the elderly, possibly reflecting a diminished cholinergic system that is associated with an age-appropriate decline in memory and attention. Combining RS-fMRI with pharmacological challenges and additional outcome measures offers a useful way to investigate age-related functional processes, which is in line with Geerligs and Tsvetanov [334], who recommend to implement an integrative approach in studying neurocognitive aging instead of merely using fMRI data. Compared to cognitive performance, RS-fMRI seems to serve as a relatively sensitive measure of drug-induced functional change. Our findings support the confidence in RS-fMRI as an important tool in psychopharmacological research, and its potential to measure disease specific alterations in neurotransmission.

Acknowledgements

This work was supported by the Netherlands Initiative Brain and Cognition (NIHC), a part of the Netherlands Organisation for Scientific Research (grant number 056-13-016). Serge Rombouts was supported by a VICI grant from NWO (grant number 016-130-677). We thank Helene van Gorsel, Jasper Stevens and Jules Heuberger (CHDR) for medical support and pharmacokinetic analyses.

Supplementary Table S5.1. Summary of group X treatment interaction effects of citalopram and galantamine vs. placebo on the NeuroCart® cognitive test battery

Parameter	Least Squares Means				Contrasts interaction effects (difference, 95% CI, p-value)			
	Young adults: Placebo	Young adults: Citalopram	Young adults: Galantamine	Older adults: Placebo	Older adults: Citalopram	Older adults: Galantamine	Young (citalopram vs. placebo) vs. older adults (citalopram vs. placebo)	Young (galantamine vs. placebo) vs. older adults (galantamine vs. placebo)
VAS Alertness (mm)	50.4	49.4	48.4	51.7	52.0	49.6	1.3 (-2.4, 5.0), <i>p</i> = 0.497	-0.1 (-3.8, 3.6), <i>p</i> = 0.940
VAS Calmness (mm)	52.1	52.0	53.6	53.2	52.8	52.7	-0.3 (-3.6, 2.9), <i>p</i> = 0.839	-2.0 (-5.3, 1.3), <i>p</i> = 0.230
VAS Mood (mm)	53.8	53.9	52.0	54.1	51.7	52.8	1.9 (-1.2, 5.0), <i>p</i> = 0.227	-1.1 (-4.3, 2.0), <i>p</i> = 0.482
VAS Nausea log (mm)	0.36	0.37	0.50	0.30	0.41	0.56	-0.021 (-0.196, 0.155), <i>p</i> = 0.813	-0.002 (-0.176, 0.171), <i>p</i> = 0.977
Adaptive tracking (%)	21.28	20.09	20.0	19.71	20.26	19.51	1.75 (-0.34, 3.83), <i>p</i> = 0.098	1.08 (-0.99, 3.16), <i>p</i> = 0.296
Simple reaction time task (sec)	283.43	293.98	286.57	294.29	291.62	296.47	-4.5 (-11.4, 3.0), <i>p</i> = 0.225	-0.4 (-7.5, 7.4), <i>p</i> = 0.922
Stroop mean RT Incongruent-Congruent (msec)	80.5	108.7	94.0	175.2	154.8	155.4	-48.7 (-108.0, 10.7), <i>p</i> = 0.105	-33.3 (-93.5, 26.9), <i>p</i> = 0.271
Stroop Correct Congruent-Incongruent	0.1	0.5	0.2	0.6	0.4	0.4	-0.5 (-1.3, 0.2), <i>p</i> = 0.159	-0.3 (-1.0, 0.5), <i>p</i> = 0.495
SDST Correct Responses	62.7	62.6	62.5	62.4	61.5	61.7	-0.9 (-2.2, 0.5), <i>p</i> = 0.206	-0.5 (-1.8, 0.9), <i>p</i> = 0.491
SDST Average Reaction Time (msec)	1966.4	2039.1	2037.1	2083.8	2142.8	2194.6	-13.8 (-144.6, 117.0), <i>p</i> = 0.830	40.7 (-91.0, 171.1), <i>p</i> = 0.536
N-back mean RT 0 back (msec)	412	414	405	478	485	473	5 (-15, 25), <i>p</i> = 0.635	2 (-18, 23), <i>p</i> = 0.812
N-back mean RT 1 back (msec)	464	464	449	547	544	526	-2 (-37, 33), <i>p</i> = 0.907	-6 (-41, 29), <i>p</i> = 0.737
N-back mean RT 2 back (msec)	559	568	552	665	654	640	-19 (-89, 52), <i>p</i> = 0.596	-17 (-87, 54), <i>p</i> = 0.633
N-back correct-incorrect/total 0 back	0.95	0.96	0.95	0.98	0.98	0.96	-0.01 (-0.06, 0.04), <i>p</i> = 0.728	-0.02 (-0.06, 0.03), <i>p</i> = 0.524
N-back correct-incorrect/total 1 back	0.96	0.96	0.94	0.94	0.93	0.96	-0.01 (-0.07, 0.04), <i>p</i> = 0.568	0.03 (-0.02, 0.09), <i>p</i> = 0.191
N-back correct-incorrect/total 2 back	0.91	0.91	0.91	0.88	0.82	0.86	-0.06 (-0.14, 0.02), <i>p</i> = 0.140	-0.03 (-0.11, 0.05), <i>p</i> = 0.430
WVLT Recall 1 correct	11.4	10.7	12	7.2	7.3	6.4	0.8 (-1.6, 3.2), <i>p</i> = 0.497	-1.4 (-3.8, 0.9), <i>p</i> = 0.231
WVLT Recall 2 correct	16.9	16.8	16.8	10.5	9.7	9.6	-0.7 (-2.8, 1.4), <i>p</i> = 0.511	-0.9 (-3.0, 1.2), <i>p</i> = 0.401
WVLT Recall 3 correct	19.8	19.9	19.6	12.6	11.2	12.7	-1.4 (-4.2, 1.3), <i>p</i> = 0.301	0.4 (-2.4, 3.2), <i>p</i> = 0.772
WVLT Delayed Recall correct	18.4	17.0	18.1	7.3	8.2	7.4	2.4 (-0.4, 5.1), <i>p</i> = 0.087	0.4 (-2.3, 3.1), <i>p</i> = 0.774
WVLT Delayed Recognition correct	25.7	26.3	26.9	23.0	22.2	20.9	-1.3 (-4.3, 1.7), <i>p</i> = 0.380	-3.3 (-6.4, -0.3), <i>p</i> = 0.032
WVLT Delayed Recognition RT correct (msec)	894.3	860.8	836.3	1017.0	1030.8	1077.6	47.4 (-40.8, 135.6), <i>p</i> = 0.286	118.6 (29.5, 207.8), <i>p</i> = 0.010

Abbreviations: VAS = Visual Analogue Scale; SDST = Symbol Digit Substitution Test; WLT = Visual Verbal Learning Test; RT = reaction time.

Chapter 6

Imaging cholinergic and serotonergic neurotransmitter networks in Alzheimer's disease in vivo

Bernadet L. Klaassens^{a,b,c,d}, Joop M.A. van Gerven^d, Erica S. Klaassen^d, Jeroen van der Grond^b, Serge A.R.B. Rombouts^{a,b,c}

^aLeiden University, Institute of Psychology, Leiden, the Netherlands, ^bLeiden University Medical Center, Department of Radiology, Leiden, the Netherlands, ^cLeiden University, Leiden Institute for Brain and Cognition, Leiden, the Netherlands, ^dCentre for Human Drug Research, Leiden, the Netherlands

ABSTRACT

Disruption of cholinergic and serotonergic neurotransmitter systems is associated with cognitive, emotional and behavioural symptoms of Alzheimer's disease (AD). To investigate the responsiveness of these systems in AD we measured the effects of a single-dose of the selective serotonin reuptake inhibitor citalopram and acetylcholinesterase inhibitor galantamine in 12 patients with AD and 12 age-matched controls on functional brain connectivity with resting state functional magnetic resonance imaging.

In this randomized, double blind, placebo-controlled crossover study, functional magnetic resonance images were repeatedly obtained before and after dosing, resulting in a dataset of 432 scans. Connectivity maps of ten functional networks were extracted using a dual regression method and drug vs. placebo effects were compared between groups with a multivariate analysis with cerebrospinal fluid, white matter, baseline and heart rate measurements as confound regressors (at $p < 0.05$, corrected).

A galantamine induced difference between groups was observed for the cerebellar network. Connectivity within the cerebellar network and between this network and the thalamus decreased after galantamine vs. placebo in AD patients, but not in elderly controls. For citalopram, voxelwise network connectivity did not show significant group x treatment interaction effects. However, we found default mode network connectivity with the precuneus and posterior cingulate cortex to be increased in AD patients, which could not be detected within the control group. Further, in contrast to the AD patients, elderly subjects showed a consistent reduction in mean connectivity with all networks after administration of citalopram.

Since AD has previously been characterized by reduced connectivity between the default mode network and the precuneus and posterior cingulate cortex, the effects of citalopram on the default mode network suggest a restoring potential of selective serotonin reuptake inhibitors in AD. The results of this study also confirm a change in cerebellar connections in AD, which is possibly related to cholinergic decline.

INTRODUCTION

In Alzheimer's disease (AD), destruction of neural tissue leads to loss of cholinergic nuclei in the basal forebrain and depleted cholinergic innervation towards the cerebral cortex, thalamus and hippocampus [229, 329, 335]. Acetylcholinesterase inhibitors (AChEIs) prevent the breakdown of acetylcholine and are often used as drug treatment to improve the cognitive symptoms of AD [189, 336]. In addition, reduced 5-hydroxytryptamine (5-HT; serotonin) activity plays a role in the cognitive deterioration [337, 338], as well as in behavioural and mood changes that frequently accompany AD [45, 51]. The cholinergic and serotonergic systems act in concert with each other with regard to functions like learning and memory [339-341], further suggesting the involvement of both systems in AD.

Single-dose administration of compounds that inhibit or excite synaptic activity can alter brain connectivity during rest, reflecting the responsiveness of neurotransmitter networks and related functions [77, 79, 311]. This pharmacological 'challenge' technique seems especially relevant for measuring deviant functional processes in AD, which is conceived as a disorder of large-scale network disconnections [18, 19]. Cholinergic network responses that have been studied so far substantiate the assumption that acetylcholine is involved in memory, learning and visual perception [189, 234]. A cholinergic challenge caused increased connectivity in healthy young subjects with regions that are implicated in visual processing, memory and attention [275]. Effects of AChEIs on connectivity in AD patients have only been examined after long-term cholinergic treatment, and show enhanced connectivity of the default mode network (DMN) and the interrelated hippocampus [89-94]. Despite the likelihood of disrupted serotonin transmission, serotonergic modulation of brain connectivity has not yet been studied in AD. Acute or short-term treatment with selective serotonin reuptake inhibitors (SSRIs) elicits reduced connectivity of the DMN and several other cortical and subcortical areas in healthy subjects [82, 83, 85-87, 199] and patients with a major depressive disorder [84].

In this randomized, placebo-controlled, crossover study, we used resting state functional MRI (RS-fMRI) to visualize cholinergic and serotonergic neurotransmitter networks in AD patients and age-matched controls. We hypothesized that single-dose AChEI and SSRI administration changes the functional integrity of neural networks differently in AD patients compared to controls, and that the altered connections would mostly apply to regions that are susceptible for AD related connectivity change such as the hippocampus, thalamus, precuneus and cingulate cortex [20, 25]. The outcomes of this study will provide fundamental knowledge on biochemical pathology in dementia, which might eventually benefit drug development and efficacy in neurodegenerative diseases.

MATERIALS AND METHODS

Included subjects

We included 12 patients with mild AD and 12 gender- and age-matched controls. The clinical diagnosis of probable AD was established according to the revised criteria of the National Institute of Neurological and Communicative Disorders and Stroke and the Alzheimer's Disease and Related Disorders Association (NINCDS-ADRDA) [15], including clinical and neuropsychological assessment. All AD patients participating in this study were recently diagnosed and had mild to moderate cognitive deficits with a Mini Mental State Examination (MMSE) score of at least 18 [274]. Furthermore, they were assessed by a physician (i.e. neurologist, geriatrician) as mentally capable of understanding the implications of study participation. The elderly subjects who served as controls had an MMSE score between 28 and 30 (see Table 6.1 for demographics).

Table 6.1. Demographics of mild AD patients and controls

	AD patients	Controls
n	12	12
Age (Mean \pm SD)	74.0 \pm 5.2	73.1 \pm 5.2
Age range	65-81	64-79
Male/female	6/6	6/6
MMSE (Mean \pm SD)	22.3 \pm 2.5	29.3 \pm 0.9
MMSE range	19-28	28-30
BMI (kg/m ²) range	22-30	22-31

All subjects underwent a thorough medical screening at the Centre for Human Drug Research (CHDR) to investigate whether they met the inclusion and exclusion criteria. They had a normal history of physical health and were able to refrain from using nicotine and caffeine during study days. Exclusion criteria included positive drug or alcohol screen on study days, regular excessive consumption of alcohol (>4 units/day), caffeine (>6 units/day) or cigarettes (>5 cigarettes/day), use of concomitant medication 2 weeks prior to study participation and involvement in an investigational drug trial 3 months prior to administration. The study was approved by the medical ethics committee of the Leiden University Medical Center (LUMC). Written informed consent was obtained from each subject prior to study participation.

Experimental design

This was a single centre, randomized, double blind, placebo-controlled crossover study with citalopram 30 mg and galantamine 8 mg [see 275]. Citalopram has an average time point of

maximum concentration (T_{max}) of 2-4 h, with a half-life ($T_{1/2}$) of 36 h. For galantamine, $T_{max} = 1-2$ h and $T_{1/2} = 7-8$ h. To correct for the different pharmacokinetic (PK) profiles, citalopram 20 mg was administered at $T = 0$ h, followed by a second dose of 10 mg at $T = 1$ h (if the first dose was tolerated). Galantamine was given as a single 8 mg dose at $T = 2$ h. Blinding was maintained by concomitant administration of double-dummy placebo's at all three time points. All subjects received an unblinded dose of granisetron 2 mg at $T = -0.5$ h, to prevent the most common drug-induced adverse effects of nausea and vomiting.

Six RS-fMRI scans were acquired during study days, two at baseline and four after administering citalopram, galantamine or placebo (at $T = 2.5, 3.5, 4.5$ and 6 h) (Figure 6.1). Each scan was followed by performance of computerized cognitive tasks (taken twice at baseline) on the NeuroCart® test battery, for quantifying pharmacological effects on the CNS [167, 204, 205]. By including multiple measurements during the T_{max} interval, this repeated measures profile increases the statistical power of the analysis and allows for identification of time related effects, associated with changing serum concentrations. Nine blood samples were taken during the course of the day to define the PK profile of citalopram, citalopram's active metabolite desmethylcitalopram, galantamine and concentrations of cortisol and prolactin [182, 206]. Washout period between study days was at least 7 days.

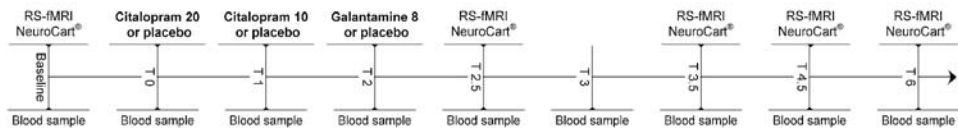


Figure 6.1. Schematic overview of a study day. Each subject received citalopram, galantamine and placebo on three different days. At baseline, two RS-fMRI scans were acquired, followed by the NeuroCart® CNS test battery. After drug administration, four more RS-fMRI scans were acquired at time points $T = 2.5, 3.5, 4.5$ and 6 h post dosing, each time followed by the NeuroCart® test battery. During the day, nine blood samples were taken to measure the concentrations of citalopram, desmethylcitalopram, galantamine, cortisol and prolactin. On each study day there were three moments of administration. The second administration only took place when subjects tolerated the first dose well (did not vomit or feel too nauseous):

Galantamine study day:	$T = 0$) placebo	$T = 1$) placebo	$T = 2$) galantamine 8 mg
Citalopram study day:	$T = 0$) citalopram 20 mg	$T = 1$) citalopram 10 mg	$T = 2$) placebo
Placebo study day:	$T = 0$) placebo	$T = 1$) placebo	$T = 2$) placebo

Outcome measures

Pharmacokinetics

PK parameters for citalopram, galantamine and citalopram's active metabolite desmethylcitalopram were calculated using a non-compartmental analysis to validate the choice of time points of pharmacodynamic endpoints (RS-fMRI, NeuroCart®, neuroendocrine measures). Blood samples were collected in 4 mL EDTA plasma tubes at baseline and 1, 2, 2.5, 3, 3.5, 4.5 and 6 h post dosing,

centrifuged (2000 *g* for 10 min) and stored at -40°C until analysis with liquid chromatography-tandem mass spectrometry (LC-MS/MS).

Neuroendocrine variables

Blood samples were obtained to determine cortisol and prolactin concentrations. Serum samples were taken in a 3.5 mL gel tube at baseline (twice) and 1, 2, 2.5, 3.5, 4.5 and 6 h post dosing, centrifuged (2000 *g* for 10 min) and stored at -40°C until analysis. Serum concentrations were quantitatively determined with electrochemiluminescence immunoassay.

NeuroCart® test battery

Each RS-fMRI scan was followed by functional CNS measures in a separate room using the computerized NeuroCart® test battery measuring alertness, mood and calmness (Visual Analogue Scales (VAS) Bond & Lader), nausea (VAS Nausea), vigilance and visual motor performance (Adaptive Tracking task), reaction time (Simple Reaction Time task), attention, short-term memory, psychomotor speed, task switching and inhibition (Symbol Digit Substitution Test and Stroop task), working memory (N-back task) and memory imprinting and retrieval (Visual Verbal Learning Test) [95-103]. The Visual Verbal Learning Test was only performed once during each day (at 3 and 4 h post dosing) as the test itself consists of different trials (imprinting and retrieval). Duration of each series of NeuroCart® brain function tests was approximately 20 min. To minimize learning effects, training for the NeuroCart® tasks occurred during the screening visit within 3 weeks prior to the first study day.

MR imaging

Scanning was performed at the LUMC on a Philips 3.0 Tesla Achieva MRI scanner (Philips Medical System, Best, The Netherlands) using a 32-channel head coil. All subjects were asked to close their eyes while staying awake prior to each RS-fMRI session on all study days. T1-weighted anatomical images were acquired once per visit. To facilitate registration to the anatomical image, each RS-fMRI scan was followed by a high-resolution T2*-weighted echo-planar scan.

RS-fMRI data were obtained with T2*-weighted echo-planar imaging (EPI) with the following scan parameters: 220 whole brain volumes, repetition time (TR) = 2180 ms; echo time (TE) = 30 ms; flip angle = 85°; field-of-view (FOV) = 220 x 220 x 130 mm; in-plane voxel resolution = 3.44 x 3.44 mm, slice thickness = 3.44 mm, including 10% interslice gap; acquisition time 8 min. For 3D T1-weighted MRI the following parameters were used: TR = 9.7 ms; TE = 4.6 ms; flip angle = 8°; FOV = 224 x 177 x 168 mm; in-plane voxel resolution = 1.17 x 1.17 mm; slice thickness = 1.2 mm; acquisition time 5 min. Parameters of high-resolution T2*-weighted EPI scans were set to: TR = 2200 ms; TE = 30 ms; flip angle = 80°; FOV = 220 x 220 x 168 mm; in-plane voxel resolution = 1.96 x 1.96 mm; slice thickness = 2.0 mm; acquisition time 30 s.

Statistical analysis

Pharmacokinetics

Maximum plasma concentrations (C_{\max}) and time of C_{\max} (T_{\max}) were obtained directly from the plasma concentration data. The area under the plasma concentration vs. time curve was calculated from time zero to the time of the last quantifiable measured plasma concentration ($AUC_{0-\text{last}}$). To investigate differences between groups, PK parameters were analysed using a mixed effects model with group as fixed effect (SAS for Windows V9.4; SAS Institute, Inc., Cary, NC, USA).

Neuroendocrine variables and NeuroCart® test battery

Treatment (drug vs. placebo) x group (AD patients vs. elderly controls) interaction effects on cortisol and prolactin concentrations and Neurocart® measures were investigated using a mixed effects model with treatment, time, group, visit, treatment by time, treatment by group and treatment by group by time as fixed effects, subject, subject by treatment and subject by time as random effects and the average of the period baseline (pre-dose) values as covariate (SAS for Windows V9.4; SAS Institute, Inc., Cary, NC, USA). The neuroendocrine data and data of the Simple Reaction Time task were not normally distributed and therefore log-transformed before analysis and back transformed after analysis. The data of the Visual Verbal Learning Test were analysed using a mixed effects model with treatment, group, visit and treatment by group as fixed effects and subject as random effect.

MR imaging

All fMRI analyses were performed using the Functional Magnetic Resonance Imaging of the Brain (FMRIB) Software Library (FSL, Oxford, United Kingdom) version 5.0.7 [119-121].

Data preprocessing

Each individual functional EPI image was inspected, brain-extracted and corrected for geometrical displacements due to head movement with linear (affine) image registration [122, 123]. Images were spatially smoothed with a 6 mm full-width half-maximum Gaussian kernel. Registration parameters for non-smoothed data were estimated to transform fMRI scans into standard space and co-registered with the brain extracted high resolution T2*-weighted EPI scans (with 6 degrees of freedom) and T1 weighted images (using the Boundary-Based-Registration method) [124]. The T1-weighted scans were non-linearly registered to the MNI 152 standard space (the Montreal Neurological Institute, Montreal, QC, Canada) using FMRIB's Non-linear Image Registration Tool. Registration parameters were estimated on non-smoothed data to transform fMRI scans into standard space after Automatic Removal of Motion Artifacts based on Independent Component Analysis (ICA-AROMA vs0.3-beta). ICA-AROMA attempts to identify and remove motion related noise components by investigating its temporal and spatial properties. As recommended, high

pass temporal filtering (with a high pass filter of 150 s) was applied after denoising the fMRI data with ICA-AROMA [207, 208].

Estimation of network connectivity

RS-fMRI networks were extracted from each individual denoised RS-fMRI dataset (24 subjects x 3 days x 6 scans = 432 datasets) with a dual regression analysis [36, 125] based on 10 predefined standard network templates [199, 275]. These standard templates have been identified using a data-driven approach [10] and comprise the following networks: three visual networks (consisting of medial, occipital pole, and lateral visual areas), default mode network, cerebellar network, sensorimotor network, auditory network, executive control network and left and right frontoparietal networks. Time series of white matter, measured from the centre of the corpus callosum, and CSF, measured from the centre of the lateral ventricles, were added as confound regressors in this analysis to account for non-neuronal signal fluctuations [126].

With the dual regression method, spatial maps representing voxel-to-network connectivity were estimated for each dataset separately in two stages and used for higher level analysis. First, the weighted network maps were used in a spatial regression into each dataset. This stage generated 12 time series per dataset that describe the average temporal course of signal fluctuations of the 10 networks plus 2 confound regressors (CSF and white matter). Next, these time series were entered in a temporal regression into the same dataset, resulting in a spatial map per network per dataset with regression coefficients referring to the weight of each voxel being associated with the characteristic signal change of a specific network. The higher the value of the coefficient, the stronger the connectivity of this voxel with a given network.

For an overall impression of connectivity alterations during study days, mean z-values of these regression coefficients within networks were calculated for each group and study day separately. By comparing the average of the four post measurements with the average of the two baseline measurements it was semi-quantitatively inspected how the average connectivity within each network changed (increased vs. decreased) during study days. Fisher's exact test was applied to investigate differences between groups in the number of networks with a specific direction of this global connectivity change.

Higher level analysis

Local group x treatment interaction effects of citalopram and galantamine were investigated with non-parametric combination (NPC) as provided by FSL's Permutation Analysis for Linear Models tool (PALM vs94-alpha) [129, 209, 210]. NPC is a multivariate method that offers the possibility to combine data of separate, possibly non-independent tests, such as our multiple time points, and investigate the presence of joint effects across time points, in a test that has fewer assumptions and is more powerful than repeated-measurements ANOVA or multivariate ANOVA (MANOVA).

First, tests were performed for each time point using 1000 synchronized permutations, followed by the fit of a generalized Pareto distribution to the tail of the approximation distribution, thus refining the p -values at the tail further than otherwise possible with a small number of permutations [318]. More specifically, to investigate group \times treatment interaction effects on voxelwise functional connectivity with each of the 10 functional networks, four two-sample t -tests (AD patients: drug - placebo vs. controls: drug - placebo) were performed for all post-dose time points ($T = 2.5, 3.5, 4.5$ and 6 h), with average heart rate (beats/m) per RS-fMRI scan as confound regressor [127]. The average of the two baseline RS-fMRI scans was used as covariate as well, by adding the coefficient spatial map as a voxel-dependent regressor in the model. This will control for the confounding influence of possibly systematic individual differences and group differences at baseline level as recently analysed and described in Klaassens et al. [319]. The same method was applied for additional investigation of treatment effects (drug vs. placebo) on the DMN within the group of AD patients and within the control group as was previously done for a group of young adults [275]. To that end, four one-sample t -tests (drug vs. placebo) were performed for all post-dose time points ($T = 2.5, 3.5, 4.5$ and 6 h), with average heart rate (beats/m) per RS-fMRI scan as confound regressor.

Second, to analyse effects across time, the tests for the four time points were combined non-parametrically via NPC using Fisher's combining function [211] and the same set of synchronized permutations as mentioned above. A liberal mask was used to investigate voxels within the MNI template, excluding voxels belonging to CSF. Threshold-free cluster enhancement was applied to the tests at each time point and after the combination, and the resulting voxelwise statistical maps were corrected for the familywise error rate using the distribution of the maximum statistic [128, 129]. Voxels were considered significant at $p < 0.05$, corrected.

RESULTS

Pharmacokinetics

PK parameters (T_{\max} , C_{\max} and $AUC_{0-\text{last}}$) in AD patients and elderly controls are summarized in Table 6.2. There were no PK differences between AD patients and controls. Figure 6.2 shows the individual and median citalopram and galantamine PK time profiles.

Neuroendocrine variables and NeuroCart® test battery

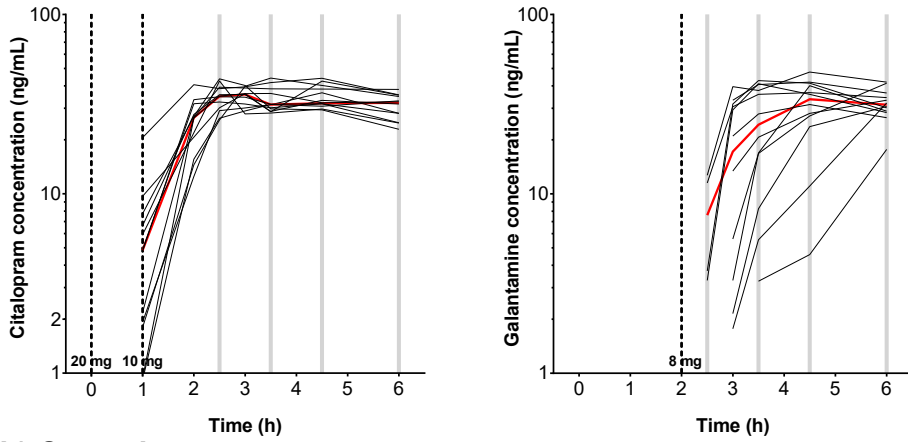
There were no significant group \times treatment interaction effects of citalopram and galantamine on cortisol and prolactin. See Supplementary Figure S6.1 for cortisol and prolactin levels in AD patients and controls. For an overview of all NeuroCart® results, we refer the reader to Supplementary Table S6.1. No significant group \times treatment interaction effects were observed for citalopram or galantamine.

Table 6.2. Pharmacokinetics of citalopram, desmethylcitalopram and galantamine in young and older adults

PK parameters	Citalopram			Desmethylcitalopram			Galantamine		
	Mean \pm SD			Mean \pm SD			Mean \pm SD		
	AD patients	Controls	Contrasts (p-value)	AD patients	Controls	Contrasts (p-value)	AD patients	Controls	Contrasts (p-value)
T_{max}	3.6 \pm 1.2	3.4 \pm 1.1	0.527	4.3 \pm 1.4	4.0 \pm 1.3	0.491	5.0 \pm 0.9	4.5 \pm 1.1	0.306
C_{max}	38.8 \pm 4.5	41.8 \pm 11.7	0.147	3.0 \pm 1.3	3.5 \pm 1.8	0.395	36.4 \pm 8.0	41.8 \pm 12.2	0.324
AUC_{0-last}	153.0 \pm 19.0	165.0 \pm 43.6	0.150	11.1 \pm 5.3	13.3 \pm 7.1	0.366	84.7 \pm 35.7	104.0 \pm 40.2	0.151

Abbreviations: AD = Alzheimer's disease; PK = pharmacokinetic; T_{max} = time point (h) of maximum concentration; C_{max} = maximum concentration (ng/mL); AUC_{0-last} = area under the plasma concentration vs. time curve (ng \cdot h/mL).

a) AD patients



b) Controls

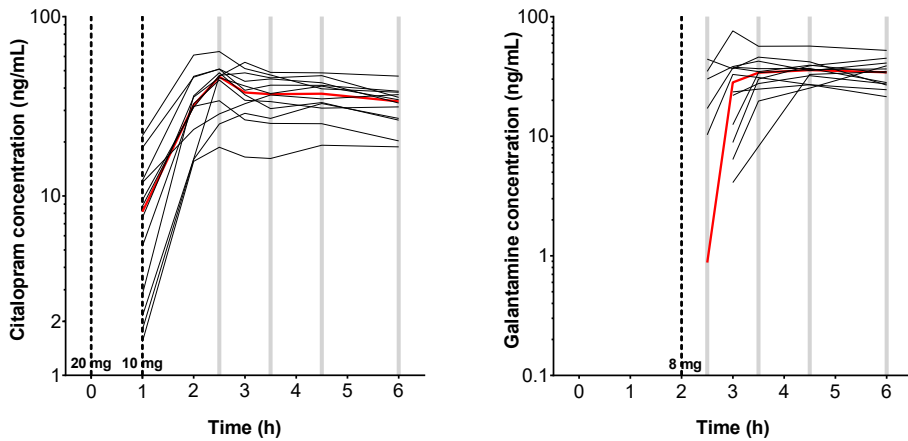


Figure 6.2. Pharmacokinetic profiles. Median (red line) and individual (black lines) PK profiles for citalopram (left) and galantamine (right) concentrations in AD patients (a) and controls (b). Vertical bars illustrate the timing of RS-fMRI acquisition post drug administration. Observations below limit of quantification were dismissed.

Imaging

Global connectivity changes

Calculations of the pre and post treatment average connectivity (mean z-values) per network, group and treatment are summarized in Table 6.3. Delta scores show that on placebo days connectivity reduced from pre to post measurement for 6 of the 10 networks in patients with AD and for 4 of the 10 networks in elderly controls. Fisher's exact test did not lead to a significant difference in prevalence in number of networks that showed a decrease in average connectivity (6/10 vs. 4/10).

Table 6.3. Mean z-scores within networks per group, per treatment; pre (average of 2 baseline measurements) and post (average of 4 measurements) drug administration, and delta scores of the difference between pre and post measurements

Group	AD patients						Controls											
	Placebo		Citalopram		Galantamine		Placebo		Citalopram		Galantamine							
Measurement	pre	post	Δ	pre	post	Δ	pre	post	Δ	pre	post	Δ						
Visual network (medial)	7.13	7.07	-0.06	6.78	7.27	0.49	6.06	6.38	0.32	4.58	5.71	1.13	5.64	4.92	-0.72	4.97	4.32	-0.65
Visual network (occipital)	5.18	5.40	0.22	4.82	5.56	0.74	4.77	4.72	-0.05	3.69	4.25	0.56	4.50	4.35	-0.15	4.03	3.74	-0.29
Visual network (lateral)	4.64	4.81	0.17	4.57	4.96	0.39	4.32	4.16	-0.16	3.82	4.13	0.31	4.57	4.14	-0.43	3.51	3.91	0.4
Default mode network	6.66	5.91	-0.75	6.42	6.55	0.13	6.76	6.20	-0.56	6.82	6.59	-0.23	6.98	6.70	-0.28	6.93	6.29	-0.64
Cerebellar network	3.55	3.94	0.39	3.01	3.61	0.6	3.11	2.85	-0.26	3.50	2.87	-0.63	2.83	2.78	-0.05	2.69	3.03	0.34
Sensorimotor network	4.23	4.71	0.48	4.68	4.46	-0.22	4.01	4.32	0.31	3.92	4.04	0.12	4.56	3.54	-1.02	3.72	3.69	-0.03
Auditory network	4.60	4.34	-0.26	4.27	4.29	0.02	4.36	4.24	-0.12	4.20	4.27	0.07	4.75	4.07	-0.68	4.28	4.01	-0.27
Executive control network	4.61	4.09	-0.52	4.42	3.80	-0.62	3.63	4.06	0.43	3.74	4.11	0.37	3.98	3.50	-0.48	3.67	3.96	0.29
Frontoparietal network right	4.55	4.38	-0.17	4.59	4.27	-0.32	4.62	3.96	-0.66	4.83	4.29	-0.54	4.82	4.61	-0.21	5.17	4.48	-0.69
Frontoparietal network left	4.94	4.18	-0.76	4.60	4.35	-0.25	4.78	4.57	-0.21	5.12	4.87	-0.25	5.45	5.21	-0.24	5.60	5.15	-0.45

Table 6.3 also presents the pre-post changes in global connectivity during treatment days. The diurnal patterns of network alterations after galantamine administration were similar between groups as well. The prevalence in number of networks that showed a decrease in connectivity in elderly controls (3/10) vs. patients with AD (7/10) did not lead to a significant difference.

In contrast to placebo and galantamine study days, group differences were observed during citalopram occasions. After citalopram administration, reduced connectivity was consistently observed for all 10 networks in elderly controls, but only in 4 out of 10 networks in patients with AD. A prevalence of 10/10 vs. 4/10 networks that showed a decrease in connectivity was tested significant ($p < 0.05$).

Local differences in drug effects between AD patients and controls

A significant group x treatment interaction effect of galantamine was found for connectivity within the cerebellar network (see Table 6.4 for specifications and extent of significant effects). In AD patients, galantamine induced a decrease in connectivity of the cerebellar network with the cerebellum, thalamus and brain stem (interaction and main effects are shown in Figure 6.3). In controls, galantamine did not induce connectivity alterations with the cerebellar network.

There were no significant differences in network effects of citalopram vs. placebo between AD patients and elderly controls. Within-group analyses showed that citalopram significantly increased connectivity between the DMN and precuneus/posterior cingulate cortex (PCC) compared to placebo in AD patients, but not in controls (Figure 6.4). Table 6.4 shows specifications and extent of significant effects.

DISCUSSION

We investigated functional network alterations after a serotonergic and cholinergic challenge to gain insight into disruptions of neurotransmitter pathways in AD. Comparing AD patients with controls, we found a significant group x treatment interaction effect after administration of the AChEI galantamine on cerebellar network connectivity. Galantamine induced a local decrease in cerebellar connectivity in AD patients, but not in controls. The SSRI citalopram did not alter regional connectivity differently between groups. However, after citalopram intake, the observed overall effect of lowered connectivity among all networks in controls was absent in AD. In addition, although there was no local interaction effect, a citalopram intensified DMN-precuneus/PCC connection was only observed in the AD group. To guarantee appropriate comparison between groups, PK properties and neuroendocrine effects of both compounds were investigated as well, and reassuring of equal absorption rates and hormone fluctuations [216], that might otherwise have led to spurious group x treatment interactions.

Table 6.4. Overview of significant citalopram and galantamine effects on functional connectivity as estimated with threshold-free cluster enhancement ($p < 0.05$, corrected)

Network effect	Region (Harvard-Oxford or Cerebellar atlas)	z*	x	y	z	# voxels
Cerebellar network (galantamine: AD patients > controls)	R Cerebellum (lobules I-VI)	4.25	20	-42	-38	414
	L Cerebellum (lobule VI)	3.91	-26	-48	-34	106
	R Cerebellum (crus I and II)	3.91	20	-84	-26	9
Cerebellar network (AD patients: galantamine < placebo)	R Cerebellum (lobules I-VI; IX, crus I), middle and inferior temporal gyrus, fusiform gyrus, temporal occipital fusiform cortex, parahippocampal gyrus	4.22	50	-34	-10	3108
	L Cerebellum (lobules IX, V, VI, crus I)	3.95	-12	-56	-34	540
	L Thalamus	4.00	-12	-12	6	168
	R Inferior frontal gyrus, pars opercularis; precentral gyrus	4.50	36	14	22	110
	M Brain stem	3.66	-4	-26	-24	66
	L Thalamus; brain stem	4.08	-8	-30	-2	22
	R Thalamus	4.03	18	-8	10	7
	L Cerebellum (lobule VIIb, crus II)	2.85	-26	-72	-50	6
	R Caudate	4.05	16	10	4	1
	L/R/M Precuneus, PCC	4.34	-6	-72	-26	685
Default mode network (AD patients: citalopram > placebo)	R Intracalcarine cortex, precuneus	3.54	4	-64	14	153

Abbreviations: AD = Alzheimer's disease; L = left; R = right; M = midline; PCC = posterior cingulate cortex. Voxel dimension = 2 mm x 2 mm x 2 mm (voxel volume 0.008 mL). * = standardized z-value of the uncorrected peak Fisher-statistic (NPC) within regions.

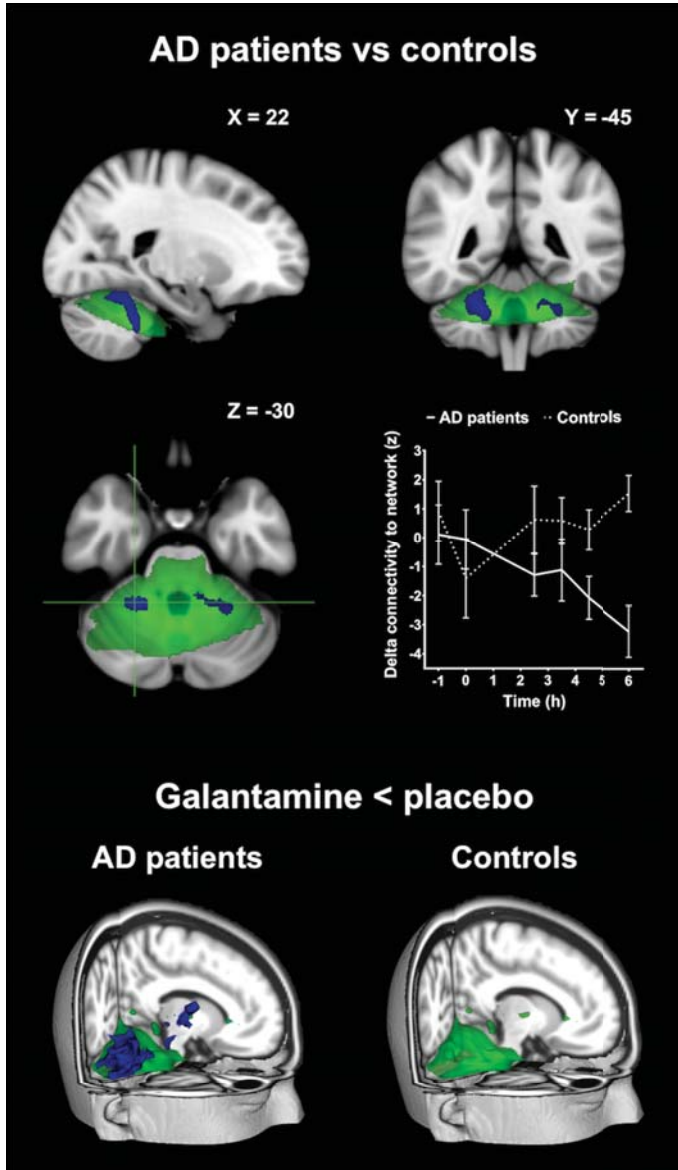


Figure 6.3. Galantamine effects on functional network connectivity. A different effect on connectivity in AD patients compared to elderly controls after galantamine vs. placebo within the cerebellar network (shown in green) for regions as shown in blue (top). The included plot visualizes the corresponding average time profiles of changes in functional connectivity per group for galantamine - placebo conditions (delta z-values with standard errors of the mean as error bars). The 3D images (bottom) show main galantamine effects per group. In AD patients connectivity between the cerebellar network (green) and regions in blue was decreased, whereas no effect was found within the group of elderly. Coronal and axial slices are displayed in radiological convention (left = right).

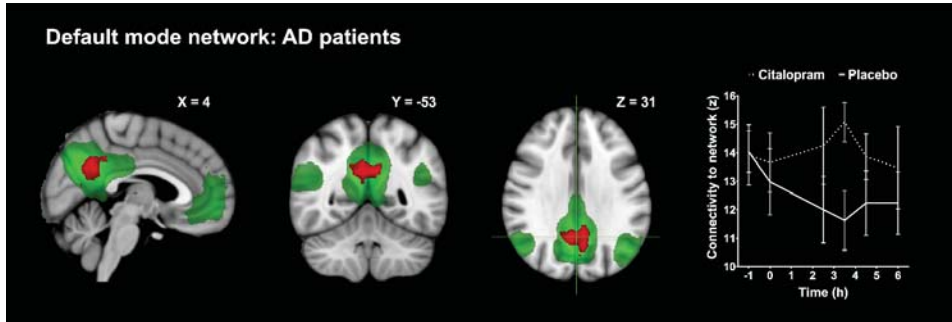


Figure 6.4. Citalopram effects on functional network connectivity. Increased connectivity in AD patients after citalopram vs. placebo was observed within the DMN (shown in green) for the precuneus/PCC (shown in red). The plot visualizes the corresponding average time profiles of changes in functional connectivity for citalopram (dotted line) and placebo (continuous line) conditions (z-values with standard errors of the mean as error bars). Coronal and axial slices are displayed in radiological convention (left = right).

Galantamine effects

This study is the first to investigate single-dose galantamine effects on resting state functional connectivity in AD, providing novel information on acute cholinergic alterations of related neural circuits that might underlie the cognitive improvements during chronic treatment. Acute AChEI administration usually does not lead to cognitive enhancement in healthy subjects or AD [214, 215]. Correspondingly, we did not find convincing effects of galantamine on any NeuroCart® task. However, galantamine did result in a diminished cerebellar network response in AD patients compared to elderly controls. Most studies in the literature describe enhanced resting state connectivity after AChEI intake in AD patients [89-94]. Contrary to our single-dose administration these studies all pertain to long-term cholinergic treatment. It is possible that neuroplasticity and modulation of cholinergic pathways over a longer period of AChEI treatment result in opposite findings. For example, increases in posterior DMN connectivity of AD patients as described by Blautzik et al. [92] were prevalent after 12 but not after 6 months of galantamine treatment, which was interpreted as indicating an insufficient time delay of 6 months to measure cholinergic effects. Solé-Padullés et al. [90] demonstrated significant increased DMN connectivity with the right-hemispheric parahippocampal gyrus in treated compared to untreated AD patients after 12 weeks of AChEI treatment but were not able to find longitudinal effects on connectivity with the DMN within treated patients. Of their 8 treated subjects, 5 even showed stable or increased connectivity when they used this area as region of interest.

Galantamine and the cerebellar network

The reduction of cerebellar-thalamic connectivity in patients with AD was partly due to an increase in cerebellar connectivity after placebo as opposed to a decrease after galantamine.

This observation underlines the importance of implementing a placebo-controlled design to investigate drug effects in comparison to diurnal fluctuations that are observed on placebo days and, as is the case for the cerebellar network, might show opposite patterns. Similarly, we found the average cerebellar network connectivity to decrease after placebo and to increase after galantamine administration. The average change in global cerebellar network connectivity during placebo days in the control group also indicates a normalizing effect of galantamine in AD patients, since the mean connectivity after galantamine in patients (mean $z = 2.85$) equals the mean connectivity after placebo days in controls (mean $z = 2.87$) instead of after placebo in patients with AD (mean $z = 3.94$).

It is increasingly recognized that the cerebellum is involved in cognitive and affective processes that are affected in neurodegenerative diseases [342-344]. Certain parts of the cerebellum have extensive fibre connections with specific cerebral areas [345, 346] and previous studies have demonstrated robust structural cerebellar-cortical atrophy connections [347] and lower functional connectivity within a network consisting of the basal ganglia and cerebellum [23] in dementia. It has also been suggested that the cerebellum contributes to the DMN, salience and executive control networks, indicating that cortico-cerebellar pathways are involved in executive and salience functioning, episodic memory and self-reflection [348], and might therefore play a role in symptoms as seen in AD.

The results of our study imply that a relation exists between cholinergic pathways and cerebellar connections in AD. Despite a lack of dense cholinergic innervation of the mammalian cerebellum, the cerebellum is known as a region with high acetylcholinesterase activity and acetylcholine seems to excite the cerebellum's muscarinic Purkinje cells and mossy fibres that are rich in choline acetyltransferase [349-355]. The observed depletion of dendritic Purkinje neurons in AD [356] possibly accounts for altered cholinergic projections after galantamine as shown in our study, which is also supported by delayed loss of Purkinje cells after AChEi treatment [349, 357]. Apart from cortical cholinergic input originating in the nucleus basalis of Meynert, a prominent cholinergic cell group in the brain stem projects towards the thalamus [243, 358]. The thalamus receives input from cerebellar nuclei, which in turn sends signals to all association areas of the cerebrum, including the prefrontal cortex [359]. In line with these pathways the observed decreased functional connections between the cerebellum, thalamus and brain stem in our mild AD group might represent diminished cholinergic trajectories in AD, which may be related to neuronal loss [347].

Citalopram effects on cognitive functions

We did not find any citalopram induced network differences between patients with AD and controls. Likewise, citalopram did not affect any behavioural or cognitive state as measured with the NeuroCart® battery differently between both groups. SSRIs are traditionally not used

as medication for cognitive symptoms, but have been proposed to treat emotional disturbances and agitation which in many AD patients are an integral part of the disease [360-362]. The included participants, motivated to comply with our intensive study program, were perhaps not representative of patients with AD with additional neuropsychiatric impairment, lowering the chance on a differentiated responsiveness of their serotonergic systems. Potentially, 5-HT hypofunction is also involved in cognitive disturbances of AD, although studies on the effect of SSRI administration on these aspects in AD patients are scarce [363]. Combining AChEI treatment with an SSRI seems to improve global cognitive functioning in AD compared to AChEI treatment alone [364], indicating a beneficial interaction between cholinergic and serotonergic stimulation, which is in line with observations on the receptor level [365]. At any rate, our findings confirm the limited cognitive effects of single-dose SSRI administration [167, 314]. A slight worsening of performance on two subtests of the N-back in the elderly was most likely due to chance. It may also be a reflection of a non-linear dose-response, as small immediate memory improvements are most consistently observed in a low (therapeutic) dose range of SSRIs [167].

Connectivity change after citalopram

Since single-dose serotonergic stimulation in non-AD subjects mainly shows effects on DMN connectivity, and DMN coherence is most often found to be altered in AD, we examined drug effects on DMN connectivity within each group separately. An increase in DMN-precuneus/PCC connectivity after citalopram was found in the AD group which could not be detected within the group of elderly subjects. We also observed a significant difference between AD patients and controls in the number of networks that showed a decrease vs. increase in connectivity after citalopram. The control group showed a reduction in connectivity after citalopram compared to baseline for all 10 networks, whereas this was only the case for 4 networks in the AD group. It is remarkable that we found this global connectivity to be enhanced after serotonergic stimulation in AD because previous studies almost uniformly show diminished network coherence after SSRI administration in healthy [83, 85-87, 199, 275] and depressed subjects [84].

Notably, depression is mainly characterized by increased connectivity [88], which may explain a lowering in connectivity after SSRI intake as antidepressant effect. AD however, is defined by decreased DMN-precuneus/PCC connectivity [23, 282, 285, 286]. The precuneus and PCC, both part of the DMN, are specifically implicated in symptomatology of AD such as impaired episodic memory retrieval, self-consciousness and visual-spatial imagery [159, 160, 287-289] and opposite findings after pharmacological enhancement in this study might therefore be regarded as beneficial neurochemical effects in AD. Our observations are concordant with the effects of memantine, an N-methyl-d-aspartate (NMDA) receptor antagonist, which is used to treat moderate and severe cases of AD. Similar to our results, memantine has been shown to strengthen connectivity of the DMN with the precuneus in AD, which was interpreted as

representing regularization of glutamatic levels that, in effect, leads to increased brain metabolic activity [291]. Although evidence on the efficacy of SSRIs as a treatment for cognitive symptoms of dementia is limited, several studies have demonstrated that serotonin might be an important target of pharmacological intervention. The serotonin antagonist and reuptake inhibitor trazodone hydrochloride has recently been discovered as a potential new disease-modifying treatment for dementia by arresting the unfolded protein response, and thereby neurodegenerative cell loss, in mice [366]. Another promising feature of SSRIs is the ability to suppress generation of beta-amyloid in CSF of mice and human volunteers [367], which implies the potential to prevent accumulation of beta-amyloid, which has also been found in the precuneus of AD patients [290]

Conclusions

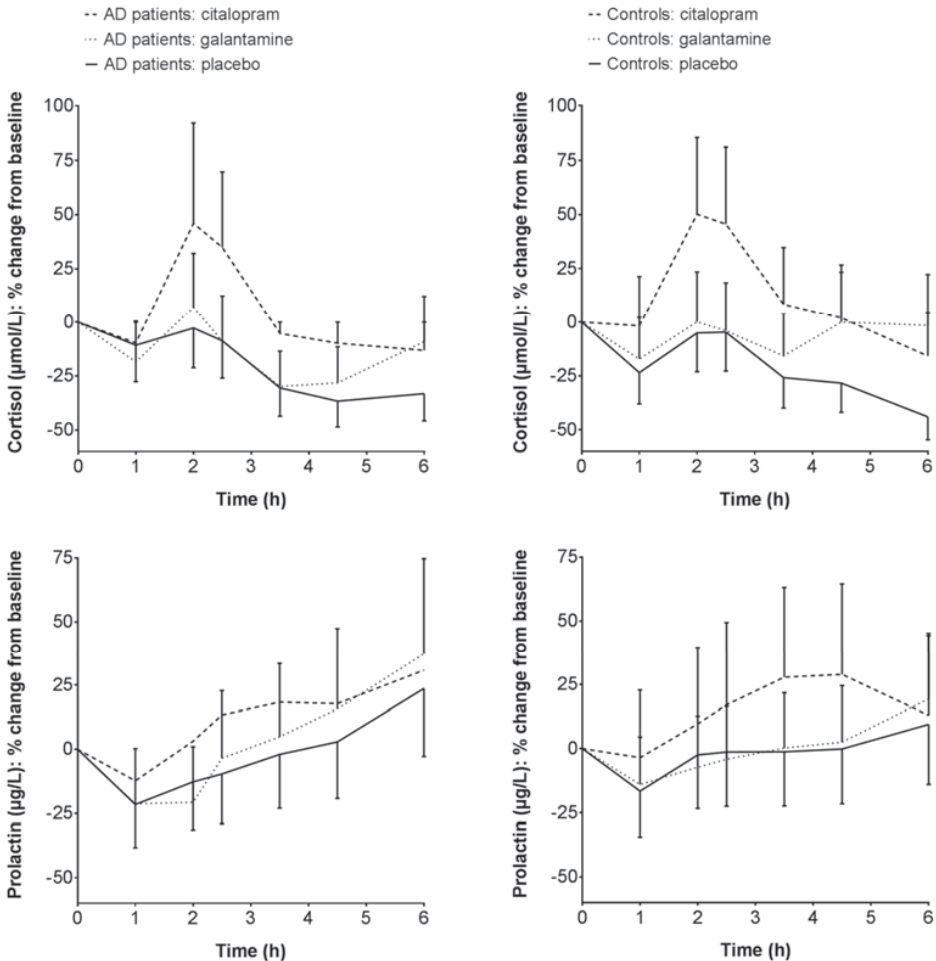
Whether serotonin dysregulation in AD mostly contributes to behavioural or cognitive symptoms, or both, has yet to be sorted out. The absence of group x treatment interaction effects after administering citalopram points to relatively similar serotonergic systems in AD patients and controls. Nevertheless, our results suggest that SSRI administration has an enhancing effect on DMN-precuneus/PCC connectivity, which has been shown to be decreased in AD [20]. This opposite finding indicates that SSRIs might have an improving effect on memory, self-referential processes and/or visual-spatial functions. We also confirm the significance of a cerebellar network in AD [347], that has been largely neglected within dementia research, but might be an important component associated with cholinergic decline. A challenge for the future is to unravel how the acute response to these compounds develops over a longer treatment period and if this response could be predictive for treatment efficacy in AD.

Acknowledgements

We are thankful for the assistance of the Alrijne Hospital Leiden, Alzheimer Nederland and GGZ Rivierduinen Leiden in the recruitment of AD patients. Helene van Gorsel, Jasper Stevens and Jules Heuberger (CHDR) are acknowledged for medical support and contribution to the non-compartmental analysis of pharmacokinetic parameters. This project was funded by the Netherlands Initiative Brain and Cognition (NIHC), a part of the Netherlands Organization for Scientific Research (NWO) (grant number 056-13-016). Serge Rombouts was supported by a VICI grant from NWO (grant number 016-130-677).

SUPPLEMENTARY MATERIAL

There was no significant group x treatment interaction effect of citalopram nor galantamine on cortisol and prolactin. In both groups, citalopram increased the level of cortisol ($p < 0.0001$) and prolactin ($p < 0.005$), relative to placebo. Galantamine did not affect the level of prolactin in any group. Cortisol was increased after galantamine vs. placebo in the elderly controls ($p < 0.005$), but not in AD patients, although this did not lead to a significant difference between groups.



Supplementary Figure S6.1. Least squares means percent change from baseline profiles of cortisol and prolactin concentrations (with standard errors of the mean as error bars).

Supplementary Table S6.1. Summary of group x treatment interaction effects and treatment effects, per group (N-back task and WLT) of citalopram and galantamine vs. placebo on the NeuroCart® test battery

Parameter	Least Squares Means				Contrasts interaction effects (difference, 95% CI, <i>p</i> -value)			
	AD patients: placebo	AD patients: citalopram	AD patients: galantamine	AD patients: placebo	Controls: citalopram	Controls: galantamine	AD patients (citalopram vs. placebo) vs. controls (citalopram vs. placebo)	AD patients (galantamine vs. placebo) vs. controls (galantamine vs. placebo)
VAS Alertness (mm)	56.9	51.7	54.9	53.6	53.3	51.0	-4.9 (-10.9, 1.1), <i>p</i> = 0.106	0.6 (-5.0, 6.1), <i>p</i> = 0.833
VAS Calmness (mm)	57.5	57.1	56.4	54.5	54.0	53.3	0.1 (-4.3, 4.5), <i>p</i> = 0.977	0.2 (-4.0, 4.3), <i>p</i> = 0.938
VAS Mood (mm)	60.1	56.2	59.4	56.8	55.7	54.2	-2.9 (-9.0, 3.1), <i>p</i> = 0.332	1.9 (-3.7, 7.5), <i>p</i> = 0.500
VAS Nausea log (mm)	0.40	0.49	0.57	0.42	0.46	0.62	0.053 (-0.147, 0.252), <i>p</i> = 0.595	-0.031 (-0.230, 0.168), <i>p</i> = 0.757
Adaptive tracking (%)	12.74	13.27	13.42	12.66	13.86	12.89	-0.67 (-2.57, 1.23), <i>p</i> = 0.479	0.46 (-1.45, 2.36), <i>p</i> = 0.632
Simple reaction time task (s)	348.57	366.38	371.72	342.56	340.53	345.04	5.7 (-3.7, 16.1), <i>p</i> = 0.231	5.9 (-3.7, 16.5), <i>p</i> = 0.230
Stroop mean RT Incongruent-Congruent (ms)	486.6	470.4	662.7	222.9	197.9	198.6	8.8 (-240.1, 257.7), <i>p</i> = 0.942	200.5 (-49.7, 450.7), <i>p</i> = 0.110
Stroop Correct Congruent-Incongruent	2.2	4.1	3.3	1.6	1.1	1.5	2.4 (-0.3, 5.1), <i>p</i> = 0.073 ²	1.2 (-1.5, 3.9), <i>p</i> = 0.347
SDST Correct Responses	47.3	47.2	49.2	48.6	48.7	47.9	-0.2 (-5.3, 5.0), <i>p</i> = 0.945	2.6 (-2.5, 7.8), <i>p</i> = 0.308
SDST Average Reaction Time (ms)	3072.9	3042.0	2929.3	2840.6	2895.3	2947.7	-85.59 (-520.3, 349.15), <i>p</i> = 0.675	-250.8 (-616.3, 114.75), <i>p</i> = 0.157

Supplementary Table S6.1 continues on next page

Supplementary Table S6.1. *Continued*

Parameter	Least Squares Means						Contrasts main treatment effects (estimate of difference, 95% CI, p-value)					
	AD patients: placebo	AD patients: citalopram	AD patients: galantamine	Controls: placebo	Controls: citalopram	Controls: galantamine	AD patients: placebo	AD patients: citalopram vs. placebo	AD patients: galantamine vs. placebo	Controls: placebo	Controls: citalopram vs. placebo	Controls: galantamine vs. placebo
N-back mean RT 0 back (ms)	542	542	527	490	495	482	0 (-31, 31), p = 0.998	-15 (-47, 18), p = 0.359	5 (-7, 16), p = 0.428	-9 (-22, 4), p = 0.167		
N-back mean RT 1 back (ms)	645	653	631	579	575	556	8 (-41, 57), p = 0.728	-14 (-64, 36), p = 0.559	-4 (-39, 31), p = 0.814	-23 (-58, 11), p = 0.172		
N-back mean RT 2 back (ms)	814	878	815	713	692	677	64 (-50, 179), p = 0.244	1 (109, 112), p = 0.978	-21 (-95, 52), p = 0.555	-37 (-110, 37), p = 0.310		
N-back correct-incorrect/total 0 back	5.74	5.84	5.90	0.97	0.94	0.95	0.10 (-0.18, 0.38), p = 0.448	0.16 (-0.13, 0.44), p = 0.254	-0.03 (-0.10, 0.04), p = 0.391	-0.02 (-0.10, 0.05), p = 0.522		
N-back correct-incorrect/total 1 back	5.11	4.93	5.22	0.95	0.88	0.96	-0.18 (-1.13, 0.77), p = 0.649	0.11 (-0.87, 1.08), p = 0.790	-0.07 (-0.12, -0.01), p = 0.023¹	0.01 (-0.04, 0.07), p = 0.612		
N-back correct-incorrect/total 2 back	3.12	3.07	3.13	0.88	0.78	0.84	-0.05 (-1.07, 0.97), p = 0.922	0.01 (-1.04, 1.06), p = 0.981	-0.10 (-0.20, -0.00), p = 0.042¹	-0.03 (-0.13, 0.06), p = 0.477		
WLT Recall 1 correct	2.2	1.9	2.3	7.5	7.2	7.4	-0.3 (-1.1, 0.5), p = 0.413	0.1 (-0.6, 0.9), p = 0.757	-0.3 (-1.6, 1.1), p = 0.704	-0.1 (-1.4, 1.3), p = 0.899		
WLT Recall 2 correct	3.6	3.4	3.5	10.7	9.8	9.8	-0.2 (-1.2, 0.8), p = 0.675	-0.1 (-1.1, 0.9), p = 0.808	-0.8 (-2.6, 0.9), p = 0.340	-0.8 (-2.6, 0.9), p = 0.340		
WLT Recall 3 correct	3.9	4.5	4.4	12.8	11.6	13.3	0.6 (-0.3, 1.4), p = 0.190	0.5 (-0.4, 1.3), p = 0.262	-1.3 (-3.5, 1.0), p = 0.269	0.5 (-1.8, 2.8), p = 0.654		
WLT Delayed Recall correct	0.8	1.5	1.1	8.0	8.2	7.7	0.7 (-0.1, 1.5), p = 0.093 ²	0.3 (-0.5, 1.2), p = 0.421	0.3 (-2.1, 2.6), p = 0.829	-0.3 (-2.6, 2.1), p = 0.829		
WLT Delayed Recognition correct	8.0	6.9	7.6	23.5	23.0	20.5	-1.1 (-2.7, 0.5), p = 0.179	-0.4 (-2.1, 1.4), p = 0.652	-0.5 (-3.0, 2.0), p = 0.682	-3.0 (-5.5, -0.5), p = 0.022¹		
WLT Delayed Recognition RT correct (ms)	1012.8	1096.3	1076.4	1015.0	1047.8	1074.6	83.5 (-56.8, 223.8), p = 0.222	63.6 (-95.9, 223.2), p = 0.408	32.8 (-40.6, 106.3), p = 0.362	59.6 (13.8, 133.0), p = 0.106		

¹Significant at $p < 0.05$; ²non-significant trend ($0.05 < p < 0.1$). Abbreviations: AD = Alzheimer's disease; CI = confidence interval; VAS = Visual Analogue Scale; SDST = Symbol Digit Substitution Test; WLT = Visual Verbal Learning Test; RT = reaction time. The N-back task and the WLT for AD patients is an adapted (easier) version. It was therefore not possible to compare performance on these tasks between AD patients and elderly controls.

Chapter 7

Summary and general discussion

SUMMARY

The purpose of this thesis was to investigate the brain's serotonergic and cholinergic systems, and the way these are altered in older age and AD. The effects of pharmacological challenges on functional brain networks as measured with resting state fMRI (RS-fMRI) may provide us more insight into neurotransmitter pathways and mechanisms of action of drugs that selectively act on the central nervous system (CNS). In addition, it was examined how functional brain connections change in aging and AD. By comparing network connectivity and the pharmacological response of this measure between healthy young and older subjects and patients with AD, we aimed to improve knowledge on the decay of brain function and neurotransmission associated with normal aging and AD. Better understanding of these (patho)physiological systems is of substantial importance considering the ongoing increase in life expectancy and AD incidence [16, 17].

In the first part of this thesis we explored the responsiveness of brain connectivity to a single-dose of the selective serotonin reuptake inhibitors (SSRIs) sertraline and citalopram and the cholinesterase inhibitor (AChEI) galantamine, and its sensitivity compared to other outcome measures in healthy young volunteers. In the second part we studied functional connections and neurotransmitter systems in old age and AD. It was examined how age-related connectivity changes compare to changes as found in AD, and whether these are dependent of structural atrophy. We thereafter investigated if network alterations after modulation with citalopram and galantamine differ between young and elderly subjects, and between elderly controls and patients with AD. The present chapter provides a summary and discussion of the main findings of the included studies and recommendations for future research.

In **chapter 2** the effects of a serotonergic challenge compared to placebo on whole-brain connectivity were measured in healthy young subjects. The single-dose administration of the SSRI sertraline caused large-scale connectivity alterations with multiple networks: the default mode network (DMN), the executive control network, the lateral, occipital and medial visual networks, the sensorimotor network and the auditory network. Regions that were most consistently affected among these network changes were the precuneus and anterior and posterior cingulate cortex (ACC and PCC). Sertraline did not alter cognitive or subjective measures that were taken by means of computerized cognitive tests and visual analogue scales to examine changes in mood, alertness, calmness, memory, emotional processing, executive functioning and reaction time. The results of this study demonstrate the widespread nature of the serotonergic system, its involvement in regions and networks that relate to emotional and sensory processing and motor control, and the sensitivity of RS-fMRI to a serotonergic challenge.

In **chapter 3** we assessed the acute effects of the SSRI citalopram and the AChEI galantamine vs. placebo on brain connectivity in young subjects. Citalopram mainly resulted in decreased connectivity within and between the sensorimotor network and areas that belong to the DMN.

Galantamine enhanced network connectivity of the medial visual network with regions as the fusiform gyrus, hippocampus, PCC and thalamus. There were no significant treatment effects on cognitive test performance or subjective states. Citalopram effects showed a clear overlap with those of sertraline and indicate that serotonin might be related to motor behavior and self-referential mechanisms. Connectivity alterations due to galantamine point to a role of acetylcholine in visual processing, learning and memory. These findings further support the use of RS-fMRI as a specific and sensitive method to measure pharmacological challenge effects.

Differences in functional network connectivity between young and elderly subjects and patients with AD were investigated in **chapter 4**. It was concluded that differences between young and older adults are considerably larger than between AD patients and elderly controls. Both comparisons point to reduced brain connectivity in old age and AD. Older age was associated with widespread diminished connectivity with nine of the ten investigated functional networks. In AD patients compared to controls, the DMN was the only network that showed reduced connectivity. When the results were corrected for regional gray matter volume, the effects were maintained but markedly attenuated (showing 58-65% loss in number of voxels with a significant effect). The findings suggest that decreased DMN-precuneus/PCC connectivity, known to be related to visuospatial functioning, episodic memory and self-consciousness, may act as a marker of AD.

In **chapter 5**, the effects of serotonergic and cholinergic challenges on network connectivity were compared between young and older adults. We showed that the SSRI citalopram reduced sensorimotor network connectivity in both young and elderly subjects. Although this decrease in connectivity was more abundant in the young subject group, citalopram did not lead to a significant group x treatment interaction effect. The drug-induced network response to galantamine was significantly diminished in elderly compared to young subjects. Whereas the young subjects showed increased connectivity as described in chapter 3, we did not find any network alterations in the elderly. There were no notable differences between groups in effect on subjective and cognitive functioning. The results indicate that older age is accompanied by a relatively unaltered serotonergic system and a decline in cholinergic neurotransmission.

Differential effects of serotonergic and cholinergic modulation in AD patients and controls were examined in **chapter 6**. There were no significant differences between groups in citalopram effects on network connectivity, although the observed effect on the sensorimotor networks as found in the elderly subjects did not reach significance in the AD group. Further, a citalopram-induced increase in DMN-precuneus/PCC connectivity was observed in AD patients, but not within the group of elderly controls. A significant difference after cholinergic enhancement was found between groups in connectivity with the cerebellar network. Galantamine did not alter functional connectivity in the elderly subjects, but reduced connectivity within the cerebellar network and in relation to the thalamus and brain stem in AD patients. The results did not reveal any convincing group x treatment interaction effects on cognitive and subjective measures.

These findings suggest that serotonergic enhancement might reverse reduced DMN-precuneus/PCC connectivity as seen in AD. The effects of galantamine point to involvement of cerebellar connections in cholinergic system alterations in AD.

GENERAL DISCUSSION

We showed that neuromodulatory effects on brain connectivity were most noticeable in healthy young subjects. Further, although the effect of older age on network connectivity (without pharmacological stimulation) was substantial, the differences in connectivity between AD patients and controls were limited. Whereas the network response to serotonergic stimulation was not significantly different between young and older adults and patients with AD, cholinergic enhancement induced a differential response in both elderly and AD patients, which might relate to the cholinergic hypothesis stating that the decay of the cholinergic system plays a role in the cognitive decline in aging and AD [53]. The findings of this thesis indicate that RS-fMRI offers a sensitive method to investigate acute pharmacological effects on the serotonergic and cholinergic systems, compared to several cognitive and subjective measures. Many results of the implemented pharmacological challenge studies were convincing with regard to location and direction of effect. This substantiates the usefulness of RS-fMRI as a method for measuring a compound's mechanism of action and its possible value in CNS drug development.

SSRI effects on brain connectivity in healthy young subjects

The results in chapter 2 and 3 show that the SSRIs sertraline and citalopram changes network connectivity in healthy young subjects. To allow for comparison of the effects of both SSRIs in healthy young subjects, the inclusion criteria and design of the sertraline study (chapter 2) were set up in agreement with the citalopram study. The twelve subjects of chapter 2 were each individually matched for age and gender with the young subjects as included in chapter 3. Despite the use of equipotent doses, the effects of sertraline on connectivity were more excessive compared to citalopram. However, the direction and areas of connectivity change were quite similar which aids the reliability of the RS-fMRI technique to show comprehensible pharmacological effects. Both SSRIs induced a decrease in connectivity with the sensorimotor network, midbrain and cortical midline structures as the precuneus, ACC, PCC and medial prefrontal areas. These effects suggest that serotonin is involved in motor function [221, 222], self-consciousness and emotion regulation [219], and the integration of sensory, motor, cognitive and emotional information [141, 368]. It has been proposed that increased brain connectivity of midline regions as seen in depression [88] represents increased self-consciousness and rumination with negative thoughts [142, 144]. Our findings therefore imply that SSRIs might reverse depression-related connectivity patterns.

Slight adjustments were made to the time schedule as sertraline and citalopram differ in their pharmacokinetic profile. In addition, we replaced the Visual Verbal Learning Test (VLT) by the Face Encoding and Recognition task. The absence of symptom relief after short periods of SSRI treatment in patients suffering from depression or anxiety disorders might be explained by the fact that improved emotional processing can only be made visible by tests that evoke an affective state [173, 174]. Accordingly, the Face Encoding and Recognition task was hypothesized to induce a larger acute response than the VLT. However, sertraline and citalopram did not affect performance on any cognitive or subjective test compared to placebo. A significant increase in neuroendocrine levels after SSRI administration implies that these unaltered measures could not be directly attributed to insufficient dosages or a lack of statistical power. It is possible that this paucity of effect is the consequence of inhibition of 5-HT_{1A} autoreceptors in the raphe nuclei during the acute stages of SSRI treatment [134]. The results of both SSRI studies verify that serotonergic tracts cover a substantial part of the brain and demonstrate the sensitivity of RS-fMRI to pharmacological challenges compared to other pharmacodynamic outcome measures.

Functional networks and neuromodulation in old age

By comparing three groups (young and older adults and patients with AD), we aimed to obtain better founded information about the effect of age vs. AD on functional network coherence and neurotransmitter systems. First, differences in network connectivity between young and older adults and between elderly and AD patients were compared in one study (chapter 4). The results of this study indicate that older age affects connectivity more extensively than AD. Of all ten investigated networks, nine showed diminished connectivity in the older adults compared to young subjects. These widespread reductions were not fully explained by loss of structural brain volume, as part of the findings was maintained after accounting for local differences in gray matter. Reduced connectivity was found for the DMN and for networks relating to language, attention, visual, auditory, motor and executive functioning, which may represent the age-appropriate decline in cognitive, sensory and motor function [254-256].

Despite the widespread loss of functional network connections at older age, the serotonergic system seemed relatively unaltered as the pharmacological effects of citalopram on brain connectivity did not differ between young and older adults (chapter 5). In both groups, citalopram caused a significant reduction of sensorimotor network connectivity. Although the citalopram induced response appeared smaller in older adults, a group x treatment interaction did not reach statistical significance. Serotonin dysregulation at older age could be related to the increased prevalence of depression in the elderly [45, 47, 310] and the similarity in response between young and old subjects is possibly the consequence of the absence of mood disorders in the older adults that were included in our study. The network response to galantamine in elderly subjects was indicative of cholinergic change at older age. In the young subjects, increased

occipital visual network connectivity was observed after galantamine with the hippocampus, precuneus, thalamus, fusiform gyrus, precentral and superior frontal gyrus, PCC and cerebellum. These specific alterations point to the role of acetylcholine in functions as learning, memory, and visual perception and processing [229, 233, 234]. In contrast, no change was found in the elderly, which was hypothesized to be the consequence of a cholinergic system decline that is characteristic for the process of normal aging and has been related to cognitive decay [329].

Functional networks and neuromodulation in Alzheimer's disease

In AD, altered network coherence was restricted to decreased DMN-precuneus connectivity (chapter 4). This is not an unexpected result and suggests a consistent and specific hallmark of AD [20, 23, 284], possibly relating to memory problems and visual-spatial symptoms [159, 160]. Our observations also indicate that functional network coherence is more affected in older age than in AD. After correction for regional GM volume the difference between AD patients and elderly controls was less profound but still involved a decrease in connectivity of the DMN with the precuneus. Measuring the effects of serotonergic and cholinergic challenges with RS-fMRI could offer us new insights into neurotransmitter system functioning and the potentially rehabilitative mechanisms of SSRIs and AChEIs in AD (chapter 6). Although we did not find any statistically significant differences between AD patients and controls in the network response after citalopram administration, the observed reduction in sensorimotor network connectivity in the elderly was not found in the group of AD patients. This might indicate the presence of a decline in serotonin networks that could not be determined with the small-sized cross-sectional studies that we performed. Figure 7.1 shows the citalopram effects on sensorimotor network connectivity in the three investigated groups.

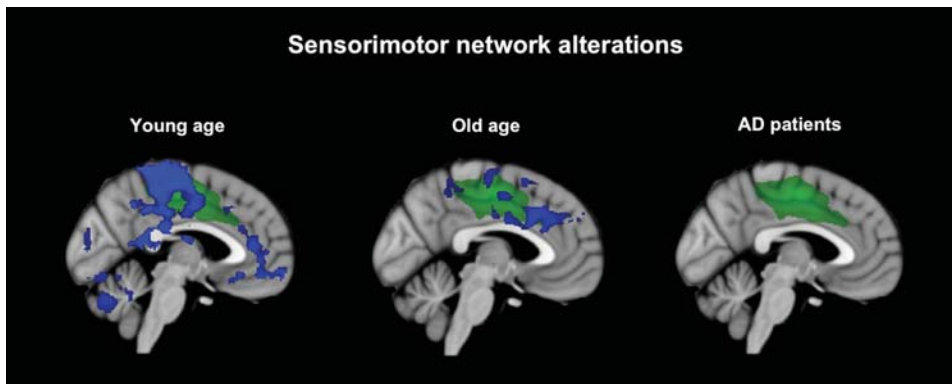


Figure 7.1. Reduced connectivity after citalopram administration between the sensorimotor network (green) and areas as shown in blue in young and older adults and patients with AD (chapter 3, 5 and 6, respectively).

The observed diminished DMN-precuneus connectivity in AD likely relates to deterioration of episodic memory, self-consciousness and visuospatial performance [159, 160]. Therefore, an interesting finding was the increase in these connections after citalopram intake. This observation seems to be fairly specific for AD as it differs from our results in healthy young and older subjects that consistently showed reduced network connections after single-dose SSRI administration. Decreased connectivity after SSRI administration has also been found in other studies that investigated SSRI effects in healthy young subjects [82, 83, 85-87] and patients with a major depressive disorder [84]. Apparently, SSRIs have a differential effect in AD patients compared to healthy or depressed subjects. The resemblance in location of the opposite findings as found in chapters 4 and 6 (see Figure 7.2) is of interest as it could signify a partial restoration of some aspects of AD associated pathology [159] by SSRIs.

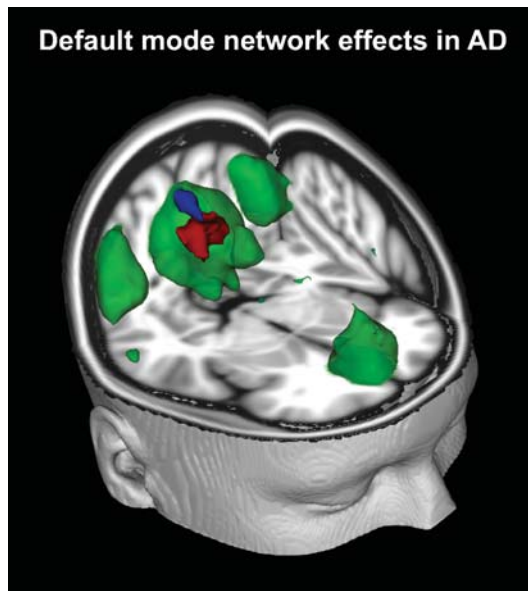


Figure 7.2. The DMN (green) shows a decrease in connectivity with the precuneus (red) in AD (chapter 4) as opposed to an increase in connectivity (blue) after citalopram administration in AD (chapter 6).

The increased functional connections with the visual network after galantamine as found in the young subjects were absent in AD patients as well. In addition, we found alterations that were specific for AD (Figure 7.3). An unexpected finding in chapter 5 was a galantamine induced increase in connectivity within the cerebellar network and between this network and the thalamus and brain stem. Although the thalamus is known to contain many acetylcholine receptors that receive input from a prominent cholinergic cell group in the brain stem [54, 358],

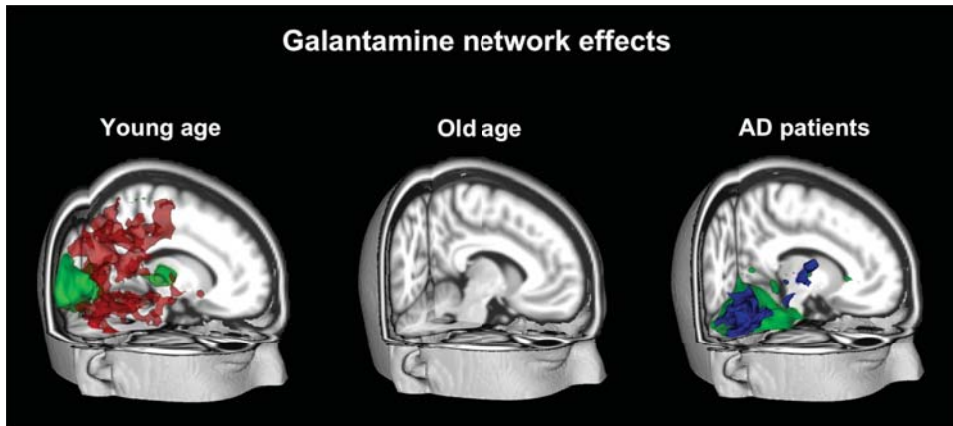


Figure 7.3. Galantamine effects on network connectivity. In the young adults, galantamine increased connectivity between the occipital visual network (green) and regions as shown in red (chapter 3). Galantamine did not alter connectivity in the older adults (chapter 5). AD patients showed a decrease in connectivity between the cerebellar network (green) and regions as shown in blue (chapter 6).

it is not straightforward to relate cerebellar connectivity change to cholinergic challenge effects. However, the cerebellum is known for a high activity of acetylcholinesterase, and acetylcholine seems to excite the cerebellum's muscarinic Purkinje cells and mossy fibres that are rich in choline acetyltransferase [349-353] and have been shown to be depleted in AD [356].

Differentiation of older subjects from patients with AD became more clear after challenging the cholinergic system, which made between-group differences in brain connectivity visible that are otherwise not apparent during rest. However, although the area was larger, this response was still restricted to one network and regions that are not typically involved in cholinergic transmission and AD. The results of this study do not directly have clinical implications for the field of dementia but they do seem to provide novel and fundamental knowledge about aspects of system decline related to AD. In our study a relatively low dosage of galantamine (8 mg) was used and it is likely that a 16 or 24 mg dosage could reveal larger and more robust differences between groups. More research is needed to replicate our findings and investigate the possible role of cerebellar network connections in relation to cholinergic decline in AD.

Strengths and limitations

A major strength of the pharmacological studies that we performed is the applied randomized, double blind, placebo-controlled, crossover design with multiple outcome measures that were acquired before and after drug administration. By collecting not only RS-fMRI data, but also cognitive and subjective measures and blood samples, we obtained a unique dataset that

allowed us to examine and discuss the results in more detail. Pharmacodynamic measurements were repeatedly obtained post dosing at time points when, based on the known T_{max} , the largest effects were expected. This design resulted in several advantages, as it made it possible to 1) inspect the pharmacokinetic profiles and neuroendocrine levels that could reassure us of sufficient absorption and choosing appropriate time points of measurements, 2) collect large datasets to increase the power of statistical tests despite small sample sizes, 3) explore diurnal fluctuations in resting state connectivity on placebo days and compare these to changes after drug administration, 4) determine the sensitivity of RS-fMRI to pharmacological challenges compared to other outcome measures, and 5) investigate differences in connectivity between groups before (chapter 4) and after pharmacological stimulation (chapter 5 and 6).

Nevertheless, our results cannot be generalized, as the small subgroups are likely not representative of larger populations. The included participants were all motivated to participate and selected based on strict inclusion and exclusion criteria. Another consideration is the chance of including 'healthy' elderly in a preclinical stage of Alzheimer's disease or another type of dementia, which was at the time of recruitment not yet identified. Likewise, although all patients have been carefully screened and diagnosed with probable AD according to the National Institute of Neurological and Communicative Disorders and Stroke and the Alzheimer's Disease and Related Disorders Association (NINCDS-ADRDA) [15], we cannot exclude the possibility that some of the included AD patients have been misdiagnosed. All patients were diagnosed very recently and especially in the early stage of the disease, clinical symptoms and biomarker alterations of different dementia types often overlap [369]. Further, although analysis of functional connectivity appears to be an informative method to investigate neurotransmitter system function, RS-fMRI cannot be used to measure neurotransmission directly. Functional connectivity is a mathematical concept of correlations between BOLD signals of different brain areas, which are not easy to interpret, prone to physiological noise such as breathing and heart rate [126], and not representative of causal or directional change [370].

Future research

In this thesis, we investigated acute drug effects on functional connectivity using RS-fMRI. Simultaneous fMRI and positron emission tomography (PET) or arterial spin labeling (ASL) acquisition could aid the interpretation of resting state fMRI results by identification of chemical pathways and the vascular pharmacological response. The advantage of PET over fMRI is that biochemical processes can be measured directly at the receptor level by localizing specific ligands *in vivo*. Ligand radiolabeling offers the possibility to measure receptor occupancy and trace the dispersion and binding of a drug in the brain [371]. But the duration, expensiveness and radioactive exposure form large drawbacks of PET imaging, making it practically impossible to execute studies with multiple repeated measures as implemented in our design. ASL, a method

to measure cerebral perfusion, is not hindered by these problems. Investigation of variations in blood flow after pharmacological modulation might be of additional value in CNS drug research.

An advantage of our repeated measures design was the possibility of examining drug effects on different time points post dosing for a detailed investigation over time in relation to pharmacokinetic properties. A challenge for the future involves PK/PD-modeling, the mathematical procedure to relate individual pharmacokinetic profiles of a drug to pharmacodynamic outcome measures [372]. Although we explored this relationship by determining the absorption rate of sertraline, citalopram and galantamine and inspecting time related effects in more detail in chapter 3, PK/PD-models are not yet available for voxelwise fMRI data. A formal model to quantify the dose-response relationship will give more insight into the value of RS-fMRI as a measure of pharmacological effects that might vary with different drug concentration levels.

We cannot draw firm conclusions about the clinical usefulness of pharmacological RS-fMRI as a means to distinguish between AD patients and controls. More research needs to be conducted to explore this possibility in detail and investigate whether drug challenge responses may also discriminate between other forms of dementia, such as frontotemporal dementia, dementia with Lewy bodies and vascular dementia. The use of pharmacological data in individual statistical classification and machine learning, and comparison with markers that are known to be most sensitive to AD might shed more light on the value of implementing pharmacological challenge paradigms as part of diagnostic procedures. For example, the inclusion of our data may improve diagnostic classification of AD [373]. Another interesting approach of the pharmacological challenge technique as applied in this research would be to examine whether the initial network response to an SSRI or AChEI could be predictive of long-term treatment effectiveness [374-376].

Conclusions

The present research suggests that older age is characterized by widespread decreases in functional network connections, which is not totally dependent of structural atrophy. This might represent the fact that normal aging is accompanied by a decline of several functions (vision, hearing, motor behavior, language, executive and cognitive function) [254-256]. The serotonergic system does not necessarily deteriorate at older age, whereas the cholinergic system shows diminished responsiveness, relating to regions and networks that are involved in memory and visual processing. Furthermore, we replicated the finding of reduced DMN connectivity in AD, and showed that this was only partly explained by loss of structural volume. Our data also indicate that the decrease in connectivity in old age is considerably larger than connectivity decline in AD. Although there was no proof of serotonergic network change in AD vs. elderly controls, our results point to an attenuation of serotonin pathways in old age and AD. In addition, the reduced DMN-precuneus connections in the AD patients are partly reversed after a citalopram challenge.

The effects of a galantamine challenge on the cerebellar network imply that cholinergic pathway disruptions in AD are related to cerebellar-thalamic connections.

Consistent with our findings, SSRIs or AChEIs do not typically alleviate the cognitive or behavioral symptoms of mood disorders and dementia immediately after drug administration [173, 174]. Pharmacological companies are therefore in search for more sensitive measures that might show specific changes even after single-dose administration. Functional connectivity analysis appears to be a promising technique in investigating brain function and neurotransmitter pathways after a pharmacological challenge. The largest pharmacological effects were found in healthy young volunteers, which might be the consequence of relatively uncompromised neurotransmitter systems. More research is needed to determine the potency of RS-fMRI to examine the way that neurotransmitter pathways are altered in normal aging, AD or other neuropsychiatric disorders. The results of our studies suggest that functional brain connectivity might serve as a sensitive and specific measure in pharmacological research, and possibly as a tool to predict treatment success in patient populations and/or characterize novel compounds under development. Future pharmacological imaging research may be improved by the integration of different imaging modalities such as PET and ASL, and the addition of PK/PD-modeling.

Chapter 8

Nederlandse samenvatting

SAMENVATTING

Hersenvuncties, zoals het cognitief functioneren, emoties en perceptie, zijn in grote mate afhankelijk van neurale communicatie en connecties tussen hersengebieden. Om meer inzicht te krijgen in het behoud en de achteruitgang van hersenvuncties, is het van belang om deze interacties en connecties te bestuderen. Een geschikte methode hiervoor is het meten van functionele hersenconnectiviteit met *resting state functional magnetic resonance imaging* (RS-fMRI). Met deze beeldvormende techniek is het mogelijk te onderzoeken welke gebieden van het brein gezamenlijk een netwerk vormen. Voor de studies die staan beschreven in dit proefschrift hebben we gebruik gemaakt van RS-fMRI om de effecten van farmacologische *challenges* op hersenconnectiviteit in beeld te brengen. Het meten van deze effecten kan ervoor zorgen dat we meer begrijpen van actiemechanismen van geneesmiddelen die selectief gericht zijn op specifieke neurotransmittersystemen, en hersenconnecties die betrokken zijn bij neurotransmitterfuncties. Door het vergelijken van netwerkconnectiviteit en de farmacologische respons op deze uitkomstmaat tussen gezonde jongeren en ouderen en patiënten met de ziekte van Alzheimer, hebben we getracht om de kennis ten aanzien van de afname van hersenvunctie en neurotransmissie die geassocieerd is aan normale veroudering en de ziekte van Alzheimer te vergroten.

Een farmacologische challenge test, of stimulatietest, houdt in dat er een middel wordt toegediend met een bekend farmacologisch werkingsmechanisme. Vervolgens worden veranderingen op bepaalde uitkomstmaten onderzocht die representatief zijn voor de werking van het middel, zoals cognitief functioneren, hormonen en hersenconnectiviteit. Deze veranderingen bieden informatie over het onderliggende biologische systeem dat wordt gestimuleerd. In dit proefschrift zijn effecten van geneesmiddelen onderzocht die van invloed zijn op de serotonerge en cholinerge neurotransmittersystemen. Neurotransmitters zorgen voor signaaloverdracht tussen hersencellen en zijn daardoor van invloed op gedrag, gevoelens en cognitie. Serotonine is betrokken bij vele functies, maar is vooral bekend door zijn bijdrage aan stemming en emoties. Medicijnen die de heropname van serotonine door presynaptische receptoren blokkeren (*selective serotonin reuptake inhibitors; SSRIs*) worden vaak gebruikt bij de behandeling van angst en depressie. Acetylcholine wordt voornamelijk gerelateerd aan functies als het leervermogen, aandacht en concentratie. Middelen die een verminderde afbraak van acetylcholine teweegbrengen (*acetylcholinesterase inhibitors; AChEIs*) worden met name gegeven aan mensen die lijden aan een vorm van dementie, zoals de ziekte van Alzheimer.

Het doel van dit proefschrift was om veranderingen in functionele connectiviteit te meten ten gevolge van serotonerge en cholinerge challenges en zo de werking van gerelateerde systemen te bestuderen. Daarnaast hebben we onderzocht welke rol hersenconnectiviteit en neurotransmittersystemen spelen bij veroudering en de ziekte van Alzheimer. Een beter begrip van deze (patho)fysiologie is van aanzienlijk belang gezien de voortdurende stijging in

levensverwachting en incidentie van de ziekte van Alzheimer. De ziekte van Alzheimer is de meest voorkomende vorm van dementie. Het is een degeneratieve hersenaandoening die vooral wordt gekenmerkt door geheugenverlies. Daarnaast treden er andere cognitieve klachten, zoals problemen met taal, oriëntatie, visueel-ruimtelijke functies en planning, en gedragsveranderingen op. Er wordt verondersteld dat het verlies van cognitieve functies en veranderingen in gedrag onder andere samenhangt met de achteruitgang in functionele hersenconnecties en neurotransmittersystemen. Zowel veroudering als de ziekte van Alzheimer gaan gepaard met een achteruitgang van serotonerge en cholinerge systemen. Een verminderde serotonine aanmaak op oudere leeftijd en bij de ziekte van Alzheimer zou samenhangen met veranderingen in stemming en gedrag. Volgens de cholinerge hypothese zijn verlaagde acetylcholine concentraties een oorzaak van de verslechtering van het geheugen en concentratievermogen.

De effecten van SSRIs en AChEIs op cognitie en gedrag zijn vaak pas na enkele weken tot maanden merkbaar. Op neuraal niveau vinden er echter al direct veranderingen plaats. Deze veranderingen kunnen zichtbaar gemaakt worden met fMRI, een beeldvormende techniek waarmee hersenactiviteit wordt gemeten. FMRI is gebaseerd op de aanname dat wanneer neuronen actief zijn, deze meer zuurstof consumeren. Hersenactiviteit wordt daarom bepaald op basis van de zuurstofconcentratie in het bloed. Deze activiteit kan worden gemeten tijdens het uitvoeren van een cognitieve taak, om te onderzoeken welke hersengebieden er op dat moment actief zijn. Maar ook in rusttoestand (*resting state*) zijn er betekenisvolle patronen in hersenactiviteit aanwezig. Tijdens een RS-fMRI scan is het alleen van belang dat de persoon in de MRI scanner zo stil mogelijk blijft liggen en niet in slaap valt. Met deze RS-fMRI scans kunnen we vervolgens functionele hersenconnectiviteit bepalen. Wanneer verschillende hersengebieden hetzelfde activatiepatroon laten zien, wordt verondersteld dat deze gebieden met elkaar verbonden zijn en betrokken zijn bij dezelfde functie. Omdat communicatie tussen hersengebieden voor een groot deel afhankelijk is van neurotransmissie, kan functionele connectiviteit ook beschouwd worden als representatief voor neurale transmissie. RS-fMRI is daarom een nuttige methode om neurotransmittersystemen te bestuderen.

Voor het uitvoeren van de studies is een uitgebreide en gestandaardiseerde methode gehanteerd. Om functionele hersenconnectiviteit te meten hebben we gebruik gemaakt van RS-fMRI. Met visuele analoge schalen en tests werden daarnaast subjectieve gevoelens (stemming, alertheid, kalmte) en cognitieve functies (geheugen, emotionele informatieverwerking, executief functioneren en reactietijd) gemeten. Bij de farmacologische experimenten werd een gerandomiseerd, dubbelblind, placebo-gecontroleerd, crossover design toegepast, waarbij er tevens bloedafnames plaatsvonden voor het bepalen van de farmacokinetiek, en cortisol en prolactine concentraties. Hiermee konden we de absorptie van de geneesmiddelen bepalen en vaststellen of de dosering voldoende was op de momenten waarop de metingen werden verricht. Herhaalde metingen na toediening van de geneesmiddelen volgden een strikt tijdschema

in overstemming met het farmacokinetisch profiel van de betreffende middelen om zeker te zijn van meetmomenten waarop de grootste effecten te verwachten waren en een adequate vergelijking te kunnen maken van effecten tussen en binnen studies.

Resultaten

In het eerste deel van dit proefschrift worden twee farmacologische challenge studies beschreven die zijn uitgevoerd bij gezonde jonge deelnemers. Het doel van deze studies was om te bepalen of hersenconnectiviteit gevoelig is als uitkomstmaat voor serotonerge en cholinerge stimulatie, en om de actiemechanismen van SSRIs en AChEIs op hersenfuncties te onderzoeken. De resultaten van de studie in **hoofdstuk 2** laten zien dat een eenmalige toediening van de SSRI sertraline (75 mg) in een steekproef van gezonde jongeren grootschalige veranderingen in connectiviteit teweegbrengen met meerdere functionele netwerken: het default mode netwerk, een centraal-executief netwerk, de laterale, occipitale en mediale visuele netwerken, een sensorisch-motorisch netwerk en een auditief netwerk. Deze veranderingen betroffen voornamelijk een afname van hersenconnectiviteit. Hersengebieden die consistent betrokken waren bij deze netwerkveranderingen waren de precuneus, en de anterieure en posterieure cingulate cortex (ACC en PCC), gebieden die onderdeel zijn van het default mode netwerk. Het is bekend dat dit netwerk relateert aan functies als introspectie, zelfbewustzijn en het episodisch geheugen. De resultaten van deze studie indiceren dat SSRIs een herstellend effect hebben op verhoogde connecties van dit netwerk zoals geobserveerd in depressieve patiënten. Sertraline had geen effect op cognitieve testen en subjectieve schalen die waren afgenomen. Deze afwezigheid van effecten toont aan dat functionele hersenconnectiviteit een zeer gevoelige uitkomstmaat is voor serotonerge challenges in vergelijking met subjectieve en cognitieve metingen.

Hoofdstuk 3 beschrijft de effecten van de SSRI citalopram (30 mg) en de AChEI galantamine (8 mg) op hersenconnectiviteit in gezonde jongeren. Citalopram leidde tot een reductie van connectiviteit binnen en tussen het sensorisch-motorische netwerk en gebieden die tot het default mode netwerk behoren. Het linker frontoparietale netwerk vertoonde ook een reductie in connectiviteit met het mesencephalon (de middenhersenen). De richting en locatie van deze effecten waren in grote mate vergelijkbaar met de effecten van sertraline. De consistentie van deze bevindingen versterkt de geloofwaardigheid van RS-fMRI als uitkomstmaat van challenge testen met SSRIs. Galantamine leidde tot een toename in hersenconnectiviteit met het mediale visuele netwerk en gebieden die vooral betrokken zijn bij het geheugen en aandachtsfuncties, namelijk de fusiform gyrus, hippocampus en thalamus. Dit beeld past bij de rol die acetylcholine speelt bij functies als het leervermogen, concentratie en visueel-ruimtelijke verwerking. Er werden wederom geen farmacologische effecten gevonden op het cognitief en subjectief functioneren.

Het tweede deel van het proefschrift was erop gericht om veranderingen in hersenconnectiviteit en cholinerge en serotonerge systemen te onderzoeken in gezonde ouderen en patiënten met

de ziekte van Alzheimer. De resultaten van deze studies kunnen leiden tot een beter begrip van veranderingen in neurotransmittersystemen in veroudering en de ziekte van Alzheimer, en de mogelijk herstellende werking hierop van SSRIs en AChEIs. **Hoofdstuk 4** betreft een studie waarin is gekeken naar verschillen in hersenconnectiviteit tussen gezonde jongeren, gezonde ouderen en patiënten met de ziekte van Alzheimer. Er werd geconcludeerd dat verschillen in connectiviteit tussen jongeren en ouderen aanzienlijk groter is dan tussen ouderen en patiënten met de ziekte van Alzheimer. Een hogere leeftijd was geassocieerd met wijdverspreide verminderde connectiviteit met negen van de tien onderzochte netwerken. De afname in connectiviteit met het default mode netwerk en netwerken gerelateerd aan functies als taal, aandacht, visueel, auditief, motorisch en executief functioneren zou representatief kunnen zijn voor de achteruitgang in cognitieve, sensorische en motorische functies die passen bij veroudering. Bij patiënten met de ziekte van Alzheimer was het default mode netwerk het enige netwerk dat een afname in connectiviteit vertoonde in vergelijking met de ouderen. Deze afname betrof vooral de precuneus, een gebied dat betrokken is bij functies als het geheugen en visueel-ruimtelijke verwerking. De verlaagde connectiviteit hangt mogelijk samen met een achteruitgang in deze functies bij de ziekte van Alzheimer. Nadat de resultaten gecorrigeerd waren voor verschillen in grijze stof volume, bleven de resultaten behouden maar waren deze wel duidelijk beperkter (met een verlies van 58-65% in het aantal voxels met een significant effect).

De volgende hoofdstukken beschrijven het verschil in farmacologische effecten van de SSRI citalopram (30 mg) en de AChEI galantamine tussen jongeren en ouderen en patiënten met de ziekte van Alzheimer te onderzoeken. In **hoofdstuk 5** zijn de verschillen tussen 12 jongeren en 17 ouderen beschreven. In beide groepen was er sprake van verlaagde connectiviteit met het sensorisch-motorische netwerk na toediening van citalopram. Hoewel deze effecten wel groter waren in de groep jonge deelnemers, leidde dit niet tot een significant verschil. Het effect van galantamine verschilde wel significant tussen jongeren en ouderen. Waar de jongeren verhoogde connectiviteit lieten zien zoals beschreven in hoofdstuk 3, konden we geen netwerkveranderingen aantonen in de ouderen. Deze afwezigheid van veranderingen in hersenconnectiviteit werd geïnterpreteerd als een kenmerk van de cholinerge achteruitgang die gerelateerd wordt aan cognitieve veroudering. Er waren geen noemenswaardige verschillen tussen groepen in het farmacologische effect op subjectieve en cognitief functioneren.

In **hoofdstuk 6** pasten we dezelfde methode toe om patiënten met de ziekte van Alzheimer en gezonde ouderen te vergelijken. Wederom vonden we op geen enkel netwerk significante verschillen tussen de groepen in het effect van citalopram op connectiviteit, hoewel het effect op het sensorisch-motorische netwerk zoals gevonden in de jongeren en ouderen niet werd geobserveerd in de groep patiënten met de ziekte van Alzheimer. Het default mode netwerk liet een toename in connectiviteit zien met de precuneus en PCC, terwijl dit niet waarneembaar was in de controlegroep. Deze bevinding lijkt specifiek te zijn voor patiënten met de ziekte van

Alzheimer, omdat er bij de gezonde deelnemers juist vrij consistent een afname in connectiviteit met deze gebieden werd aangetoond. Een significant verschil tussen de groepen na cholinerge stimulatie werd gevonden voor het cerebellaire netwerk. Galantamine leidde tot verlaagde connectiviteit binnen het cerebellaire netwerk en in relatie tot de thalamus en hersenstam in patiënten met de ziekte van Alzheimer. Mogelijk speelt het cerebellum een rol bij de effecten van AChEIs vanwege connecties met de hersenstam, een belangrijke bron van acetylcholine richting de thalamus. Beide studies lieten geen overtuigende farmacologische effecten zien op cognitieve en subjectieve metingen met de NeuroCart® testbatterij.

Conclusie

Samenvattend laten de studies zien dat resting state fMRI, in vergelijking met verscheidene cognitieve en subjectieve maten, een gevoelige techniek is voor het meten van farmacologische effecten op de serotonerge en cholinerge neurotransmittersystemen. De responsiviteit van functionele netwerken werd vooral aangetoond in gezonde jongeren, wat mogelijk het gevolg is van relatief behouden neurotransmittersystemen op jongere leeftijd. Een oudere leeftijd bleek gerelateerd te zijn aan een aanzienlijke afname in hersenconnectiviteit, waarbij de veranderingen in connectiviteit in patiënten met de ziekte van Alzheimer vs. controles beperkt was. Ook lieten we zien dat farmacologisch challenge effecten op connectiviteit tijdens rust betekenisvolle en fundamentele inzichten kunnen opleveren in veranderingen van neurotransmitterbanen bij veroudering en de ziekte van Alzheimer. Hoewel serotonerge netwerken niet significant lijken te veranderen ten gevolge van veroudering en de ziekte van Alzheimer, vonden we veranderingen in cholinerge systemen in zowel ouderen als patiënten met de ziekte van Alzheimer. Deze veranderingen zijn mogelijk representatief voor de achteruitgang in cognitieve functies in veroudering en dementie.

Analyse van functionele hersenconnectiviteit is een nuttige methode waarmee het mogelijk is om neurotransmittersystemen en hersenconnecties, en de manier waarop deze aangedaan raken in veroudering en de ziekte van Alzheimer, in beeld te brengen. Op dit moment is de RS-fMRI echter nog niet geschikt als methode voor individuele diagnoses. Wel lijken er mogelijkheden te zijn voor RS-fMRI als instrument voor farmacologisch onderzoek. Een eigenschap van SSRIs en AChEIs is dat de verbeteringen in cognitieve en gedragsfuncties niet onmiddellijk na de eerste toediening optreden. Farmacologische bedrijven zijn daarom sterk geïnteresseerd in gevoelige indicatoren die al na een enkele dosering neurale veranderingen kunnen laten zien. Op basis van onze bevindingen bevelen we RS-fMRI aan als een gevoelige en specifieke tool in farmacologisch onderzoek, met de potentie om behandelactiviteit van geneesmiddelen te voorspellen en bij te dragen aan de ontwikkeling van nieuwe geneesmiddelen. Voor een dergelijke toepasbaarheid is het van belang dat er verder onderzoek wordt uitgevoerd. Toekomstig farmacologisch beeldvormend onderzoek kan gebaat zijn bij de integratie van verschillende neuroimaging

modaliteiten zoals *arterial spin labelling* en *positron emission tomography*, en het vaststellen van een dosis-respons relatie door middel van PK/PD-modellering.

Appendix

Abbreviations

References

Dankwoord

Curriculum vitae

ABBREVIATIONS

5-HT	5-hydroxytryptamine
([¹¹ C]PIB	Pittsburgh compound B
ACC	Anterior cingulate cortex
ACh	Acetylcholine
AChEI	Acetylcholinesterase inhibitor
AD	Alzheimer's disease
ANOVA	Analysis of variance
ASL	Arterial spin labelling
AUC	Area under the curve
AUC _{0-last}	Area under the plasma concentration vs. time curve
BOLD	Blood-oxygen level dependent
CHDR	Centre for Human Drug Research
C _{max}	Maximum concentration
CNS	Central nervous system
DMN	Default mode network
EPI	Echo-planar imaging
FAST	FMRIB's Automated Segmentation Tool
FMRI	Functional magnetic resonance imaging
FMRIB	Functional Magnetic Resonance Imaging of the Brain
FOV	Field-of-view
FSL	Functional Magnetic Resonance Imaging of the Brain Software Library
GM	Gray matter
ICA-AROMA	Automatic Removal of Motion Artifacts based on Independent Component Analysis
LC-MS/MS	Liquid chromatography-tandem mass spectrometry
LUMC	Leiden University Medical Center
MANOVA	Multivariate analysis of variance
MCI	Mild cognitive impairment
MMSE	Mini mental state examination
MNI	Montreal Neurological Institute
MRI	Magnetic resonance imaging
NINCDS-ADRDA	National Institute of Neurological and Communicative Disorders and Stroke and the Alzheimer's Disease and Related Disorders Association
NMDA	N-methyl-d-aspartate
NPC	Non-parametric combination
NWO	Netherlands Organization for Scientific Research
PALM	Permutation Analysis for Linear Models

PCC	Posterior cingulate cortex
PD	Pharmacodynamic
PET	Positron emission tomography
PK	Pharmacokinetic
RS-fMRI	Resting state functional magnetic resonance imaging
SDST	Symbol-Digit Substitution Test
SMA	Supplementary motor area
SSRI	Selective serotonin reuptake inhibitor
$T_{1/2}$	Half-life
TE	Echo time
THC	$\Delta 9$ -tetrahydrocannabinol
T_{max}	Time point of maximum concentration
TR	Repetition time
VAS	Visual Analogue Scales
VVLT	Visual Verbal Learning Test

REFERENCES

1. Friston, K.J., Frith, C.D., Liddle, P.F. and Frackowiak, R.S.J. (1993). Functional connectivity: The principal-component analysis of large (PET) data sets. *J. Cereb. Blood Flow Metab.* 13 (1):5-14.
2. Ogawa, S., Lee, T.M., Kay, A.R. and Tank, D.W. (1990). Brain magnetic resonance imaging with contrast dependent on blood oxygenation. *Proc. Natl. Acad. Sci. U. S. A.* 87 (24):9868-9872.
3. Raichle, M.E. (2009). A brief history of human brain mapping. *Trends Neurosci.* 32 (2):118-126.
4. Huettel, S.A., McKeown, M.J., Song, A.W., et al. (2004). Linking hemodynamic and electrophysiological measures of brain activity: Evidence from functional MRI and intracranial field potentials. *Cereb. Cortex* 14 (2):165-173.
5. Mesulam, M.M. (1998). From sensation to cognition. *Brain* 121:1013-1052.
6. van Dijk, K.R.A., Hedden, T., Venkataraman, A., Evans, K.C., Lazar, S.W. and Buckner, R.L. (2010). Intrinsic functional connectivity as a tool for human connectomics: Theory, properties, and optimization. *J. Neurophysiol.* 103 (1):297-321.
7. Fox, M.D. and Raichle, M.E. (2007). Spontaneous fluctuations in brain activity observed with functional magnetic resonance imaging. *Nat. Rev. Neurosci.* 8 (9):700-711.
8. Zhang, D.Y. and Raichle, M.E. (2010). Disease and the brain's dark energy. *Nat. Rev. Neurol.* 6 (1):15-28.
9. Beckmann, C.F., DeLuca, M., Devlin, J.T. and Smith, S.M. (2005). Investigations into resting-state connectivity using independent component analysis. *Philos. T. Roy. Soc. B* 360 (1457):1001-1013.
10. Smith, S.M., Fox, P.T., Miller, K.L., et al. (2009). Correspondence of the brain's functional architecture during activation and rest. *Proc. Natl. Acad. Sci. U.S.A.* 106 (31):13040-13045.
11. Greicius, M.D., Krasnow, B., Reiss, A.L. and Menon, V. (2003). Functional connectivity in the resting brain: A network analysis of the default mode hypothesis. *Proc. Natl. Acad. Sci. U. S. A.* 100 (1):253-258.
12. Raichle, M.E. and Snyder, A.Z. (2007). A default mode of brain function: A brief history of an evolving idea. *Neuroimage* 37 (4):1083-1090.
13. Spreng, R.N., Mar, R.A. and Kim, A.S.N. (2009). The common neural basis of autobiographical memory, prospection, navigation, theory of mind, and the default mode: A quantitative meta-analysis. *J. Cogn. Neurosci.* 21 (3):489-510.
14. Andrews-Hanna, J.R. (2012). The brain's default network and its adaptive role in internal mentation. *Neuroscientist* 18 (3):251-270.
15. McKhann, G.M., Knopman, D.S., Chertkow, H., et al. (2011). The diagnosis of dementia due to Alzheimer's disease: Recommendations from the National Institute on Aging-Alzheimer's Association workgroups on diagnostic guidelines for Alzheimer's disease. *Alzheimers Dement.* 7 (3):263-269.
16. Alzheimer's Association (2017). 2017 Alzheimer's disease facts and figures. *Alzheimers Dement.* 12 (4):459-509.
17. Mathers, C.D., Stevens, G.A., Boerma, T., White, R.A. and Tobias, M.I. (2015). Causes of international increases in older age life expectancy. *Lancet* 385 (9967):540-548.
18. Seeley, W.W., Crawford, R.K., Zhou, J., Miller, B.L. and Greicius, M.D. (2009). Neurodegenerative diseases target large-scale human brain networks. *Neuron* 62 (1):42-52.

19. Delbeuck, X., Van der Linden, M. and Collette, F. (2003). Alzheimer's disease as a disconnection syndrome? *Neuropsychol. Rev.* 13 (2):79-92.
20. Hafkemeijer, A., van der Grond, J. and Rombouts, S.A.R.B. (2012). Imaging the default mode network in aging and dementia. *B.B.A.-Mol. Basis Dis.* 1822 (3):431-441.
21. Krajcovicova, L., Marecek, R., Mikl, M. and Rektorova, I. (2014). Disruption of resting functional connectivity in Alzheimer's patients and at-risk subjects. *Curr. Neurol. Neurosci. Rep.* 14 (10).
22. Agosta, F., Pievani, M., Geroldi, C., Copetti, M., Frisoni, G.B. and Filippi, M. (2012). Resting state fMRI in Alzheimer's disease: beyond the default mode network. *Neurobiol. Aging* 33 (8):1564-1578.
23. Binnewijzend, M.A.A., Schoonheim, M.M., Sanz-Arigita, E., et al. (2012). Resting-state fMRI changes in Alzheimer's disease and mild cognitive impairment. *Neurobiol. Aging* 33 (9):2018-2028.
24. Brier, M.R., Thomas, J.B., Snyder, A.Z., et al. (2012). Loss of intranetwork and internetwork resting state functional connections with Alzheimer's disease progression. *J. Neurosci.* 32 (26):8890-8899.
25. Sheline, Y.I. and Raichle, M.E. (2013). Resting state functional connectivity in preclinical Alzheimer's disease. *Biol. Psychiatry* 74 (5):340-347.
26. Zhou, J., Greicius, M.D., Gennatas, E.D., et al. (2010). Divergent network connectivity changes in behavioural variant frontotemporal dementia and Alzheimer's disease. *Brain* 133:1352-1367.
27. Horwitz, B. (1985). Brain metabolism and blood-flow during aging. *Electroencephalogr. Clin. Neurophysiol.* 61 (3):S14-S15.
28. Andrews-Hanna, J.R., Snyder, A.Z., Vincent, J.L., et al. (2007). Disruption of large-scale brain systems in advanced aging. *Neuron* 56 (5):924-935.
29. Madden, D.J., Bennett, I.J., Burzynska, A., Potter, G.G., Chen, N.K. and Song, A.W. (2012). Diffusion tensor imaging of cerebral white matter integrity in cognitive aging. *B.B.A.-Mol. Basis Dis.* 1822 (3):386-400.
30. O'Sullivan, M., Jones, D.K., Summers, P.E., Morris, R.G., Williams, S.C.R. and Markus, H.S. (2001). Evidence for cortical "disconnection" as a mechanism of age-related cognitive decline. *Neurology* 57 (4):632-638.
31. Aizenstein, H.J., Nebes, R.D., Saxton, J.A., et al. (2008). Frequent amyloid deposition without significant cognitive impairment among the elderly. *Arch. Neurol.* 65 (11):1509-1517.
32. Frisoni, G.B., Fox, N.C., Jack, C.R., Scheltens, P. and Thompson, P.M. (2010). The clinical use of structural MRI in Alzheimer disease. *Nat. Rev. Neurol.* 6 (2):67-77.
33. He, X.X., Qin, W., Liu, Y., et al. (2014). Abnormal salience network in normal aging and in amnesic mild cognitive impairment and Alzheimer's disease. *Hum. Brain Mapp.* 35 (7):3446-3464.
34. Gardini, S., Venneri, A., Sambataro, F., et al. (2015). Increased functional connectivity in the default mode network in mild cognitive impairment: A maladaptive compensatory mechanism associated with poor semantic memory performance. *J. Alzheimers Dis.* 45 (2):457-470.
35. Wang, L., Roe, C.M., Snyder, A.Z., et al. (2012). Alzheimer disease family history impacts resting state functional connectivity. *Ann. Neurol.* 72 (4):571-577.
36. Filippini, N., MacIntosh, B.J., Hough, M.G., et al. (2009). Distinct patterns of brain activity in young carriers of the APOE-ε4 allele. *Proc. Natl. Acad. Sci. U. S. A.* 106 (17):7209-7214.
37. Damoiseaux, J.S., Beckmann, C.F., Arigita, E.J.S., et al. (2008). Reduced resting-state brain activity in the "default network" in normal aging. *Cereb. Cortex* 18 (8):1856-1864.

38. Ferreira, L.K. and Busatto, G.F. (2013). Resting-state functional connectivity in normal brain aging. *Neurosci. Biobehav. Rev.* 37 (3):384-400.
39. Onoda, K., Ishihara, M. and Yamaguchi, S. (2012). Decreased functional connectivity by aging is associated with cognitive decline. *J. Cogn. Neurosci.* 24 (11):2186-2198.
40. Wu, T., Zang, Y.F., Wang, L., et al. (2007). Aging influence on functional connectivity of the motor network in the resting state. *Neurosci. Lett.* 422 (3):164-168.
41. Allen, E.A., Erhardt, E.B., Damaraju, E., et al. (2011). A baseline for the multivariate comparison of resting-state networks. *Front. Syst. Neurosci.* 5:2.
42. Tomasi, D. and Volkow, N.D. (2012). Aging and functional brain networks. *Mol. Psychiatry* 17 (5):549-558.
43. Selkoe, D.J. (2002). Alzheimer's disease is a synaptic failure. *Science* 298 (5594):789-791.
44. Mahncke, H.W., Bronstone, A. and Merzenich, M.M. (2006). Brain plasticity and functional losses in the aged: Scientific bases for a novel intervention. *Prog. Brain Res.* 157:81-109.
45. Meltzer, C.C., Smith, G., DeKosky, S.T., et al. (1998). Serotonin in aging, late-life depression, and Alzheimer's disease: The emerging role of functional imaging. *Neuropsychopharmacol* 18 (6):407-430.
46. Bowen, D.M., Allen, S.J., Benton, J.S., et al. (1983). Biochemical assessment of serotonergic and cholinergic dysfunction and cerebral atrophy in Alzheimer's disease. *J. Neurochem.* 41 (1):266-272.
47. Daubert, E.A. and Condron, B.G. (2010). Serotonin: A regulator of neuronal morphology and circuitry. *Trends Neurosci.* 33 (9):424-434.
48. Nichols, D.E. and Nichols, C.D. (2008). Serotonin receptors. *Chem. Rev.* 108 (5):1614-1641.
49. Hoyer, D., Hannon, J.P. and Martin, G.R. (2002). Molecular, pharmacological and functional diversity of 5-HT receptors. *Pharmacol. Biochem. Behav.* 71 (4):533-554.
50. Carr, G.V. and Lucki, I. (2011). The role of serotonin receptor subtypes in treating depression: A review of animal studies. *Psychopharmacology (Berl.)* 213 (2-3):265-287.
51. Ownby, R.L., Crocco, E., Acevedo, A., John, V. and Loewenstein, D. (2006). Depression and risk for Alzheimer disease: Systematic review, meta-analysis, and metaregression analysis. *Arch. Gen. Psychiatry* 63 (5):530-538.
52. McRae, A., McRae, K. and Brady (2001). Review of sertraline and its clinical applications in psychiatric disorders. *Expert Opin. Pharmacother.* 2 (5):883-892.
53. Dumas, J.A. and Newhouse, P.A. (2011). The cholinergic hypothesis of cognitive aging revisited again: Cholinergic functional compensation. *Pharmacol. Biochem. Beh.* 99 (2):254-261.
54. Mesulam, M.M. (2013). Cholinergic circuitry of the human nucleus basalis and its fate in Alzheimer's disease. *J. Comp. Neurol.* 521 (18):4124-4144.
55. Caulfield, M.P. and Birdsall, N.J.M. (1998). International Union of Pharmacology. XVII. Classification of muscarinic acetylcholine receptors. *Pharmacol. Rev.* 50 (2):279-290.
56. Millar, N.S. and Harkness, P.C. (2008). Assembly and trafficking of nicotinic acetylcholine receptors (Review). *Mol. Membr. Biol.* 25 (4):279-292.
57. Kalamida, D., Poulas, K., Avramopoulou, V., et al. (2007). Muscle and neuronal nicotinic acetylcholine receptors: Structure, function and pathogenicity. *Febs J.* 274 (15):3799-3845.

58. Colovic, M.B., Krstic, D.Z., Lazarevic-Pasti, T.D., Bondzic, A.M. and Vasic, V.M. (2013). Acetylcholinesterase inhibitors: Pharmacology and toxicology. *Curr. Neuropharmacol.* 11 (3):315-335.
59. Benarroch, E.E. (2010). Acetylcholine in the cerebral cortex: Effects and clinical implications. *Neurology* 75 (7):659-665.
60. Ruberg, M., Mayo, W., Brice, A., et al. (1990). Choline acetyltransferase activity and [³H] vesamicol binding in the temporal cortex of patients with Alzheimer's disease, Parkinson's disease, and rats with basal forebrain lesions. *Neuroscience* 35 (2):327-333.
61. Herholz, K., Weisenbach, S., Zundorf, G., et al. (2004). In vivo study of acetylcholine esterase in basal forebrain, amygdala, and cortex in mild to moderate Alzheimer disease. *Neuroimage* 21 (1):136-143.
62. Bartus, R.T., Dean, R.L., Beer, B. and Lippa, A.S. (1982). The cholinergic hypothesis of geriatric memory dysfunction. *Science* 217 (4558):408-417.
63. Perry, E., Walker, M., Grace, J. and Perry, R. (1999). Acetylcholine in mind: A neurotransmitter correlate of consciousness? *Trends Neurosci.* 22 (6):273-80.
64. Teipel, S.J., Flatz, W.H., Heinsen, H., et al. (2005). Measurement of basal forebrain atrophy in Alzheimer's disease using MRI. *Brain* 128:2626-2644.
65. Geula, C., Mesulam, M.M., Saroff, D.M. and Wu, C.K. (1998). Relationship between plaques, tangles, and loss of cortical cholinergic fibers in Alzheimer disease. *J. Neuropathol. Exp. Neurol.* 57 (1):63-75.
66. Kar, S., Slowikowski, S.P.M., Westaway, D. and Mount, H.T.J. (2004). Interactions between beta-amyloid and central cholinergic neurons: Implications for Alzheimer's disease. *J. Psychiatry Neurosci.* 29 (6):427-441.
67. Auld, D.S., Kornecook, T.J., Bastianetto, S. and Quirion, R. (2002). Alzheimer's disease and the basal forebrain cholinergic system: Relations to beta-amyloid peptides, cognition, and treatment strategies. *Prog. Neurobiol.* 68 (3):209-245.
68. Campos, C., Rocha, N.B.F., Vieira, R.T., et al. (2016). Treatment of cognitive deficits in Alzheimer's disease: A psychopharmacological review. *Psychiat. Danub.* 28 (1):2-12.
69. Ngo, J. and Holroyd-Leduc, J.M. (2015). Systematic review of recent dementia practice guidelines. *Age Ageing* 44 (1):25-33.
70. Farlow, M.R. and Cummings, J.L. (2007). Effective pharmacologic management of Alzheimer's disease. *Am. J. Med.* 120 (5):388-397.
71. Husain, M. and Mehta, M.A. (2011). Cognitive enhancement by drugs in health and disease. *Trends Cogn. Sci.* 15 (1):28-36.
72. Kaduszkiewicz, H., Zimmermann, T., Beck-Bornholdt, H.P. and van den Bussche, H. (2005). Cholinesterase inhibitors for patients with Alzheimer's disease: systematic review of randomised clinical trials. *Br. Med. J.* 331 (7512):321-323.
73. Lanni, C., Lenzken, S.C., Pascale, A., et al. (2008). Cognition enhancers between treating and doping the mind. *Pharmacol. Res.* 57 (3):196-213.
74. Honey, G. and Bullmore, E.T. (2004). Human pharmacological MRI. *Trends Pharmacol. Sci.* 25 (7):366-374.

75. Gijssman, H.J., Cohen, A.F. and van Gerven, J.M.A. (2004). The application of the principles of clinical drug development to pharmacological challenge tests of the serotonergic system. *J. Psychopharmacol.* 18 (1):7-13.
76. Klumpers, L.E., Cole, D.M., Khalili-Mahani, N., et al. (2012). Manipulating brain connectivity with $\delta(9)$ -tetrahydrocannabinol: A pharmacological resting state fMRI study. *Neuroimage* 63 (3):1701-1711.
77. Kleinloog, D., Rombouts, S., Zoethout, R., et al. (2015). Subjective effects of ethanol, morphine, delta(9)-tetrahydrocannabinol, and ketamine following a pharmacological challenge are related to functional brain connectivity. *Brain Connect.* 5 (10):641-8.
78. Niesters, M., Khalili-Mahani, N., Martini, C., et al. (2012). Effect of subanesthetic ketamine on intrinsic functional brain connectivity: A placebo-controlled functional magnetic resonance imaging study in healthy male volunteers. *Anesthesiology* 117 (4):868-877.
79. Khalili-Mahani, N., Niesters, M., van Osch, M.J., et al. (2015). Ketamine interactions with biomarkers of stress: A randomized placebo-controlled repeated measures resting-state fMRI and PCASL pilot study in healthy men. *Neuroimage* 108:396-409.
80. Khalili-Mahani, N., Zoethout, R.M.W., Beckmann, C.F., et al. (2012). Effects of morphine and alcohol on functional brain connectivity during "resting state": A placebo-controlled crossover study in healthy young men. *Hum. Brain Mapp.* 33 (5):1003-1018.
81. Cole, D.M., Beckmann, C.F., Oei, N.Y.L., Both, S., van Gerven, J.M.A. and Rombouts, S.A.R.B. (2013). Differential and distributed effects of dopamine neuromodulations on resting-state network connectivity. *Neuroimage* 78:59-67.
82. van de Ven, V., Wingen, M., Kuypers, K.P.C., Ramaekers, J.G. and Formisano, E. (2013). Escitalopram decreases cross-regional functional connectivity within the default-mode network. *PLoS One* 8 (6):e68355.
83. Schaefer, A., Burmann, I., Regenthal, R., et al. (2014). Serotonergic modulation of intrinsic functional connectivity. *Curr. Biol.* 24 (19):2314-2318.
84. Li, B.J., Liu, L., Friston, K.J., et al. (2013). A treatment-resistant default mode subnetwork in major depression. *Biol. Psychiatry* 74 (1):48-54.
85. McCabe, C. and Mishor, Z. (2011). Antidepressant medications reduce subcortical-cortical resting-state functional connectivity in healthy volunteers. *Neuroimage* 57 (4):1317-1323.
86. McCabe, C., Mishor, Z., Filippini, N., Cowen, P.J., Taylor, M.J. and Harmer, C.J. (2011). SSRI administration reduces resting state functional connectivity in dorso-medial prefrontal cortex. *Mol. Psychiatry* 16 (6):592-594.
87. van Wingen, G.A., Tendolkar, I., Urner, M., et al. (2014). Short-term antidepressant administration reduces default mode and task-positive network connectivity in healthy individuals during rest. *Neuroimage* 88:47-53.
88. Sundermann, B., Beverborg, M.O.L. and Pfeleiderer, B. (2014). Toward literature-based feature selection for diagnostic classification: A meta-analysis of resting-state fMRI in depression. *Front. Hum. Neurosci.* 8:692.
89. Li, W., Antuono, P.G., Xie, C., et al. (2012). Changes in regional cerebral blood flow and functional connectivity in the cholinergic pathway associated with cognitive performance in subjects with mild Alzheimer's disease after 12-week donepezil treatment. *Neuroimage* 60 (2):1083-1091.

90. Solé-Padullés, C., Bartres-Faz, D., Llado, A., et al. (2013). Donepezil treatment stabilizes functional connectivity during resting state and brain activity during memory encoding in Alzheimer's disease. *J. Clin. Psychopharmacol.* 33 (2):199-205.
91. Goveas, J.S., Xie, C.M., Ward, B.D., et al. (2011). Recovery of hippocampal network connectivity correlates with cognitive improvement in mild Alzheimer's disease patients treated with donepezil assessed by resting-state fMRI. *J. Magn. Reson. Imaging* 34 (4):764-773.
92. Blautzik, J., Keeser, D., Paolini, M., et al. (2016). Functional connectivity increase in the default-mode network of patients with Alzheimer's disease after long-term treatment with Galantamine. *Eur. Neuropsychopharmacol.* 26 (3):602-613.
93. Griffanti, L., Wilcock, G.K., Voets, N., et al. (2016). Donepezil enhances frontal functional connectivity in Alzheimer's disease: A pilot study. *Dement. Geriatr. Cogn. Dis. Extra* 6 (3):518-528.
94. Zaidel, L., Allen, G., Cullum, C.M., et al. (2012). Donepezil effects on hippocampal and prefrontal functional connectivity in Alzheimer's disease: Preliminary report. *J. Alzheimers Dis.* 31 Suppl 3:S221-S226.
95. Borland, R.G. and Nicholson, A.N. (1984). Visual motor coordination and dynamic visual-acuity. *Brit. J. Clin. Pharmacol.* 18 (Suppl 1):S69-S72.
96. Bond, A. and Lader, M. (1974). Use of analog scales in rating subjective feelings. *Brit. J. Med. Psychol.* 47 (3):211-218.
97. Laeng, B., Lag, T. and Brennen, T. (2005). Reduced stroop interference for opponent colors may be due to input factors: Evidence from individual differences and a neural network simulation. *J. Exp. Psychol. Human.* 31 (3):438-452.
98. Lezak, M.D. (2004) *Neuropsychological Assessment*. New York. Oxford University Press.
99. Lim, H.K., Juh, R., Pae, C.U., et al. (2008). Altered verbal working memory process in patients with Alzheimer's disease. *Neuropsychobiology* 57 (4):181-187.
100. Norris, H. (1971). The action of sedatives on brain stem oculomotor systems in man. *Neuropharmacology* 10 (21):181-191.
101. Stroop, J.R. (1935). Studies of interference in serial verbal reactions. *J. Exp. Psychol.* 18:643-662.
102. Rogers, M.A., Kasai, K., Koji, M., et al. (2004). Executive and prefrontal dysfunction in unipolar depression: A review of neuropsychological and imaging evidence. *Neurosci. Res.* 50 (1):1-11.
103. Wechsler, D. (1981). The psychometric tradition: Developing the Wechsler Adult Intelligence Scale. *Contemp. Educ. Psychol.* 6 (2):82-85.
104. Sagud, M., Pivac, N., Muck-Seler, D., Jakovljevic, M., Mihaljevic-Peles, A. and Korsic, M. (2002). Effects of sertraline treatment on plasma cortisol, prolactin and thyroid hormones in female depressed patients. *Neuropsychobiology* 45 (3):139-143.
105. von Bardeleben, U., Steiger, A., Gerken, A. and Holsboer, F. (1989). Effects of fluoxetine upon pharmacoendocrine and sleep-EEG parameters in normal controls. *Int. Clin. Psychopharmacol.* 4:1-5.
106. Cozantitis, D., Dessypris, A. and Nuutila, K. (1980). The effect of galanthamine hydrobromide on plasma ACTH in patients undergoing anesthesia and surgery. *Acta Anaesthesiol. Scand.* 24 (3):166-168.
107. Guye, M., Bettus, G., Bartolomei, F. and Cozzone, P.J. (2010). Graph theoretical analysis of structural and functional connectivity MRI in normal and pathological brain networks. *Magn. Reson. Mater. Phy.* 23 (5-6):409-421.

108. van den Heuvel, M.P. and Pol, H.E.H. (2010). Exploring the brain network: A review on resting-state fMRI functional connectivity. *Eur. Neuropsychopharmacol.* 20 (8):519-534.
109. Jacobs, B.L. and Azmitia, E.C. (1992). Structure and function of the brain serotonin system. *Physiol. Rev.* 72 (1):165-229.
110. Barnes, N.M. and Sharp, T. (1999). A review of central 5-HT receptors and their function. *Neuropharmacology* 38 (8):1083-1152.
111. Smith, G.S., Ma, Y., Dhawan, V., et al. (2002). Serotonin modulation of cerebral glucose metabolism measured with positron emission tomography (PET) in human subjects. *Synapse* 45 (2):105-112.
112. Geday, J., Hermansen, F., Rosenberg, R. and Smith, D.F. (2005). Serotonin modulation of cerebral blood flow measured with positron emission tomography (PET) in humans. *Synapse* 55 (4):224-229.
113. McKie, S., Del-Ben, C., Elliott, R., et al. (2005). Neuronal effects of acute citalopram detected by pharmacofMRI. *Psychopharmacology (Berl.)* 180 (4):680-686.
114. Klomp, A., Caan, M.W.A., Denys, D., Nederveen, A.J. and Reneman, L. (2012). Feasibility of ASL-based phMRI with a single dose of oral citalopram for repeated assessment of serotonin function. *Neuroimage* 63 (3):1695-1700.
115. Viviani, R., Abler, B., Seeringer, A. and Stingl, J.C. (2012). Effect of paroxetine and bupropion on human resting brain perfusion: An arterial spin labeling study. *Neuroimage* 61 (4):773-779.
116. Anderson, I.M., Del-Ben, C.M., McKie, S., et al. (2007). Citalopram modulation of neuronal responses to aversive face emotions: a functional MRI study. *Neuroreport* 18 (13):1351-1355.
117. Bruhl, A.B., Jancke, L. and Herwig, U. (2011). Differential modulation of emotion processing brain regions by noradrenergic and serotonergic antidepressants. *Psychopharmacology (Berl.)* 216 (3):389-399.
118. Lu, H. and Stein, E.A. (2014). Resting state functional connectivity: Its physiological basis and application in neuropharmacology. *Neuropharmacology* 84:79-89.
119. Smith, S.M., Jenkinson, M., Woolrich, M.W., et al. (2004). Advances in functional and structural MR image analysis and implementation as FSL. *Neuroimage* 23 (Suppl 1):S208-S219.
120. Woolrich, M.W., Jbabdi, S., Patenaude, B., et al. (2009). Bayesian analysis of neuroimaging data in FSL. *Neuroimage* 45 (Suppl 1):S173-S186.
121. Jenkinson, M., Beckmann, C.F., Behrens, T.E., Woolrich, M.W. and Smith, S.M. (2012). FSL. *Neuroimage* 62 (2):782-790.
122. Smith, S.M. (2002). Fast robust automated brain extraction. *Hum. Brain Mapp.* 17 (3):143-155.
123. Jenkinson, M., Bannister, P., Brady, M. and Smith, S. (2002). Improved optimization for the robust and accurate linear registration and motion correction of brain images. *Neuroimage* 17 (2):825-841.
124. Greve, D.N. and Fischl, B. (2009). Accurate and robust brain image alignment using boundary-based registration. *Neuroimage* 48 (1):63-72.
125. Beckmann, C.F., Mackay, C.E., Filippini, N. and Smith, S.M. (2009). Group comparison of resting-state FMRI data using multi-subject ICA and dual regression. *OHBM*.
126. Birn, R.M. (2012). The role of physiological noise in resting-state functional connectivity. *Neuroimage* 62 (2):864-70.

127. Khalili-Mahani, N., Chang, C., van Osch, M.J., et al. (2013). The impact of “physiological correction” on functional connectivity analysis of pharmacological resting state fMRI. *Neuroimage* 65:499-510.
128. Smith, S.M. and Nichols, T.E. (2009). Threshold-free cluster enhancement: Addressing problems of smoothing, threshold dependence and localisation in cluster inference. *Neuroimage* 44 (1):83-98.
129. Winkler, A.M., Ridgway, G.R., Webster, M.A., Smith, S.M. and Nichols, T.E. (2014). Permutation inference for the general linear model. *Neuroimage* 92:381-397.
130. Adell, A., Celada, P., Abellan, M.T. and Artigas, F. (2002). Origin and functional role of the extracellular serotonin in the midbrain raphe nuclei. *Brain Res Rev* 39 (2-3):154-180.
131. Morgane, P.J., Galler, J.R. and Mokler, D.J. (2005). A review of systems and networks of the limbic forebrain/limbic midbrain. *Progr. Neurobiol.* 75 (2):143-160.
132. Celada, P., Puig, M.V. and Artigas, F. (2013). Serotonin modulation of cortical neurons and networks. *Front. Integr. Neurosci.* 7:25.
133. Peroutka, S.J. and Snyder, S.H. (1979). Multiple serotonin receptors: Differential binding of [³H]5-hydroxytryptamine, [³H]lysergic acid diethylamide and [³H]spiroperidol. *Mol. Pharmacol.* 16 (3):687-699.
134. Briley, M. and Moret, C. (1993). Neurobiological mechanisms involved in antidepressant therapies. *Clin. Neuropharmacol.* 16 (5):387-400.
135. Whale, R., Clifford, E.M., Bhagwagar, Z. and Cowen, P.J. (2001). Decreased sensitivity of 5-HT_{1D} receptors in melancholic depression. *Brit. J. Psychiatry* 178:454-457.
136. Joseph, R. (1992). The limbic system: Emotion, laterality, and unconscious mind. *Psychoanal. Rev.* 79 (3):405-456.
137. Anand, A., Li, Y., Wang, Y., et al. (2005). Activity and connectivity of brain mood regulating circuit in depression: A functional magnetic resonance study. *Biol. Psychiatry* 57 (10):1079-1088.
138. Mayberg, H.S. (1997). Limbic-cortical dysregulation: A proposed model of depression. *J. Neuropsychiatr. Clin. Neurosci.* 9 (3):471-481.
139. Seminowicz, D.A., Mayberg, H.S., McIntosh, A.R., et al. (2004). Limbic-frontal circuitry in major depression: A path modeling metanalysis. *Neuroimage* 22 (1):409-418.
140. Hensler, J.G. (2006). Serotonergic modulation of the limbic system. *Neurosci. Biobehav. Rev.* 30 (2):203-214.
141. Fransson, P. and Marrelec, G. (2008). The precuneus/posterior cingulate cortex plays a pivotal role in the default mode network: Evidence from a partial correlation network analysis. *Neuroimage* 42 (3):1178-1184.
142. Zhu, X.L., Wang, X., Xiao, J., et al. (2012). Evidence of a dissociation pattern in resting-state default mode network connectivity in first-episode, treatment-naive major depression patients. *Biol. Psychiatry* 71 (7):611-617.
143. Sheline, Y.I., Price, J.L., Yan, Z.Z. and Mintun, M.A. (2010). Resting-state functional MRI in depression unmasks increased connectivity between networks via the dorsal nexus. *Proc. Natl. Acad. Sci. U.S.A.* 107 (24):11020-11025.
144. Hamilton, J.P., Furman, D.J., Chang, C., Thomason, M.E., Dennis, E. and Gotlib, I.H. (2011). Default-mode and task-positive network activity in major depressive disorder: Implications for adaptive and maladaptive rumination. *Biol. Psychiatry* 70 (4):327-333.

145. Greicius, M.D., Flores, B.H., Menon, V., et al. (2007). Resting-state functional connectivity in major depression: Abnormally increased contributions from subgenual cingulate cortex and thalamus. *Biol. Psychiatry* 62 (5):429-437.
146. Kraus, C., Ganger, S., Losak, J., et al. (2014). Gray matter and intrinsic network changes in the posterior cingulate cortex after selective serotonin reuptake inhibitor intake. *Neuroimage* 84:236-244.
147. Thompson, G.C., Thompson, A.M., Garrett, K.M. and Britton, B.H. (1994). Serotonin and serotonin receptors in the central auditory system. *Otolaryngol.-Head and Neck Surg.* 110 (1):93-102.
148. Morrison, J.H., Foote, S.L., Molliver, M.E., Bloom, F.E. and Lidov, H.G. (1982). Noradrenergic and serotonergic fibers innervate complementary layers in monkey primary visual cortex: An immunohistochemical study. *Proc. Natl. Acad. Sci. U.S.A.* 79 (7):2401-2405.
149. Lidow, M.S., Goldman-rakic, P.S., Gallager, D.W., Geschwind, D.H. and Rakic, P. (1989). Distribution of major neurotransmitter receptors in the motor and somatosensory cortex of the rhesus monkey. *Neuroscience* 32 (3):609-627.
150. Kahkonen, S., Ahveninen, J., Pennanen, S., Liesivuori, J., Ilmoniemi, R.J. and Jaaskelainen, I.P. (2002). Serotonin modulates early cortical auditory processing in healthy subjects: Evidence from MEG with acute tryptophan depletion. *Neuropsychopharmacology* 27 (5):862-868.
151. Amargos-Bosch, M., Bortolozzi, A., Puig, M.V., et al. (2004). Co-expression and in vivo interaction of serotonin_{1A} and serotonin_{2A} receptors in pyramidal neurons of prefrontal cortex. *Cereb. Cortex* 14 (3):281-299.
152. Lidow, M.S., Goldman-rakic, P.S., Gallager, D.W. and Rakic, P. (1989). Quantitative autoradiographic mapping of serotonin 5-HT₁ and 5-HT₂ receptors and uptake sites in the neocortex of the rhesus monkey. *J. Comp. Neurol.* 280 (1):27-42.
153. Oliveri, M. and Calvo, G. (2003). Increased visual cortical excitability in ecstasy users: A transcranial magnetic stimulation study. *J. Neurol. Neurosurg. Psychiatry* 74 (8):1136-1138.
154. Jacobs, B.L. and Fornal, C.A. (1999). Activity of serotonergic neurons in behaving animals. *Neuropsychopharmacology* 21 (Suppl 2):S9-S15.
155. Loubinoux, I., Pariente, J., Boulanouar, K., et al. (2002). A single dose of the serotonin neurotransmission agonist paroxetine enhances motor output: Double-blind, placebo-controlled, fMRI study in healthy subjects. *Neuroimage* 15 (1):26-36.
156. Loubinoux, I., Pariente, J., Rascol, O., Celsis, P. and Chollet, F. (2002). Selective serotonin reuptake inhibitor paroxetine modulates motor behavior through practice. A double-blind, placebo-controlled, multi-dose study in healthy subjects. *Neuropsychologia* 40 (11):1815-1821.
157. Shima, K. and Tanji, J. (1998). Role for cingulate motor area cells in voluntary movement selection based on reward. *Science* 282 (5392):1335-1338.
158. Vogt, B.A., Finch, D.M. and Olson, C.R. (1992). Functional heterogeneity in cingulate cortex: The anterior executive and posterior evaluative regions. *Cereb. Cortex* 2 (6):435-443.
159. Cavanna, A.E. and Trimble, M.R. (2006). The precuneus: A review of its functional anatomy and behavioural correlates. *Brain* 129:564-583.
160. Zhang, S. and Li, C.S.R. (2012). Functional connectivity mapping of the human precuneus by resting state fMRI. *Neuroimage* 59 (4):3548-3562.

161. Robinson, S. (2007). Antidepressants for treatment of tinnitus. *Prog. Brain Res.* 166:263-71.
162. Burton, H., Wineland, A., Bhattacharya, M., Nicklaus, J., Garcia, K.S. and Piccirillo, J.F. (2012). Altered networks in bothersome tinnitus: A functional connectivity study. *BMC Neurosci.* 13 (3):1-15.
163. Kim, J.Y., Kim, Y.H., Lee, S., et al. (2012). Alteration of functional connectivity in tinnitus brain revealed by resting-state fMRI?: A pilot study. *Int. J. Audiol.* 51 (5):413-417.
164. Maudoux, A., Lefebvre, P., Cabay, J.E., et al. (2012). Auditory resting-state network connectivity in tinnitus: A functional MRI study. *PLoS One* 7 (5):e36222.
165. Maudoux, A., Lefebvre, P., Cabay, J.E., et al. (2012). Connectivity graph analysis of the auditory resting state network in tinnitus. *Brain Res.* 1485:10-21.
166. Ueyama, T., Donishi, T., Ukai, S., et al. (2013). Brain regions responsible for tinnitus distress and loudness: A resting-state fMRI study. *PLoS One* 8 (6):e67778.
167. Dumont, G.J.H., de Visser, S.J., Cohen, A.F. and van Gerven, J.M.A. (2005). Biomarkers for the effects of selective serotonin reuptake inhibitors (SSRIs) in healthy subjects. *Brit. J. Clin. Pharmacol.* 59 (5):495-510.
168. Rijnbeek, B., De Visser, S., Franson, K., Cohen, A. and Van Gerven, J. (2002). REM sleep reduction as a biomarker for the effects of antidepressants in healthy volunteers. *Brit. J. Clin. Pharmacol.* 54 (5):561-562.
169. Bruhl, A.B., Kaffenberger, T. and Herwig, U. (2010). Serotonergic and noradrenergic modulation of emotion processing by single dose antidepressants. *Neuropsychopharmacology* 35 (2):521-533.
170. Del-Ben, C.M., Deakin, J.F.W., Mckie, S., et al. (2005). The effect of citalopram pretreatment on neuronal responses to neuropsychological tasks in normal volunteers: An fMRI study. *Neuropsychopharmacology* 30 (9):1724-1734.
171. Murphy, S.E., Norbury, R., O'Sullivan, U., Cowen, P.J. and Harmer, C.J. (2009). Effect of a single dose of citalopram on amygdala response to emotional faces. *Brit. J. Psychiatry* 194 (6):535-540.
172. Outhred, T., Hawkshead, B.E., Wager, T.D., Das, P., Malhi, G.S. and Kemp, A.H. (2013). Acute neural effects of selective serotonin reuptake inhibitors versus noradrenaline reuptake inhibitors on emotion processing: Implications for differential treatment efficacy. *Neurosci. Biobehav. Rev.* 37 (8):1786-1800.
173. Frazer, A. and Benmansour, S. (2002). Delayed pharmacological effects of antidepressants. *Mol. Psychiatry* 7 (Suppl 1):S23-S28.
174. Harmer, C.J., Goodwin, G.M. and Cowen, P.J. (2009). Why do antidepressants take so long to work? A cognitive neuropsychological model of antidepressant drug action. *Br. J. Psychiatry* 195 (2):102-108.
175. Bhagwagar, Z., Cowen, P.J., Goodwin, G.M. and Harmer, C.J. (2004). Normalization of enhanced fear recognition by acute SSRI treatment in subjects with a previous history of depression. *Am. J. Psychiatry* 161 (1):166-168.
176. Browning, M., Reid, C., Cowen, P.J., Goodwin, G.M. and Harmer, C.J. (2007). A single dose of citalopram increases fear recognition in healthy subjects. *J. Psychopharmacol.* 21 (7):684-690.
177. Harmer, C.J., Bhagwagar, Z., Perrett, D.I., Vollm, B.A., Cowen, P.J. and Goodwin, G.M. (2003). Acute SSRI administration affects the processing of social cues in healthy volunteers. *Neuropsychopharmacology* 28 (1):148-152.

178. Harmer, C.J., Hill, S.A., Taylor, M.J., Cowen, P.J. and Goodwin, G.M. (2003). Toward a neuropsychological theory of antidepressant drug action: Increase in positive emotional bias after potentiation of norepinephrine activity. *Am. J. Psychiatry* 160 (5):990-992.
179. Harmer, C.J. (2008). Serotonin and emotional processing: Does it help explain antidepressant drug action? *Neuropharmacology* 55 (6):1023-1028.
180. Carrasco, J.L. and Sandner, C. (2005). Clinical effects of pharmacological variations in selective serotonin reuptake inhibitors: An overview. *Int. J. Clin. Pract.* 59 (12):1428-1434.
181. Jacobs, G.E., Kamerling, I.M.C., de Kam, M.L., et al. (2010). Enhanced tolerability of the 5-hydroxytryptophane challenge test combined with granisetron. *J. Psychopharmacol.* 24 (1):65-72.
182. Jacobs, G.E., van der Grond, J., Teeuwisse, W.M., et al. (2010). Hypothalamic glutamate levels following serotonergic stimulation: A pilot study using 7-Tesla magnetic resonance spectroscopy in healthy volunteers. *Prog. Neuro-Psychopharmacol. Biol. Psychiatry* 34 (3):486-491.
183. Veer, I.M., Oei, N.Y.L., Spinhoven, P., van Buchem, M.A., Elzinga, B.M. and Rombouts, S.A.R.B. (2012). Endogenous cortisol is associated with functional connectivity between the amygdala and medial prefrontal cortex. *Psychoneuroendocrinology* 37 (7):1039-1047.
184. Reynell, C. and Harris, J.J. (2013). The BOLD signal and neurovascular coupling in autism. *Dev. Cogn. Neurosci.* 6:72-79.
185. Wong, C.W., Olafsson, V., Tal, O. and Liu, T.T. (2012). Anti-correlated networks, global signal regression, and the effects of caffeine in resting-state functional MRI. *Neuroimage* 63 (1):356-364.
186. Rack-Gomer, A.L. and Liu, T.T. (2012). Caffeine increases the temporal variability of resting-state BOLD connectivity in the motor cortex. *Neuroimage* 59 (3):2994-3002.
187. Rack-Gomer, A.L., Liu, J. and Liu, T.T. (2009). Caffeine reduces resting-state BOLD functional connectivity in the motor cortex. *Neuroimage* 46 (1):56-63.
188. Feczko, E., Miezin, F.M., Constantino, J.N., Schlaggar, B.L., Petersen, S.E. and Pruett, J.R. (2012). The hemodynamic response in children with Simplex Autism. *Dev. Cogn. Neurosci.* 2 (4):396-408.
189. Soreq, H. and Seidman, S. (2001). Acetylcholinesterase - New roles for an old actor. *Nat. Rev. Neurosci.* 2 (4):294-302.
190. Tork, I. (1990). Anatomy of the serotonergic system. *Ann. Ny. Acad. Sci.* 600:9-33.
191. Baxter, D.A., Canavier, C.C., Clark, J.W. and Byrne, J.H. (1999). Computational model of the serotonergic modulation of sensory neurons in *Aplysia*. *J. Neurophysiol.* 82 (6):2914-2935.
192. Doya, K. (2002). Metalearning and neuromodulation. *Neural Netw.* 15 (4-6):495-506.
193. Marder, E. and Thirumalai, V. (2002). Cellular, synaptic and network effects of neuromodulation. *Neural Netw.* 15 (4-6):479-493.
194. Bargmann, C.I. (2012). Beyond the connectome: How neuromodulators shape neural circuits. *Bioessays* 34 (6):458-465.
195. Khalili-Mahani, N., van Osch, M.J., de Rooij, M., et al. (2014). Spatial heterogeneity of the relation between resting-state connectivity and blood flow: An important consideration for pharmacological studies. *Hum. Brain Mapp.* 35 (3):929-942.

196. Damoiseaux, J.S., Rombouts, S.A.R.B., Barkhof, F., et al. (2006). Consistent resting-state networks across healthy subjects. *Proc. Natl. Acad. Sci. U. S. A.* 103 (37):13848-13853.
197. Seeley, W.W., Menon, V., Schatzberg, A.F., et al. (2007). Dissociable intrinsic connectivity networks for salience processing and executive control. *J. Neurosci.* 27 (9):2349-2356.
198. Wang, L., Zang, Y., He, Y., et al. (2006). Changes in hippocampal connectivity in the early stages of Alzheimer's disease: evidence from resting state fMRI. *Neuroimage* 31 (2):496-504.
199. Klaassens, B.L., van Gorsel, H.C., Khalili-Mahani, N., et al. (2015). Single-dose serotonergic stimulation shows widespread effects on functional brain connectivity. *Neuroimage* 122:440-50.
200. Wang, L., Day, J., Roe, C.M., et al. (2014). The effect of APOE ϵ 4 allele on cholinesterase inhibitors in patients with Alzheimer disease: Evaluation of the feasibility of resting state functional connectivity magnetic resonance imaging. *Alz. Dis. Assoc. Dis.* 28 (2):122-127.
201. Gu, Q. (2002). Neuromodulatory transmitter systems in the cortex and their role in cortical plasticity. *Neuroscience* 111 (4):815-835.
202. Hasselmo, M.E. (1995). Neuromodulation and cortical function: Modeling the physiological basis of behavior. *Behav. Brain Res.* 67 (1):1-27.
203. Foehring, R.C. and Lorenzon, N.M. (1999). Neuromodulation, development and synaptic plasticity. *Can. J. Exp. Psychol.* 53 (1):45-61.
204. Liem-Moolenaar, M., de Boer, P., Timmers, M., et al. (2011). Pharmacokinetic-pharmacodynamic relationships of central nervous system effects of scopolamine in healthy subjects. *Brit. J. Clin. Pharmacol.* 71 (6):886-898.
205. Gijssman, H.J., van Gerven, J.M.A., Verkes, R.J., et al. (2002). Saccadic peak velocity and EEG as end-points for a serotonergic challenge test. *Hum. Psychopharm. Clin.* 17 (2):83-89.
206. Umegaki, H., Yamamoto, A., Suzuki, Y. and Iguchi, A. (2009). Responses of hypothalamo-pituitary-adrenal axis to a cholinesterase inhibitor. *Neuroreport* 20 (15):1366-1370.
207. Pruim, R.H.R., Mennes, M., van Rooij, D., Llera, A., Buitelaar, J.K. and Beckmann, C.F. (2015). ICA-AROMA: A robust ICA-based strategy for removing motion artifacts from fMRI data. *Neuroimage* 112:267-277.
208. Pruim, R.H.R., Mennes, M., Buitelaar, J.K. and Beckmann, C.F. (2015). Evaluation of ICA-AROMA and alternative strategies for motion artifact removal in resting state fMRI. *Neuroimage* 112:278-287.
209. Pesarin, F. (1990). On a nonparametric combination method for dependent permutation tests with applications. *Psychother. Psychosom.* 54 (2-3):172-179.
210. Winkler, A.M., Webster, M.A., Brooks, J.C., Tracey, I., Smith, S.M. and Nichols, T.E. (2016). Non-parametric combination and related permutation tests for neuroimaging. *Hum. Brain Mapp.* 37:1486-1511.
211. Fisher, R.A. (1932) *Statistical methods for research workers*. Edinburgh. Oliver and Boyd.
212. Burke, W.J., Gergel, I. and Bose, A. (2002). Fixed-dose trial of the single isomer SSRI escitalopram in depressed outpatients. *J. Clin. Psychiat.* 63 (4):331-336.
213. Wagner, K.D., Robb, A.S., Findling, R.L., Jin, J.Q., Gutierrez, M.M. and Heydorn, W.E. (2004). A randomized, placebo-controlled trial of citalopram for the treatment of major depression in children and adolescents. *Am. J. Psychiat.* 161 (6):1079-1083.

214. Lanctot, K.L., Herrmann, N., Yau, K.K., et al. (2003). Efficacy and safety of cholinesterase inhibitors in Alzheimer's disease: A meta-analysis. *Can. Med. Assoc. J.* 169 (6):557-564.
215. Repantis, D., Laisney, O. and Heuser, I. (2010). Acetylcholinesterase inhibitors and memantine for neuroenhancement in healthy individuals: A systematic review. *Pharmacol. Res.* 61 (6):473-481.
216. Seifritz, E., Baumann, P., Muller, M.J., et al. (1996). Neuroendocrine effects of a 20-mg citalopram infusion in healthy males: A placebo-controlled evaluation of citalopram as 5-HT function probe. *Neuropsychopharmacology* 14 (4):253-263.
217. Bruhl, A. and Herwig, U. (2009). Differential modulation of emotion processing by single dose serotonergic and noradrenergic antidepressants: A pharmacofMRI study. *Pharmacopsychiatry* 42 (5):214-214.
218. Baumgarten, H.G. and Grozdanovic, Z. (1995). Psychopharmacology of central serotonergic systems. *Pharmacopsychiatry* 28:73-79.
219. Kupfer, D.J., Frank, E. and Phillips, M.L. (2012). Major depressive disorder: new clinical, neurobiological, and treatment perspectives. *Lancet* 379 (9820):1045-1055.
220. Wilson, M.A. and Molliver, M.E. (1991). The organization of serotonergic projections to cerebral cortex in primates: Regional distribution of axon terminals. *Neuroscience* 44 (3):537-553.
221. Geyer, M.A. (1996). Serotonergic functions in arousal and motor activity. *Behav. Brain Res.* 73 (1-2):31-35.
222. Hindmarch, I. (1995). The Behavioral Toxicity of the Selective Serotonin Reuptake Inhibitors. *Int. Clin. Psychopharm.* 9:13-17.
223. Bel, N. and Artigas, F. (1992). Fluvoxamine preferentially increases extracellular 5-hydroxytryptamine in the raphe nuclei: An in vivo microdialysis study. *Eur. J. Pharmacol.* 229 (1):101-103.
224. Stahl, S.M. (2000). Placebo-controlled comparison of the selective serotonin reuptake inhibitors citalopram and sertraline. *Biol Psychiat* 48 (9):894-901.
225. Ekselius, L., von Knorring, L. and Eberhard, G. (1997). A double-blind multicenter trial comparing sertraline and citalopram in patients with major depression treated in general practice. *Int. Clin. Psychopharmacol.* 12 (6):323-331.
226. Urani, A., Romieu, P., Portales-Casamar, E., Roman, F.J. and Maurice, T. (2002). The antidepressant-like effect induced by the sigma₁ (σ_1) receptor agonist igmesine involves modulation of intracellular calcium mobilization. *Psychopharmacology (Berl.)* 163 (1):26-35.
227. Villemagne, V.L., Dannals, R.F., Sanchezroa, P.M., et al. (1991). Imaging histamine H1 receptors in the living human brain with carbon-11-pyramine. *J. Nucl. Med.* 32 (2):308-311.
228. Kasa, P., Rakonczay, Z. and Gulya, K. (1997). The cholinergic system in Alzheimer's disease. *Prog. Neurobiol.* 52 (6):511-535.
229. Schliebs, R. and Arendt, T. (2011). The cholinergic system in aging and neuronal degeneration. *Behav. Brain Res.* 221 (2):555-563.
230. Selden, N.R., Gitelman, D.R., Salamon-Murayama, N., Parrish, T.B. and Mesulam, M.M. (1998). Trajectories of cholinergic pathways within the cerebral hemispheres of the human brain. *Brain* 121:2249-2257.
231. Bentley, P., Driver, J. and Dolan, R.J. (2008). Cholinesterase inhibition modulates visual and attentional brain responses in Alzheimer's disease and health. *Brain* 131:409-424.

232. Sarter, M. and Bruno, J.P. (1998). Cortical acetylcholine, reality distortion, schizophrenia, and Lewy Body Dementia: Too much or too little cortical acetylcholine? *Brain Cognition* 38 (3):297-316.
233. Dotigny, F., Ben Amor, A.Y., Burke, M. and Vaucher, E. (2008). Neuromodulatory role of acetylcholine in visually-induced cortical activation: Behavioral and neuroanatomical correlates. *Neuroscience* 154 (4):1607-1618.
234. Kang, J.I., Huppe-Gourgues, F. and Vaucher, E. (2014). Boosting visual cortex function and plasticity with acetylcholine to enhance visual perception. *Front. Syst. Neurosci.* 8:172.
235. Bentley, P., Husain, M. and Dolan, R.J. (2004). Effects of cholinergic enhancement on visual stimulation, spatial attention, and spatial working memory. *Neuron* 41 (6):969-982.
236. Bentley, P., Vuilleumier, P., Thiel, C.M., Driver, J. and Dolan, R.J. (2003). Cholinergic enhancement modulates neural correlates of selective attention and emotional processing. *Neuroimage* 20 (1):58-70.
237. Hashimoto, M., Kazui, H., Matsumoto, K., Nakano, Y., Yasuda, M. and Mori, E. (2005). Does donepezil treatment slow the progression of hippocampal atrophy in patients with Alzheimer's disease? *Am. J. Psychiatry* 162 (4):676-682.
238. Gron, G., Kirstein, M., Thielscher, A., Riepe, M.W. and Spitzer, M. (2005). Cholinergic enhancement of episodic memory in healthy young adults. *Psychopharmacology (Berl.)* 182 (1):170-179.
239. Kircher, T.T.J., Erb, M., Grodd, W. and Leube, D.T. (2005). Cortical activation during cholinesterase-inhibitor treatment in Alzheimer disease: Preliminary findings from a pharmacofMRI study. *Am. J. Geriatr. Psychiat.* 13 (11):1006-1013.
240. Rombouts, S.A.R.B., Barkhof, F., van Meel, C.S. and Scheltens, P. (2002). Alterations in brain activation during cholinergic enhancement with rivastigmine in Alzheimer's disease. *J. Neurol. Neurosur. Psych.* 73 (6):665-671.
241. Goekoop, R., Scheltens, P., Barkhof, F. and Rombouts, S.A.R.B. (2006). Cholinergic challenge in Alzheimer patients and mild cognitive impairment differentially affects hippocampal activation: A pharmacological fMRI study. *Brain* 129:141-157.
242. Goekoop, R., Rombouts, S.A.R.B., Jonker, C., et al. (2004). Challenging the cholinergic system in mild cognitive impairment: A pharmacological fMRI study. *Neuroimage* 23 (4):1450-1459.
243. McCance, I., Phillis, J.W. and Westerman, R.A. (1968). Acetylcholine-sensitivity of thalamic neurones: Its relationship to synaptic transmission. *Br. J. Pharmacol.* 32 (3):635-651.
244. Phillis, J.W., Tebecis, A.K. and York, D.H. (1967). A study of cholinceptive cells in the lateral geniculate nucleus. *J. Physiol.* 192 (3):695-713.
245. Sillito, A.M., Cudeiro, J. and Jones, H.E. (2006). Always returning: Feedback and sensory processing in visual cortex and thalamus. *Trends Neurosci.* 29 (6):307-316.
246. Furey, M.L., Pietrini, P. and Haxby, J.V. (2000). Cholinergic enhancement and increased selectivity of perceptual processing during working memory. *Science* 290 (5500):2315-2319.
247. Murphy, P.C. and Sillito, A.M. (1991). Cholinergic enhancement of direction selectivity in the visual cortex of the cat. *Neuroscience* 40 (1):13-20.
248. Schmahmann, J.D. (2004). Disorders of the cerebellum: Ataxia, dysmetria of thought, and the cerebellar cognitive affective syndrome. *J. Neuropsych. Clin. Neurosc.* 16 (3):367-378.

249. Schmahmann, J.D. and Sherman, J.C. (1998). The cerebellar cognitive affective syndrome. *Brain* 121:561-579.
250. Trindade, E., Menon, D., Topfer, L.A. and Coloma, C. (1998). Adverse effects associated with selective serotonin reuptake inhibitors and tricyclic antidepressants: A meta-analysis. *Can. Med. Assoc. J.* 159 (10):1245-1252.
251. Gauthier, S. (2001). Cholinergic adverse effects of cholinesterase inhibitors in Alzheimer's disease: Epidemiology and management. *Drugs Aging* 18 (11):853-862.
252. Rosengarten, B., Paulsen, S., Burr, O. and Kaps, M. (2009). Neurovascular coupling in Alzheimer patients: Effect of acetylcholine-esterase inhibitors. *Neurobiol. Aging* 30 (12):1918-1923.
253. Stephenson, L.A. and Kolka, M.A. (1990). Acetylcholinesterase inhibitor, pyridostigmine bromide, reduces skin blood flow in humans. *Am. J. Physiol.* 258 (4):R951-R957.
254. Fandakova, Y., Sander, M.C., Werkle-Bergner, M. and Shing, Y.L. (2014). Age differences in short-term memory binding are related to working memory performance across the lifespan. *Psychol. Aging* 29 (1):140-149.
255. Li, K.Z.H. and Lindenberger, U. (2002). Relations between aging sensory/sensorimotor and cognitive functions. *Neurosci. Biobehav. Rev.* 26 (7):777-783.
256. Salthouse, T.A. (1996). The processing-speed theory of adult age differences in cognition. *Psychol. Rev.* 103 (3):403-428.
257. Barkhof, F., Haller, S. and Rombouts, S.A.R.B. (2014). Resting-state functional MR Imaging: A new window to the brain. *Radiology* 272 (1):28-48.
258. Betzel, R.F., Byrge, L., He, Y., Goni, J., Zuo, X.N. and Sporns, O. (2014). Changes in structural and functional connectivity among resting-state networks across the human lifespan. *Neuroimage* 102:345-357.
259. Sala-Llonch, R., Bartres-Faz, D. and Junque, C. (2015). Reorganization of brain networks in aging: a review of functional connectivity studies. *Front. Psychol.* 6:663.
260. Sperling, R. (2011). The potential of functional MRI as a biomarker in early Alzheimer's disease. *Neurobiol. Aging* 32:537-543.
261. Greicius, M.D., Srivastava, G., Reiss, A.L. and Menon, V. (2004). Default-mode network activity distinguishes Alzheimer's disease from healthy aging: Evidence from functional MRI. *Proc. Natl. Acad. Sci. U.S.A.* 101 (13):4637-4642.
262. Lundstrom, B.N., Ingvar, M. and Petersson, K.M. (2005). The role of precuneus and left inferior frontal cortex during source memory episodic retrieval. *Neuroimage* 27 (4):824-834.
263. Buckner, R.L., Snyder, A.Z., Shannon, B.J., et al. (2005). Molecular, structural, and functional characterization of Alzheimer's disease: Evidence for a relationship between default activity, amyloid, and memory. *J. Neurosci.* 25 (34):7709-7717.
264. Biswal, B.B., Mennes, M., Zuo, X.N., et al. (2010). Toward discovery science of human brain function. *Proc. Natl. Acad. Sci. U.S.A.* 107 (10):4734-4739.
265. Dennis, E.L. and Thompson, P.M. (2014). Functional brain connectivity using fMRI in aging and Alzheimer's disease. *Neuropsychol. Rev.* 24 (1):49-62.
266. Koch, W., Teipel, S., Mueller, S., et al. (2010). Effects of aging on default mode network activity in resting state fMRI: Does the method of analysis matter? *Neuroimage* 51 (1):280-287.

267. Pievani, M., de Haan, W., Wu, T., Seeley, W.W. and Frisoni, G.B. (2011). Functional network disruption in the degenerative dementias. *Lancet Neurol.* 10 (9):829-843.
268. Zhang, H.Y., Wang, S.J., Liu, B., et al. (2010). Resting brain connectivity: Changes during the progress of Alzheimer disease. *Radiology* 256 (2):598-606.
269. Mowinckel, A.M., Espeseth, T. and Westlye, L.T. (2012). Network-specific effects of age and in-scanner subject motion: A resting-state fMRI study of 238 healthy adults. *Neuroimage* 63 (3):1364-1373.
270. Wu, T., Zang, Y.F., Wang, L., Long, X.Y., Li, K.C. and Chan, P. (2007). Normal aging decreases regional homogeneity of the motor areas in the resting state. *Neurosci. Lett.* 423 (3):189-193.
271. Yan, L., Zhuo, Y., Wang, B. and Wang, D.J. (2011). Loss of coherence of low frequency fluctuations of BOLD fMRI in visual cortex of healthy aged subjects. *Open Neuroimag. J.* 5:105-111.
272. Sluimer, J.D., van der Flier, W.M., Karas, G.B., et al. (2009). Accelerating regional atrophy rates in the progression from normal aging to Alzheimer's disease. *Eur. Radiol.* 19 (12):2826-2833.
273. Oakes, T.R., Fox, A.S., Johnstone, T., Chung, M.K., Kalin, N. and Davidson, R.J. (2007). Integrating VBM into the general linear model with voxelwise anatomical covariates. *Neuroimage* 34 (2):500-508.
274. Folstein, M., Folstein, S. and McHugh, P. (1975). Mini-Mental State: A practical method for grading the cognitive state of patients for the clinician. *J. Psychiatr. Res.* 12:189-198.
275. Klaassens, B.L., Rombouts, S.A.R.B., Winkler, A.M., van Gorsel, H.C., van der Grond, J. and van Gerven, J.M.A. (2017). Time related effects on functional brain connectivity after serotonergic and cholinergic neuromodulation. *Hum. Brain Mapp.* 38 (1):308-325.
276. Zhang, Y.Y., Brady, M. and Smith, S. (2001). Segmentation of brain MR images through a hidden Markov random field model and the expectation-maximization algorithm. *IEEE Trans. Med. Imaging* 20 (1):45-57.
277. Sohn, W.S., Yoo, K., Lee, Y.B., Seo, S.W., Na, D.L. and Jeong, Y. (2015). Influence of ROI selection on resting state functional connectivity: An individualized approach for resting state fMRI analysis. *Front. Neurosci.* 9:280.
278. Adriaanse, S.M., Sanz-Arigita, E.J., Binnewijzend, M.A.A., et al. (2014). Amyloid and its association with default network integrity in Alzheimer's disease. *Hum. Brain Mapp.* 35 (3):779-791.
279. Utevsky, A.V., Smith, D.V. and Huettel, S.A. (2014). Precuneus is a functional core of the default-mode network. *J. Neurosci.* 34 (3):932-940.
280. Gusnard, D.A. and Raichle, M.E. (2001). Searching for a baseline: Functional imaging and the resting human brain. *Nat. Rev. Neurosci.* 2 (10):685-694.
281. Achard, S., Salvador, R., Whitcher, B., Suckling, J. and Bullmore, E.T. (2006). A resilient, low-frequency, small-world human brain functional network with highly connected association cortical hubs. *J. Neurosci.* 26 (1):63-72.
282. Damoiseaux, J.S., Prater, K.E., Miller, B.L. and Greicius, M.D. (2012). Functional connectivity tracks clinical deterioration in Alzheimer's disease. *Neurobiol. Aging* 33 (4):828.e19-828.e30.
283. He, Y., Wang, L., Zang, Y.F., et al. (2007). Regional coherence changes in the early stages of Alzheimer's disease: A combined structural and resting-state functional MRI study. *Neuroimage* 35 (2):488-500.
284. Kim, J., Kim, Y.H. and Lee, J.H. (2013). Hippocampus-precuneus functional connectivity as an early sign of Alzheimer's disease: A preliminary study using structural and functional magnetic resonance imaging data. *Brain Res.* 1495:18-29.

285. Sheline, Y.I., Morris, J.C., Snyder, A.Z., et al. (2010). APOE4 allele disrupts resting state fMRI connectivity in the absence of amyloid plaques or decreased CSF A β 42. *J. Neurosci.* 30 (50):17035-17040.
286. Tahmasian, M., Pasquini, L., Scherr, M., et al. (2015). The lower hippocampus global connectivity, the higher its local metabolism in Alzheimer disease. *Neurology* 84 (19):1956-1963.
287. Karas, G., Scheltens, P., Rombouts, S., et al. (2007). Precuneus atrophy in early-onset Alzheimer's disease: A morphometric structural MRI study. *Neuroradiology* 49 (12):967-976.
288. Rombouts, S.A.R.B., Barkhof, F., Goekoop, R., Stam, C.J. and Scheltens, P. (2005). Altered resting state networks in mild cognitive impairment and mild Alzheimer's disease: An fMRI study. *Hum. Brain Mapp.* 26 (4):231-239.
289. Sperling, R.A., Dickerson, B.C., Pihlajamaki, M., et al. (2010). Functional alterations in memory networks in early Alzheimer's disease. *Neuromolecular Med.* 12 (1):27-43.
290. Mintun, M.A., LaRossa, G.N., Sheline, Y.I., et al. (2006). [11]PIB in a nondemented population: Potential antecedent marker of Alzheimer disease. *Neurology* 67 (3):446-452.
291. Lorenzi, M., Beltramello, A., Mercuri, N.B., et al. (2011). Effect of memantine on resting state default mode network activity in Alzheimer's disease. *Drugs Aging* 28 (3):205-217.
292. Grady, C.L., Protzner, A.B., Kovacevic, N., et al. (2010). A multivariate analysis of age-related differences in default mode and task-positive networks across multiple cognitive domains. *Cereb. Cortex* 20 (6):1432-1447.
293. Mevel, K., Chetelat, G., Eustache, F. and Desgranges, B. (2011). The default mode network in healthy aging and Alzheimer's disease. *Int. J. Alzheimers Dis.* 2011:535816.
294. Giorgio, A., Santelli, L., Tomassini, V., et al. (2010). Age-related changes in grey and white matter structure throughout adulthood. *Neuroimage* 51 (3):943-951.
295. Good, C.D., Johnsrude, I.S., Ashburner, J., Henson, R.N.A., Friston, K.J. and Frackowiak, R.S.J. (2001). A voxel-based morphometric study of ageing in 465 normal adult human brains. *Neuroimage* 14 (1):21-36.
296. Habes, M., Janowitz, D., Erus, G., et al. (2016). Advanced brain aging: Relationship with epidemiologic and genetic risk factors, and overlap with Alzheimer disease atrophy patterns. *Transl. Psychiatry* 6:1-8.
297. Glahn, D.C., Winkler, A.M., Kochunov, P., et al. (2010). Genetic control over the resting brain. *Proc. Natl. Acad. Sci. U.S.A.* 107 (3):1223-1228.
298. Chan, D., Fox, N.C., Jenkins, R., Scahill, R.I., Crum, W.R. and Rossor, M.N. (2001). Rates of global and regional cerebral atrophy in AD and frontotemporal dementia. *Neurology* 57 (10):1756-1763.
299. Matsuda, H. (2013). Voxel-based Morphometry of Brain MRI in Normal Aging and Alzheimer's Disease. *Aging Dis.* 4 (1):29-37.
300. Bailly, M., Destrieux, C., Hommet, C., et al. (2015). Precuneus and cingulate cortex atrophy and hypometabolism in patients with Alzheimer's disease and mild cognitive impairment: MRI and 18 F-FDG PET quantitative analysis using FreeSurfer. *Biomed. Res. Int.* 2015:583931.
301. Baron, J.C., Chetelat, G., Desgranges, B., et al. (2001). In vivo mapping of gray matter loss with voxel-based morphometry in mild Alzheimer's disease. *Neuroimage* 14 (2):298-309.
302. Huettel, S.A., Singerman, J.D. and McCarthy, G. (2001). The effects of aging upon the hemodynamic response measured by functional MRI. *Neuroimage* 13 (1):161-175.

303. Mohr, P.N.C. and Nagel, I.E. (2010). Variability in brain activity as an individual difference measure in neuroscience? *J. Neurosci.* 30 (23):7755-7757.
304. Brier, M.R., Thomas, J.B., Snyder, A.Z., et al. (2014). Unrecognized preclinical Alzheimer disease confounds rs-fMRI studies of normal aging. *Neurology* 83 (18):1613-1619.
305. Elman, J.A., Madison, C.M., Baker, S.L., et al. (2016). Effects of beta-amyloid on resting state functional connectivity within and between networks reflect known patterns of regional vulnerability. *Cereb. Cortex* 26 (2):695-707.
306. Li, S.C., Lindenberger, U. and Sikstrom, S. (2001). Aging cognition: From neuromodulation to representation. *Trends Cogn. Sci.* 5 (11):479-486.
307. Gallagher, M. and Colombo, P.J. (1995). Ageing: The cholinergic hypothesis of cognitive decline. *Curr. Opin. Neurobiol.* 5 (2):161-168.
308. Hasselmo, M.E. (1999). Neuromodulation: Acetylcholine and memory consolidation. *Trends Cogn. Sci.* 3 (9):351-359.
309. Decker, M.W. (1987). The effects of aging on hippocampal and cortical projections of the forebrain cholinergic system. *Brain Res. Rev.* 12 (4):423-438.
310. Gareri, P., De Fazio, P. and De Sarro, G. (2002). Neuropharmacology of depression in aging and age-related diseases. *Ageing Res. Rev.* 1 (1):113-134.
311. Niesters, M., Sitsen, E., Oudejans, L., et al. (2014). Effect of deafferentation from spinal anesthesia on pain sensitivity and resting-state functional brain connectivity in healthy male volunteers. *Brain Connect.* 4 (6):404-416.
312. Honey, G.D., Suckling, J., Zelaya, F., et al. (2003). Dopaminergic drug effects on physiological connectivity in a human cortico-striato-thalamic system. *Brain* 126 (8):1767-1781.
313. Borsook, D., Becerra, L. and Hargreaves, R. (2006). A role for fMRI in optimizing CNS drug development. *Nat. Rev. Drug. Discov.* 5 (5):411-424.
314. van Laar, M.W., van Willigenburg, A.P.P. and Volkerts, E.R. (1995). Acute and subchronic effects of nefazodone and imipramine on highway driving, cognitive functions, and daytime sleepiness in healthy adult and elderly subjects. *J. Clin. Psychopharmacol.* 15 (1):30-40.
315. Arranz, B., Eriksson, A., Mellerup, E., Plenge, P. and Marcusson, J. (1993). Effect of aging in human cortical pre- and postsynaptic serotonin binding sites. *Brain Res.* 620 (1):163-166.
316. Bartus, R.T. (1979). Physostigmine and recent memory: Effects in young and aged nonhuman primates. *Science* 206 (4422):1087-1089.
317. Lotrich, F.E. and Pollock, B.G. (2005). Aging and clinical pharmacology: Implications for antidepressants. *J. Clin. Pharmacol.* 45 (10):1106-1122.
318. Winkler, A.M., Ridgway, G.R., Douaud, G., Nichols, T.E. and Smith, S.M. (2016). Faster permutation inference in brain imaging. *Neuroimage* 141:502-516.
319. Klaassens, B.L., van Gerven, J.M.A., van der Grond, J., de Vos, F., Moller, C. and Rombouts, S. (2017). Diminished posterior precuneus connectivity with the default mode network differentiates normal aging from Alzheimer's disease. *Front. Aging Neurosci.* 9:97.
320. Sachenko, V.V. and Khorevin, V.I. (2001). Serotonin and central mechanisms underlying motor control. *Neurophysiology* 33 (3):180-196.

321. Leo, R.J. (1996). Movement disorders associated with the serotonin selective reuptake inhibitors. *J. Clin. Psychiatry* 57 (10):449-454.
322. Anderson, L.B., Anderson, P.B., Anderson, T.B., Bishop, A. and Anderson, J. (2009). Effects of selective serotonin reuptake inhibitors on motor neuron survival. *Int. J. Gen. Med.* 2:109-115.
323. Capitaio, L.P., Murphy, S.E., Browning, M., Cowen, P.J. and Harmer, C.J. (2015). Acute fluoxetine modulates emotional processing in young adult volunteers. *Psychol. Med.* 45 (11):2295-2308.
324. Wu, J.H., Zhang, S., Li, W.Q., et al. (2015). Cortisol awakening response predicts intrinsic functional connectivity of the medial prefrontal cortex in the afternoon of the same day. *Neuroimage* 122:158-165.
325. Boyce, R.D., Handler, S.M., Karp, J.F. and Hanlon, J.T. (2012). Age-related changes in antidepressant pharmacokinetics and potential drug-drug interactions: A comparison of evidence-based literature and package insert information. *Am. J. Geriatr. Pharmacother.* 10 (2):139-150.
326. Wixted, J.T. and Squire, L.R. (2011). The medial temporal lobe and the attributes of memory. *Trends Cogn. Sci.* 15 (5):210-217.
327. van der Werf, Y.D., Witter, M.P., Uylings, H.B.M. and Jolles, J. (2000). Neuropsychology of infarctions in the thalamus: A review. *Neuropsychologia* 38 (5):613-627.
328. Garoff, R.J., Slotnick, S.D. and Schacter, D.L. (2005). The neural origins of specific and general memory: The role of the fusiform cortex. *Neuropsychologia* 43 (6):847-859.
329. Muir, J.L. (1997). Acetylcholine, aging, and Alzheimer's disease. *Pharmacol. Biochem. Behav.* 56 (4):687-696.
330. Dunbar, F., Zhu, Y. and Brashear, H.R. (2006). Post hoc comparison of daily rates of nausea and vomiting with once- and twice-daily galantamine from a double-blind, placebo-controlled, parallel-group, 6-month study. *Clin. Ther.* 28 (3):365-372.
331. Tan, C.C., Yu, J.T., Wang, H.F., et al. (2014). Efficacy and safety of donepezil, galantamine, rivastigmine, and memantine for the treatment of Alzheimer's disease: A systematic review and meta-analysis. *J. Alzheimers Dis.* 41 (2):615-631.
332. Beglinger, L.J., Tangphao-Daniels, O., Kareken, D.A., Zhang, L., Mohs, R. and Siemers, E.R. (2005). Neuropsychological test performance in healthy elderly volunteers before and after donepezil administration: A randomized, controlled study. *J. Clin. Psychopharmacol.* 25 (2):159-165.
333. Beglinger, L.J., Gaydos, B.L., Kareken, D.A., Tangphao-Daniels, O., Siemers, E.R. and Moh, R.C. (2004). Neuropsychological test performance in healthy volunteers before and after donepezil administration. *J. Psychopharmacol.* 18 (1):102-108.
334. Geerligns, L. and Tsvetanov, K.A. (2017). The use of resting state data in an integrative approach to studying neurocognitive ageing: Commentary on Campbell and Schacter (2016). *Lang. Cogn. Neurosci.* 32 (6):684-691.
335. Mesulam, M.M. and Geula, G. (1988). Nucleus basalis (Ch4) and cortical cholinergic innervation in the human brain: Observations based on the distribution of acetylcholinesterase and choline acetyltransferase. *J. Comp. Neurol.* 275 (2):216-240.
336. Pepeu, G. and Giovannini, M.G. (2009). Cholinesterase inhibitors and beyond. *Curr. Alzheimer Res.* 6 (2):86-96.

337. Geldenhuys, W.J. and Van der Schyf, C.J. (2011). Role of serotonin in Alzheimer's disease: A new therapeutic target? *CNS Drugs* 25 (9):765-781.
338. Claeysen, S., Bockaert, J. and Giannoni, P. (2015). Serotonin: A new hope in Alzheimer's disease? *ACS Chem. Neurosci.* 6 (7):940-943.
339. McEntee, W.J. and Crook, T.H. (1991). Serotonin, memory, and the aging brain. *Psychopharmacology (Berl.)* 103 (2):143-149.
340. Riekkinen, M., Tolonen, R. and Riekkinen, P. (1994). Interaction between 5-HT_{1a} and nicotinic cholinergic receptors in the regulation of water maze navigation behavior. *Brain Res.* 649 (1-2):174-180.
341. Richter-Levin, G. and Segal, M. (1993). Age-related cognitive deficits in rats are associated with a combined loss of cholinergic and serotonergic functions. *Ann. N.Y. Acad. Sci.* 695:254-257.
342. Samson, M. and Claassen, D.O. (2017). Neurodegeneration and the cerebellum. *Neurodegener. Dis.* 17 (4-5):155-165.
343. Colloby, S.J., O'Brien, J.T. and Taylor, J.P. (2014). Patterns of cerebellar volume loss in dementia with Lewy bodies and Alzheimer's disease: A VBM-DARTEL study. *Psychiatr. Res.-Neuroim.* 223 (3):187-191.
344. Thomann, P.A., Schlafer, C., Seidl, U., Dos Santos, V., Essig, M. and Schroder, J. (2008). The cerebellum in mild cognitive impairment and Alzheimer's disease - A structural MRI study. *J. Psychiatr. Res.* 42 (14):1198-1202.
345. Glickstein, M. and Doron, K. (2008). Cerebellum: Connections and functions. *Cerebellum* 7 (4):589-594.
346. Buckner, R.L., Krienen, F.M., Castellanos, A., Diaz, J.C. and Yeo, B.T.T. (2011). The organization of the human cerebellum estimated by intrinsic functional connectivity. *J. Neurophysiol.* 106 (5):2322-2345.
347. Guo, C.C., Tan, R., Hodges, J.R., Hu, X.T., Sami, S. and Hornberger, M. (2016). Network-selective vulnerability of the human cerebellum to Alzheimer's disease and frontotemporal dementia. *Brain* 139:1527-1538.
348. Habas, C., Kamdar, N., Nguyen, D., et al. (2009). Distinct cerebellar contributions to intrinsic connectivity networks. *J. Neurosci.* 29 (26):8586-8594.
349. Mount, H.T.J., Dreyfus, C.F. and Black, I.B. (1994). Muscarinic stimulation promotes cultured Purkinje-cell survival: A role for acetylcholine in cerebellar development. *J. Neurochem.* 63 (6):2065-2073.
350. Jaarsma, D., Ruigrok, T.J.H., Caffè, R., et al. (1997). Cholinergic innervation and receptors in the cerebellum. *Prog. Brain Res.* 114:67-96.
351. Kwong, W.H., Chan, W.Y., Lee, K.K.H., Fan, M. and Yew, D.T. (2000). Neurotransmitters, neuropeptides and calcium binding proteins in developing human cerebellum: A review. *Histochem. J.* 32 (9):521-534.
352. McCance, I. and Phillis, J.W. (1968). Cholinergic mechanisms in the cerebellar cortex. *Int. J. Neuropharmacol.* 7 (5):447-462.
353. Jaarsma, D., Dino, M.R., Cozzari, C. and Mugnaini, E. (1996). Cerebellar choline acetyltransferase positive mossy fibres and their granule and unipolar brush cell targets: A model for central cholinergic nicotinic neurotransmission. *J. Neurocytol.* 25 (12):829-842.
354. Atack, J.R., Perry, E.K., Bonham, J.R., Candy, J.M. and Perry, R.H. (1986). Molecular forms of acetylcholinesterase and butyrylcholinesterase in the aged human central nervous system. *J. Neurochem.* 47 (1):263-277.

355. Iyo, M., Namba, H., Fukushi, K., et al. (1997). Measurement of acetylcholinesterase by positron emission tomography in the brains of healthy controls and patients with Alzheimer's disease. *Lancet* 349 (9068):1805-1809.
356. Mavroudis, I.A., Fotiou, D.F., Adipepe, L.F., et al. (2010). Morphological changes of the human Purkinje cells and deposition of neuritic plaques and neurofibrillary tangles on the cerebellar cortex of Alzheimer's disease. *Am. J. Alzheimers Dis.* 25 (7):585-591.
357. Seo, Y., Shin, Y., Kim, H.S., et al. (2014). Donepezil enhances Purkinje cell survival and alleviates motor dysfunction by inhibiting cholesterol synthesis in a murine model of Niemann Pick disease type C. *J. Neuropathol. Exp. Neurol.* 73 (3):234-243.
358. Heckers, S., Geula, C. and Mesulam, M.M. (1992). Cholinergic innervation of the human thalamus: Dual origin and differential nuclear distribution. *J. Comp. Neurol.* 325 (1):68-82.
359. Palesi, F., Tournier, J.D., Calamante, F., et al. (2015). Contralateral cerebello-thalamo-cortical pathways with prominent involvement of associative areas in humans in vivo. *Brain Structure & Function* 220 (6):3369-3384.
360. Nyth, A.L. and Gottfries, C.G. (1990). The clinical efficacy of citalopram in treatment of emotional disturbances in dementia disorders: A Nordic multicenter study. *Br. J. Psychiatry* 157:894-901.
361. Leonpacher, A.K., Peters, M.E., Drye, L.T., et al. (2016). Effects of citalopram on neuropsychiatric symptoms in Alzheimer's dementia: Evidence from the CitAD Study. *Am. J. Psychiatry* 173 (5):473-480.
362. Porsteinsson, A.P., Drye, L.T., Pollock, B.G., et al. (2014). Effect of citalopram on agitation in Alzheimer disease: The CitAD randomized clinical trial. *J. Am. Med. Assoc.* 311 (7):682-691.
363. Schmitt, J.A.J., Wingen, M., Ramaekers, J.G., Evers, E.A.T. and Riedel, W.J. (2006). Serotonin and human cognitive performance. *Curr. Pharm. Des.* 12 (20):2473-2486.
364. Mowla, A. (2009). Does serotonin augmentation have any effect on cognition and activities of daily living in Alzheimer's dementia?: A double-blind clinical trial. *Eur. Psychiatry* 24 (5):484-487.
365. Buhot, H.C., Martin, S. and Segu, L. (2000). Role of serotonin in memory impairment. *Ann. Med.* 32 (3):210-221.
366. Halliday, M., Radford, H., Zents, K.A.M., et al. (2017). Repurposed drugs targeting eIF2 α -P-mediated translational repression prevent neurodegeneration in mice. *Brain* 140 (6):1768-1783.
367. Sheline, Y.I., West, T., Yarasheski, K., et al. (2014). An antidepressant decreases CSF A β production in healthy individuals and in transgenic AD mice. *Sci. Transl. Med.* 6 (236):236re4.
368. Bush, G., Luu, P. and Posner, M.I. (2000). Cognitive and emotional influences in anterior cingulate cortex. *Trends Cogn. Sci.* 4 (6):215-222.
369. Arlt, S. (2013). Non-Alzheimer's disease-related memory impairment and dementia. *Dialogues Clin. Neurosci.* 15 (4):465-473.
370. Friston, K.J. (2011). Functional and effective connectivity: A review. *Brain Connect.* 1 (1):13-36.
371. Farde, L. (1996). The advantage of using positron emission tomography in drug research. *Trends Neurosci.* 19 (6):211-214.
372. Derendorf, H. and Meibohm, B. (1999). Modeling of pharmacokinetic/pharmacodynamic (PK/PD) relationships: Concepts and perspectives. *Pharm. Res.* 16 (2):176-185.

373. Schouten, T.M., Koini, M., de Vos, F., et al. (2016). Combining anatomical, diffusion, and resting state functional magnetic resonance imaging for individual classification of mild and moderate Alzheimer's disease. *Neuroimage-Clinical* 11:46-51.
374. Merello, M., Nouzeilles, M.I., Arce, G.P. and Leiguarda, R. (2002). Accuracy of acute levodopa challenge for clinical prediction of sustained long-term levodopa response as a major criterion for idiopathic Parkinson's disease diagnosis. *Mov. Disord.* 17 (4):795-798.
375. Malone, K.M., Thase, M.E., Mieczkowski, T., et al. (1993). Fenfluramine challenge test as a predictor of outcome in major depression. *Psychopharmacol. Bull.* 29 (2):155-161.
376. Kuzmickiene, J. and Kaubrys, G. (2015). Selective ability of some CANTAB battery test measures to detect cognitive response to a single dose of donepezil in Alzheimer disease. *Med. Sci. Monit.* 21:2572-2582.

DANKWOORD

Dit proefschrift had ik onmogelijk kunnen voltooien zonder de waardevolle hulp en ondersteuning van velen.

Ten eerste wil ik alle deelnemers hartelijk bedanken voor hun inzet en motivatie tijdens de lange onderzoeksdagen. Zonder hen waren deze studies niet mogelijk geweest.

Vervolgens natuurlijk mijn promotoren Serge Rombouts en Joop van Gerven en copromotor Jeroen van der Grond. Beste Serge, Joop en Jeroen, bedankt voor de prettige samenwerking en begeleiding, waarbij er altijd ruimte was voor overleg, en de kans die jullie mij hebben gegeven om dit project uit te voeren. Jullie hebben mij hierbij al die jaren gesteund en dat waardeer ik enorm.

Graag wil ik ook de leden van de promotie- en oppositiecommissie bedanken voor het lezen en beoordelen van dit proefschrift.

Ik heb met heel veel plezier bij de Faculteit der Sociale Wetenschappen gewerkt, waarvoor ik al mijn collega's daar wil bedanken. In het bijzonder Frank en Tijn: dank voor alle welkome onderbrekingen tijdens werkdagen en jullie hulp bij fMRI analyses. En Roy, Manja en Kerwin, bedankt voor alle momenten van ontspanning tijdens en buiten het werk.

De samenwerking met het Centre for Human Drug Research was van essentieel belang voor de opzet en uitvoering van de studies, waarvoor veel dank aan alle betrokken afdelingen. Ik ben met name Helene, Erica en Petra zeer dankbaar voor de tijd die zij hebben geïnvesteerd in het onderzoek.

Veel dank aan de collega's van het Leids Universitair Medisch Centrum (Radiologie, Anesthesiologie, KCL) en het LIBC support team, en in het bijzonder aan Wouter, Michel, Michèle en Mattanja, voor alle technische en praktische ondersteuning.

Daarnaast gaat mijn dank uit naar de instellingen (Alrijne Ziekenhuis Leiden en GGZ Rivierduinen Leiden) die hebben geholpen bij de inclusie van patiënten.

Alle coauteurs wil ik graag bedanken voor hun bijdrage. Many thanks to Naj Khalili-Mahani and Anderson Winkler for the valuable methodological support and advice, and Brandon Witcher and Brad Wyman for cooperating during the sertraline study.

Ik heb heel veel gehad aan de studenten die hebben meegewerkt aan de dataverzameling en voorbereiding van de onderzoeksdagen. Lotte, Liselot, Ingrid en Jurriën, bedankt voor jullie inzet en enthousiasme.

Verder wil ik mijn collega's van het Brain Research Center, en vooral mijn kamergenoten, bedanken voor hun interesse en support tijdens de laatste fase van mijn promotie.

Monika en Janice, wat fijn dat jullie mij als paranimfen willen bijstaan tijdens de laatste etappe van dit traject. Dank voor jullie hulp, relativerende woorden en gezelligheid.

Lieve vrienden, heel erg bedankt voor alle aanmoedigingen en adviezen, het luisteren naar mijn verhalen, en het zorgen voor ontspanning de afgelopen jaren. Jullie steun betekent veel voor mij.

Lieve mama en Eline, bedankt voor jullie betrokkenheid, interesse in mijn onderzoek en het meedenken waar mogelijk. Als laatste wil ik mijn oma Grietje bedanken, die op de leeftijd van 100 jaar nog altijd belangstelling heeft voor mijn werk.

CURRICULUM VITAE

Bernadet Louise Klaassens was born on August 26, 1980 in Leiderdorp, the Netherlands. She graduated from high school at the Bonaventuracollege in Leiden in 1998. In 2005, she received her bachelor's degree in Psychology and in 2007, she completed the study Psychology with a master's degree in Clinical Neuropsychology at Leiden University. During this master, she followed a clinical internship at the adult and old-age clinic of the Erasmus Medical Center in Rotterdam. After working as



a junior researcher at Palier in The Hague and as thesis and internship coordinator for the master program Clinical Neuropsychology at Leiden University, she continued with a second master specialization in Methodology and Statistics in Psychology in 2010. Under supervision of Prof. Serge Rombouts and Prof. Mark de Rooij she wrote a thesis on different methods for network modeling of resting state fMRI data of the Leiden Longevity Study. She obtained this master's degree in 2011, and subsequently started her PhD research under guidance of Prof. Serge Rombouts, Prof. Joop van Gerven and Dr. Jeroen van der Grond at Leiden University. This project, as described in this thesis, was performed in collaboration with the Leiden Institute for Brain and Cognition, the Centre for Human Drug Research and the Leiden University Medical Center. In 2017, Bernadet started working as a neuropsychologist at the Brain Research Center in Amsterdam, where clinical trials are executed to investigate novel pharmacological agents for the treatment of Alzheimer's disease.

